PROJECT DELIVERABLE
ANNUAL (2006-2007) AND FINAL REPORT

Task agreement no: J5284 05 0047
Cooperative agreement no: H5000 02 0409-Florida Atlantic University

PHOSPHORUS KINETICS AND BIOGEOCHEMICAL STUDIES TO SUPPORT A SEAGRASS ECOSYSTEM SIMULATION MODEL FOR FLORIDA BAY MANAGEMENT

May 30, 2007

PI: Dr. Marguerite S. Koch
Florida Atlantic University
Aquatic Plant Ecology Lab
Department of Biological Sciences
Boca Raton, Fl, 33431
Phone: (561) 297 3325
Fax: (561) 297 2749
mkoch@fau.edu

CoPIs: Ole Nielsen[1], Henning Jensen[2], Christopher J. Madden[3]
[1]Florida Atlantic University, [2]University of Southern Denmark,
[3]South Florida Water Management District

Graduate Students on Project
Ms. Kara Rosch, Mr. Demetris Keltou

EXECUTIVE SUMMARY

Overall Reasearch

The research presented in this report significantly improves our understanding of nutrient cycling, and P-cycling specifically, in Florida Bay. Herein, we (1) quantify nutrient uptake kinetics of inorganic phosphorus in major ecosystem components of the bay, (2) determine the potential for the hydrolysis of organic phosphorus in the water column, (3) provide estimates for organic matter turnover of seagrass, and (4) examine the potential for carbonate dissolution to recycle the large solid phase inorganic P pool in the bay.

Inorganic Phosporus Uptake Kinetics (Chapter 1)

Tropical and subtropical estuaries dominated by fine carbonate sediments frequently exhibit P limitation of primary producers. Nevertheless, P cycling in these ecosystems is not well understood. We deployed chambers to determine seasonal phosphate (P*i*) uptake kinetics for the water column, sediment and the entire system (water column + sediment + seagrass/epiphyte) in Florida Bay (FB) during 2003-2006 and on the Little Bahama Bank (LBB) during a cruise June, 2004. P*i* concentration over time fit an exponential decay model (R^2>0.92), demonstrating that P*i* uptake is a linear function of concentration in these systems at low P*i* levels (<2 µmol L^{-1}). Applying the P*i* system rate constant (S_p) from western (177 ± 50 x 10^{-6} m s^{-1}) and eastern (272 ± 66 x 10^{-6} m s^{-1}) bay sites, and using P*i* measured during the study (0.02 to 0.177 µmol P*i* L^{-1}), we calculated an P*i* uptake rate ranging from 0.30 to 2.62 mmol P*i* m^{-2} d^{-1} for western and 0.47 to 4.16 mmol P*i* m^{-2} d^{-1} for eastern bay sites. These data indicate a higher P*i* affinity in the east, consistent with greater P limitation for this region; however, high inter-annual variance tempers this conclusion. During non-bloom conditions, phytoplankton dominated P*i* uptake in the east

(46%) and both phytoplankton and the seagrass-epiphyte consortium in the west (32 and 52%, respectively), with a smaller contribution by the sediment (15-20%). On the highly oligotrophic LBB interior sites, the water column always dominated (≥94%) P*i* uptake in the system with a higher S_p (573-881 x 10^{-6} m s^{-1}) than FB. During a cyanobacterial bloom in FB (chl a 17 µg L^{-1}), the water column also dominated P*i* uptake (~100%) and S_p was the highest (>2,800 x 10^{-6} m s^{-1}) found in the bay or on the bank. Fractionating this P taken up showed that phytoplankton accounted for 88% of sequestered P*i*, with only 12% in the acid extractable fraction, most likely as inorganic calcium bound and/or surface adsorbed P, and only 1% attributable to small heterotrophs. When chl a levels declined (2 µg L^{-1}) P*i* uptake was still dominated by phytoplankton (77%); however, the acid extractable pool increased (18%) and the smaller heterotrophic community became more important (22%). We propose that in carbonate-dominated seagrass systems, P*i* is primarily taken up by the water column biota, particularly when driven by cyanobacteria with extremely rapid P*i* uptake rates. In the absence of algal blooms, suspended sediments and heterotrophs in the water column, as well as the benthos (seagrass ≥ sediment) become more important; although in highly oligotrophic systems, such as on the interior of the LBB, P*i* uptake appears to always be controlled by the water column, even in the absence of phytoplankton blooms. Once sequestered by the water column, P is remineralized/hydrolyzed in the water column or settles to the benthos where it is incorporated into sediment porewater or solid phase pools supporting benthic primary production.

Organic Phosphorus Hydrolysis – Alkaline Phosphatase Activity (Chapter 2)

Few phosphorus (P) depleted coastal marine ecosystems have been examined for their capacity to hydrolyze phosphomonoesters (PMEs; organic labile P). The purpose of this study,

was to examine seasonal alkaline phosphatase activity (APA-enzyme that hydrolyzes PMEs) partitioned between water column fractions (phytoplankton, bacteria and freely dissolved) and the dominant benthic autotroph (*Thalassia testudinum*) in Florida Bay, a seagrass-dominated, P limited shallow estuary using low fluorescent substrate (MUF-P) concentrations (≤ 2.0 µM). Comparisons of APA among sites across a nutrient gradient in the bay showed both temporal and spatial differences in substrate hydrolysis rates at 2 µmol L^{-1} MUF-P. APA was higher at the nutrient rich western and northcentral (751 and 695 nmol L^{-1} h^{-1}) sites, driven primarily by microbial and phytoplankton activities in the water column during the fall and winter, compared to the P limited northeastern (359 nmol L^{-1} h^{-1}) site. Highest AP activities (~1,000 nmol L^{-1} h^{-1}) were attributed to cyanobacterial blooms (~15 µg Chl. a L^{-1}) that occurred in the central and western regions of the bay. The free dissolved fraction (<0.2 µm) accounted for most of the APA (~50%), followed by phytoplankton (>1.2 µm; 30%) and bacteria fractions (>0.2-<1.2 µm; 8%). *Thalassia testudinum* leaves with their associated epiphytes contributed modestly to water column APA (14 and 20%), and only during non-bloom conditions. The finding that PMEs are primarily undetectable in the bay, suggests a rapid turnover of this labile organic P pool. A high capacity for organic P hydrolysis in Florida Bay is probably driven by the close association of the shallow water column (<2 m) with the underlying seagrass community and adjacent Everglades wetlands. This association provides organic substrates for microbial and cyanobacterial activity, which in turn appears to both directly stimulate APA and indirectly lead to an accumulation of free enzymes in the water column which may be important in recycling organic P in the system.

Seagrass Nutrient Recycling in Florida Bay (Chapter 3)

Nutrient cycling in tropical estuaries dominated by seagrasses, which are important ecologically as well as constitute an important dynamic nutrient pool, is not well understood. Nitrogen (N) and phosphorus (P) retention by leaves on short shoots, as a measure of resorption (retaining nutrients before senescence), and the subsequent decay of senescent leaves, roots and rhizomes were examined for the dominant Atlantic/Caribbean seagrass species, *Thalassia testudinum*, across a nutrient gradient in Florida Bay. Loss of leaf nutrients while still attached to the short shoot, from both resorption and decay, was highest (88% P; 51% N) at the nutrient-rich compared to nutrient-poor site (49% P; 25% N). Leaf nutrient resorption or loss from senescent leaves did not increase with decreasing nutrient availability, but was enhanced by enrichment through increased decomposition. This high rate of seagrass leaf nutrient loss (12-81 µmol P and 0.46-2.43 mmol N m^{-2} d^{-1}), while still attached to short shoots, represents significant recycling (46-87% P and 17-48% N) of total estimated external nutrient loads to the bay, and affected subsequent leaf decay constants. Senescent leaf, rhizome and root nutrient loss rates were >10-fold lower than intact leaves, particularly at high nutrient sites. Thus, there are linkages between site trophic state and *T. testudinum* nutrient recycling. However, rather than increasing plant nutrient resorption at low nutrient sites, enhanced seagrass leaf decomposition at high nutrient sites increases nutrient flux to the water column, potentially serving as a nutrient pump that translocates porewater nutrients to overlying waters. This transfer of nutrients at sites with high trophic states may influence recurrent phytoplankton blooms in the western and central bay.

Sediment Inorganic P Pool Availability to Seagrass (Chapter 4)

Metabolic sulphide and organic matter oxidation in seagrass rhizopheres may be important in the dissolution of solid-phase TP*i* (e.g. calcium flouro apatite) in carbonate-dominated sediments. We measured sulphate reduction rates (SRR) and simulated metabolic oxidation by adding sulfuric acid (10-50 µmoles cm^{-3} sediment) to sediment slurries from high- and low-P sites in Florida Bay, a seagrass-dominated carbonate estuary. Mobilization of P*i*, F^- and Ca^{2+} was monitored for 6 h followed by extraction of surface-bound P pools. We also examined re-adsorption and carbonate matrix incorporation using ^{33}P. In our dissolution experiment, the highest H_2SO_4 amendments, 112±36 and 53±0.2 µmol H_2SO_4 gdwt, dropped pH values in the sediment slurry to 6.6-6.8, on par with seagrass sediment pore waters with high SRR. Although Ca^{2+} and F^- was released at all sites in response to acid treatments, the P*i* recovered was higher in western (0.60-0.14 nmol P*i* μmol^{-1} H_2SO_4) than eastern (0.08-0 nmol P*i* μmol^{-1} H_2SO_4) bay sites, spanning 1-2 orders of magnitude, while TP*i* levels in the sediment were only 2- to 4-fold higher in the P-enriched western bay. Based on our radiotracer experiment, after 5 h 73% of ^{33}P was detected in HCl-extractable $CaCO_3$-bound pools in eastern bay sediments, while after 55 h, the majority of radioactivity was still found in the surface-bound exchangeable pool in western bay sediments. These experimental results suggest that Ca-bound P is tightly adsorbed and/or incorporated into the sediment matrix at eastern bay sites, perhaps as a result of fine grain size (83% < 63 µm). In contrast, at the most enriched western bay site, SRR (1.9 µmol SO_4^{2-} $gdwt^{-1}$ d^{-1}), assuming a 1:1 stoichiometry of the S redox coupling, could dissolve ~2.8 µmol Ca $gdwt^{-1}$ d^{-1}, applying a 2:1 ratio of Ca dissolved to SR, that would generate 1.5 nmol P*i* $gdwt^{-1}$ d^{-1}, based on P*i* released as a function of $CaCO_3$ dissolution in this study. This P*i*

from TP*i* would meet ~50% (53 µmol P m^{-2} d^{-1} to 14 cm) of the daily P requirement for *T. testudinum* (~100 µmol P m^{-2} d^{-1}), and together with P regenerated from mineralization of organic material (66 µmol P m^{-2} d^{-1}; with a C:P 2,000 and 2 mol C per mol SO_4^{2-} reduced), would provide a surplus of P*i*, probably contributing to the lack of seagrass P limitation in the western bay. Thus, carbonate dissolution may be an important source of P recycling in Florida Bay; but, resorption and reincorporation of P by carbonates may limit its availability for seagrass production in the eastern bay.

Overall Conclusions

I. While the water column of Florida Bay maintains a relatively stable and low inorganic P concentration, even across the sediment nutrient gradient, it represents the site of rapid sequestration and recycling of nutrients that are regenerated in the system. This is evidenced by (1) inorganic P uptake kinetics being dominated by the water column, (2) the high activity of organic P hydrolysis in the water column, (3) high rates of seagrass leaf decomposition occurring in the water column while still attached to short shoots, the dominating flux of seagrass nutrients in the bay which represents a large nutrient storage component, and (4) the low rates of organic, and perhaps inorganic, nutrient flux to the pore water from seagrass detritus and the solid phase inorganic sediment pool.

II. Water column potential to sequester inorganic P, the primary macro-nutrient limiting autotrophs in the bay, increases exponentially with the onset of algal blooms, dominated by cyanobacteria. This “feed-back” system allows blooms to perpetuate once initiated, because of cyanobacteria’s extremely high affinity for inorganic and

organic P, at least potential for organic P hydrolysis. The first-order rate of P*i* uptake by phytoplankton, at the low concentrations in the bay, also controls P uptake rates, maintaining relatively low concentrations across the bay.

III. The ultimate fate of the water column sequestered P, as well as N, into the benthos, through settlement and incorporation into the detrital and inorganic-solid phase pools, defines the uptake potential for seagrass sequestration. The seagrass, also affected by a "feed-back" system, increase in biomass in the western bay, subsequently supporting greater recycling of nutrients, primarily to the water column, but also to the pore water through increased organic matter decomposition. Seagrasses show first-order P uptake kinetics at levels found in the bay surface and pore waters; making pore waters the ultimate site of seagrass sequestration, as these concentrations are frequently 10-fold higher than surface waters. Also, seagrasses would have to compete with epiphytes and phytoplankton for nutrients in the water column, and while their kinetics show this possibility; their uptake rates would not support seagrass high nutrient requirements.

IV. Seagrass density and productivity is much higher in western than eastern bay sediments, not only a result of loading rates, but internal recycling of nutrients in these regions of the bay. Aerobic respiration rates at the sediment-water interface in the seagrass canopy are 3-fold higher than the eastern bay. Sulfate reduction rates, the dominant anaerobic pathway for organic matter decomposition in marine sediments, in western and central Florida Bay are at least 2-fold higher than in eastern bay sites. Therefore, turnover of organic matter, not only attributable to seagrass decomposition because it also includes the more labile organic matter from phytoplankton, is higher in the western and central portions of the bay. This fact probably also contributes to

increased occurrences of phytoplankton blooms in the western and central regions of the bay.

V. Another major potential source of P in the bay is in the solid phase inorganic P pool in the carbonate sediments. As recent geochemical research indicates, the once considered stable calcium carbonate sediment undergoes a significant amount of dissolution, primarily generated by metabolic oxidation of organic matter (releasing carbonic acid) and/or the re-oxidation of hydrogen sulfide produced through anaerobic decomposition of organic matter. Therefore in seagrass sediments, particularly those of very dense beds found in the western bay, generating high rates of sulfate reduction and oxygen leakage from seagrass roots to the rhizosphere (zone of oxidized microlayer at the sediment-root interface), high dissolution rates of $CaCO_3$ can be realized. This is particularly the case during nighttime when respiration rates are high and CO_2 is not being concomitantly sequestered in the overlying water column. While carbonate dissolution through acidification could release a significant amount of inorganic P for seagrass production, we only found this to be the case at enriched western bay sites. In eastern bay sites, where very fine carbonate particles, with a high free surface energy, and that are relatively un-enriched with respect to P, readily adsorb and incorporate inorganic P that is released with acidification. Although more work is clearly needed on understanding P-cycling under carbonate precipitation-dissolution processes across the bay, these data indicate another potential nutrient “feed-back” mechanism in the bay. Nutrient enriched sites with higher organic matter for decomposition promote an increased potential for seagrass to sequester the very large inorganic solid phase P pool, perpetuating high seagrass biomass densities seen across the bay.

VI. Finally, the stability of the entire Florida Bay ecosystem is fundamentally linked to nutrient cycling and biogeochemical processes. While this report focused on increasing our understanding of nutrient cycling in the bay, based on our seagrass stressor work (summarized in Koch et al. in press. Journal Experimental Marine Biology and Ecology) and major contributions by others, the dominant factor in the bay that can cause sudden mortality of entire seagrass meadows is plant hypoxia, driven by plant, sediment, and water column decomposition processes, and the ability of the autotrophs in the system, as well as physical mixing, to balance this oxygen demand. We suggest, based on data reported herein, that repeated seagrass die-off events from western Florida Bay is probably an indirect response to the multiple nutrient recycling "feed-back" mechanisms discussed in this report which destabilize the ecosystem under subtle eutrophication processes. Restricted circulation, warm temperatures, and biota with efficient nutrient uptake kinetics compound the problem by retaining and efficiently recycling nutrients once loaded into the system. Although Florida Bay is considered a nutrient limited estuary, its shallow depth, long hydraulic residence time and extremely high organic matter loads for a carbonate-dominated estuary, make moderate eutrophication processes a major concern.

TABLE OF CONTENTS

Page #

List of Figures xiii
List of Tables xv
Acknowledgements xviii

Chapter 1. INORGANIC PHOSPHORUS UPTAKE IN A CARBONATE-DOMINATED SEAGRASS ECOSYSTEM-FLORIDA BAY 19
1.0. Introduction 20
1.1. Methods 22
1.1.1. Study Area 22
1.1.2. P*i* Uptake Experiments 23
1.1.3. Chamber tests 25
1.1.4. Water column P fractions 27
1.1.5. Nutrient Analyses 28
1.1.6. Chemotaxonomy 28
1.1.7. Parameter Estimates and Statistics 29

1.2. Results 30
1.2.1. P*i* Uptake Kinetics 30
1.2.2. P*i* uptake rate constant (S_p) 30
1.2.3. Threshold for P*i* Uptake (C_0) 37
1.2.4. Water column P fractions and chemotaxonomy 37
1.3. Discussion 41
1.4. Literature Cited 47

Chapter 2 ALKALINE PHOSPHATASE ACTIVITY OF SEAGRASS AND WATER COLUMN FRACTIONS IN FLORIDA BAY 51
2.0. Introduction 52
2.1. Methods 54
2.1.1. Study Sites 54
2.1.2. Sampling and APA Analysis 56
2.1.3. Field Collections and Incubations 57
2.1.4. Water column TP, TDP, Pi and PME analyses 58
2.1.5. Data Analyses 59
2.2. Results 60
2.2.1. Seasonal Patterns of APA 60
2.2.2. Size Fractionated APA 64
2.2.3. Alkaline Phosphatase Kinetics 67
2.3.4. PME Levels in Florida Bay 70
2.3. Discusssion 71
2.4. Literature Cited 81

Chapter 3. SEAGRASS (*THALASSIA TESTUDINUM*) NUTRIENT RECYCLING ALONG A NUTRIENT GRADIENT IN FLORIDA BAY 92
3.0. Introduction 93
3.1. Methods 96
3.1.1. Site Description 96
3.1.2. Leaf Nutrient Resorption Study 98
3.1.2.1. Resorption Experiment 98
3.1.2.2. Senescent Leaf Decomposing Tissue 99
3.1.2.3. Leaf Biomass and Nutrient Production 99
3.1.3. Decomposition Study 100
3.1.3.1. Litterbag Experiments 100
3.1.3.2. Decomposition and Nutrient Loss Calculations 101
3.1.4. Site Temperature, Salinity, and O_2 Dynamics 102
3.1.5. Statistical Analyses 103
3.1.6. Calculation of Bay-wide Nutrient Fluxes 103
3.2. Results 105
3.2.1. Resorption Study 105
3.2.1.1. Leaf Nutrient Retention 105
3.2.1.2. Senescent Leaf Decomposing Tissue 106
3.2.1.3. Nutrient Declines versus Percent Decomposing Tissue 107
3.2.1.4. Leaf Nutrient Content 110
3.2.2. Decomposition Experiment 112
3.2.2.1. Seasonal Effect on Decay Constants 112
3.2.2.2. Site Effects on Decay Constants 113
3.2.2.3. Seagrass Tissue Nutrient Loss Rates 119
3.3. Discussion 122
3.4. Literature Cited 130

Chapter 4. THE POTENTIAL ROLE OF METABOLIC OXIDATION AND SEDIMENT DISSOLUTION IN RELEASING PHOSPHORUS FROM CARBONATE SEAGRASS SEDIMENTS IN FL BAY 134
4.0. Introduction 135
4.1. Methods 137
4.1.1. Sampling Sites 137
4.1.2. P mobilization experiment 139
4.1.3. Sediment Characteristics 141
4.1.4. Sediment P-pool labeling experiment 141
4.1.5. Sulfate reduction rates (SRR) 142
4.2. Results 142
4.2.1. General Sediment Characteristics - Solid Phase 142
4.2.2. Sulfuric acid addition experiment 143
4.2.3. Tracer experiment 151
4.2.4. Sulfate reduction rates 152
4.3. Discussion 154
4.4. Literature Cited 163

LIST OF FIGURES

Chapter 1. INORGANIC PHOSPHORUS UPTAKE IN A CARBONATE-DOMINATED SEAGRASS ECOSYSTEM-FLORIDA BAY

Figure 1.1. Study area in Florida Bay and Bahamas for field P*i* uptake experiments 23

Figure 1.2. P*i* disappearance in chambers with artificial seawater and P spikes 26

Figure 1.3. Average P*i* rate constants, S_p, for seagrass ecosystem components water column, water column + sediment and system in Florida Bay and on the Little Bahama Bank 35

Figure 1.4. Inorganic and organic fractions of sequestered P*i* in the water column.....40

Figure 1.5. Conceptual model illustrating P*i* cycling in Florida Bay 46

Chapter 2. ALKALINE PHOSPHATASE ACTIVITY OF SEAGRASS AND WATER COLUMN FRACTIONS IN FLORIDA BAY

Figure 2.1. APA seasonal sites and sites for spatial PME analysis across Florida Bay 55

Figure 2.2. Seasonal alkaline phosphatase enzyme kinetics using the Michaelis-Menten hyperbolic model for non-filtered (NF), <1.2 µm, and <0.2 µm size fractionated water column 62

Figure 2.3. Seasonal alkaline phosphatase enzyme kinetics using the Michaelis-Menten hyperbolic model for non-filtered (NF) water and NF water with 5 cm leaf segments of *Thalassia testudinum* both with and without epiphytes 63

Chapter 3. SEAGRASS (*THALASSIA TESTUDINUM*) NUTRIENT RECYCLING IN FLORIDA BAY, A CARBONATE-DOMINATED SHALLOW ESTUARY

Figure 3.1. Study sites in Florida Bay for resorption and decomposition experiments 97

Figure 3.2. Seasonal senescent leaf phosphorus and nitrogen leaf decline as they senesced on the short shoot 105

Figure 3.3. Relationship between decomposing tissue on senescent leaves and the P decline between senescent and new fully emergent leaves on intact short shoots 107

Figure 3.4. Linear relationship between leaf tissue N and P loss (%) as leaves senesced on the short shoots 109

Figure 3.5. Temperature and salinity in the water column at each site: Black Betsy Key, Dump Key, and Rabbit Key over the study period 114

Figure 3.6. Proportional loss of senescent leaf biomass deployed at each site in litterbags at Black Betsy Key, Dump Key, and Rabbit Key fit over time for each site and season with a 2-parameter exponential decay model. 116

Figure 3.7. Proportional loss of root biomass deployed at each site in litterbags at Black Betsy Key, Dump Key, and Rabbit Key fit over time for each site and season with a 2-parameter exponential decay model 117

Figure 3.8. Proportional loss of senescent rhizome biomass (mean ± SE; n = 3) deployed at each site in litterbags at Black Betsy Key, Dump Key, and Rabbit Key fit over time for each site and season with a 2-parameter exponential decay model 118

Figure 3.9. Proportion of original N remaining (N_t/N_0) over time for all tissue types following winter and summer deployment at Black Betsy Key, Dump Key, and Rabbit Key 120

Figure 3.10. Proportion of original P remaining (P_t/P_0) over time for all tissue types following winter and summer deployment at Black Betsy Key, Dump Key, and Rabbit Key 121

Figure 3.11. Nutrient standing stocks and fluxes into the water column and sediment from *Thalassia testudinum* above- and below-ground tissue in western, northcentral, and eastern Florida Bay.....125

Chapter 4. THE POTENTIAL ROLE OF METABOLIC OXIDATION AND SEDIMENT DISSOLUTION IN RELEASING PHOSPHORUS FROM CARBONATE SEAGRASS SEDIMENTS IN FL BAY.

Figure 4.1. Study sites where sediment was collected for sulfate reduction, acid dissolution, and ^{33}P radiotracer experiments 138

Figure 4.2. Efflux of inorganic P, fluoride and Ca^{2+} into the seawater sediment slurry as a function of decreasing pH exposed to 3 different acidification treatments 145

Figure 4.3. Total P and F recovered from the soluble (seawater) and exchangeable (HCl and BD extractable) pools after dissolution with sulfuric acid comparing eastern and western bay sites 147

Figure 4.4. Relationship between sulfuric acid additions and release of inorganic P, fluoride and Ca^{2+} into the seawater sediment slurry (soluble phase) normalized to per g dw^{-1} 149

Figure 4.5. Changes in the ^{33}P radioactivity over time in the aqueous phase of the sediment slurry over time using sediment from eastern and western bay 151

Figure 4.6. Depth profiles of microbial sulfate reduction rates incubated at in situ temperatures in intact sediment cores October 2005 and July 2006 from western and eastern Florida Bay 153

LIST OF TABLES

Chapter 1. INORGANIC PHOSPHORUS UPTAKE IN A CARBONATE-DOMINATED SEAGRASS ECOSYSTEM-FLORIDA BAY

Table 1.1. Inorganic N and P concentrations, molar ratios, and physical parameters in the surface waters at three study sites during field experiments.....31

Table 1.2. Test of P*i* rate constants (S_p) in large and small chambers.....32

Table. 1.3. Seasonal apparent first order P*i* rate constants (S_p) from study sites 33

Table. 1.4. Three-way ANOVA results on ranked data for the apparent first order P*i* rate constant (S_p).....34

Table. 1.5. Seasonal inorganic P uptake kinetic parameter C_0, the P*i* concentration where net uptake is zero, from study sites.....38

Table. 1.6. Chlorophyll a (chl.a) and phytoplankton group percentages in the community predicted based on accessory pigment data 39

Chapter 2. ALKALINE PHOSPHATASE ACTIVITY OF SEAGRASS AND WATER COLUMN FRACTIONS IN FLORIDA BAY

Table 2.1. Seasonal APA at 2 µmol L^{-1} MUF-P in the water column with sequential size fractions.....60

Table 2.2. Seasonal salinity, temperature, pH, total phosphorus, total dissolved phosphorus, inorganic soluble reactive phosphorus and phospho-monoester concentrations 61

Table 2.3. Water column chlorophyll a and phytoplankton group dominance based on chemotaxonomy.....64

Table 2.4. Percent (%) APA contribution to total APA (at 2 µmol L^{-1} MUF-P) in the water column by each size fraction averaged across seasons 65

Table 2.5. Seasonal alkaline phosphatase enzyme hydrolysis kinetic parameter, V_{max} (µmol P L^{-1} h^{-1}) 68-69

Table 2.6. Soluble reactive phosphorus and phosphomonoester concentrations measured at Florida Bay long-term monitoring sites 70-71

Table 2.7. Literature comparisons of APA in marine ecosystems comparing reported activities from a) south Florida estuaries, b) other estuarine/shelf systems, and c) open ocean systems 73-74

Chapter 3. SEAGRASS (*THALASSIA TESTUDINUM*) NUTRIENT RECYCLING IN FLORIDA BAY, A CARBONATE-DOMINATED SHALLOW ESTUARY

Table 3.1. Decline in *Thalassia testudinum* total phosphorus (TP) and total nitrogen (TN) from yellowing to decomposing tissue on the same senescent leaves at three sites across Florida Bay. 107

Table 3.2. *Thalassia testudinum* leaf biomass, total phosphorus, and total nitrogen production at three study sites in the bay 108

Table 3.3. Seasonal differences in total nitrogen and phosphorus concentration and molar ratios of carbon, nitrogen, and phosphorus in newly fully emergent and senescent leaves 111

Table 3.4. Net production and respiration at each study site 113

Table 3.5. Decay rate constants (k ± SE) for loss of plant tissue biomass and total mass of P (TMP) and N (TMN) over time 115

Chapter 4. THE POTENTIAL ROLE OF METABOLIC OXIDATION AND SEDIMENT DISSOLUTION IN RELEASING PHOSPHORUS FROM CARBONATE SEAGRASS SEDIMENTS IN FL BAY.

Table 4.1. Sediment total inorganic Ca, F and TP*i*, and total P, molar ratios of fluoride to calcium and inorganic P to calcium and fluoride, and bulk density, porosity, and % sediment < 60 µm. 144

Table. 4.2. Soluble reactive phosphorus (ΔP*i*), fluoride (ΔF^-), and calcium (ΔCa^{2+}) mobilized in seawater (SW) after acidification treatments (150, 400, and 800 µmol H_2SO_4) and ΔSRP and ΔF^- re-adsorbed but recovered in specific

sequential extracts with $MgCl_2$ (loosely adsorbed) and BD (strongly adsorbed). 146

Table. 4.3. Ratios between P*i*, F^-, and Ca^{2+} mobilized after sulfuric acid additions. 150

Table 4.4. Distribution of ^{33}P in various P-pools as a function of time following addition of trace amounts of $^{33}PO_4^{3-}$ to sediment slurries from the western and northeastern Florida Bay sites 152

Table 4.5. Seasonal variations in sulfate reduction rates (SRR) integrated to14 cm depth and mean SRR normalized to sediment volume 154

ACKNOWLEDGEMENTS

This work was initiated to support the development of water quality and seagrass ecosystem models being applied to the management of Florida Bay, a critical ecosystem component of the Greater Everglades Complex. We appreciate this funding opportunity leading to an increased understanding of nutrient cycling in the Bay. This research was funded by the Critical Ecosystem Studies Initiative (CESI) program of the U.S. Department of Interior (DOI) through Everglades National Park (ENP; Cooperative Agreement H5000 02 0409, #J5284 05 0047). This work is a continuation of work initiated under a National Oceanic and Atmospheric Administration Coastal Ocean Program grant NA160P2547 and supplemented by the Danish Natural Science Research Council grant 21030013/21040034. Florida Institute of Oceanography provided logistical support for ship time on the R.V. Bellow for our P uptake work on the Little Bahama Bank. We thank Dr. Louda at FAU for chemotaxonomy and chl a analyses. We also appreciate the logistical field support provided by ENP through the Florida Bay Science Center at the Key Largo Ranger Station and the Florida Institute of Oceanography's (FIO) Keys Marine Lab facilities. Graduate and undergraduate students and research associates from the aquatic plant ecology lab at FAU are also recognized for their assistance in the research presented in this report in particular Ms. Stephanie Schopmeyer, Rosanna Tursi, and Connor Irwin. Discussions on AP kinetics and organic P analyses with Drs. Joe Boyer, Phil Monbet, Susan Newman, Ed Proffitt, Carlos Coronado and Gregg Fields assisted in this research project and to whom we are grateful for their time. Data by Boyer, 2006 was provided by the SERC-FIU Water Quality Monitoring Network which is supported by SFWMD/SERC Cooperative Agreement #C-15397 as well as EPA Agreement #X994621-94-0. We also thank Steve Kelly at the South Florida Water Management District for funding tissue nutrient analyses in our decomposition study.

CHAPTER 1

INORGANIC PHOSPHORUS UPTAKE IN A CARBONATE-DOMINATED SEAGRASS ECOSYSTEM-FLORIDA BAY

1.0. Introduction

Tropical and subtropical estuaries with autochthonous internal sediment generation are dominated by fine carbonate particles that efficiently sequester inorganic phosphorus (P*i*) (Howarth 1988; McGlathery et al. 1994; Jensen et al. 1998; Koch et al. 2001). This capacity to readily bind P*i* into solid phase pools, such as fluoroapatite (Kitano et al. 1978), and low terrestrial P loads has led to P limitation of tropical seagrass production (Powell et al. 1989; Short et al. 1990; Fourqurean et al. 1992a,b). Nevertheless, P cycling in these carbonate-dominated ecosystems is not well understood. While P*i* uptake has been examined on coral reef flats (Atkinson 1987; Bilger and Atkinson 1995; Steven and Atkinson 2003), to date little information is available on P uptake kinetics in carbonate-dominated seagrass ecosystems with the exception of a few studies focused on the water column (Cotner et al. 2000; Glibert et al. 2004; Thingstad et al. 2005). Partitioning of P uptake among the various components of a seagrass system, including the water column, seagrass and sediment has not been elucidated.

Isotherm experiments with calcite and aragonite (de Kanel and Morse 1978; Kitano et al. 1978; Millero et al. 2001) and field carbonate sediments in suspension (Nielsen et al. 2006) indicate a high capacity for carbonate sediments to sequester P*i*. However, picoplankton, principally cyanobacteria and bacteria in tropical oligotrophic marine environments, take up P*i* at nanomolar levels (Phlips et al. 1999; Cotner et al. 2000; Glibert et al. 2004; Thingstad et al. 2005), suggesting that the water column biota can efficiently compete for labile P with carbonate particles suspended in the water and/or at the sediment-water interface. In addition, seagrass leaves have been shown to take up P*i* at nanomolar concentrations (Nielsen et al. 2006) on par with microorganisms (Currie and Kalff 1984; Falkner et al. 1989).

In this study, we develop P*i* uptake kinetic parameters for the water column, sediment, and the entire "system" (water column + sediment + seagrass) of carbonate seagrass ecosystems with very low P*i* concentrations. Small chambers were used to isolate the various components of the system and detect small differences in concentration at low ambient P*i* levels. Kinetics were established in Florida Bay (FB), a carbonate seagrass-dominated estuary, over several seasons and across an established nutrient gradient (Fourqurean et al. 1992a,b; Zhang et al. 2004). We hypothesized that fine sediments in the eastern bay would rapidly sequester P*i* and dominate P*i* uptake in the system, while low chl a in this region of the bay (Phlips et al. 1999) would limit water column uptake. We also hypothesized that P*i* uptake rates would be low in the western bay which receives a relatively higher P load from the Gulf of Mexico (Boyer et al. 1997; Rudnick et al. 1999) resulting in P-enriched sediments, relative to the eastern bay (Zhang et al. 2004). In this study, we also compared FB P*i* uptake kinetics to those measured on the Little Bahama Bank (LBB), a highly oligotrophic site remote from anthropogenic nutrient sources, particularly in the bank interior. FB and the LBB support extensive seagrass meadows dominated by the tropical seagrass *Thalassia testudinum*. Water column biotic and abiotic fractions responsible for P*i* sequestration were also discriminated when we examined the mechanism of water column uptake in FB. In summary, we present a conceptual model illustrating P uptake and cycling in a carbonate seagrass-dominated estuary, using FB as a case study.

1.1. Methods

1.1.1. Study Area

P*i* uptake experiments were conducted both seasonally and inter-annually (2003-2006) at 5 sites in FB, a shallow (< 3 m) semi-enclosed carbonate estuarine lagoon (~2,000 km^2) at the southern tip of the Florida peninsula (Fig. 1.1). P*i* uptake kinetics were also determined shipboard on a cruise (June 6-9, 2004 onboard the RV Bellows) along three transects on the LBB, a highly oligotrophic shallow (<20 m) carbonate bank situated north of Grand Bahama Island (Fig. 1.1). In FB, *T. testudinum* biomass and primary production decrease from the western to the eastern regions as a consequence of decreasing P availability, evidenced by sediment P concentrations (Zhang et al 2004), sediment P isotherms (Nielsen et al. 2006) and leaf C:P stoichiometry (Fourqurean et al. 1992a, b). The bay sites chosen for this study (Fig. 1.1a) encompass this nutrient gradient with sites in the western bay, Green Mangrove Key (GMK; 24°55'20"N/80°47'33"W) and Rabbit Key (RK; 24°58'50"N/80°50'11"W), in the eastern bay, Eagle Key (25°09'30"N/80°34'59"W) and Black Betsy Key (BLBK; 25°08'23"N/80°38'51"W), and in the central bay, Dump Key (DK; 25°06'40"N/80°46'15"W).

On the LBB (Fig. 1.1b), the first site on transect one (T_1) was located close to the western edge of the bank, while sites on transect two (T_2) and three (T_3) were located in the bank interior. These sites were also dominated by *T. testudinum* and represent a P trophic gradient based on leaf tissue molar C:P stoichiometry (1097, 1161, and 1361, respectively; Koch unpublished data), although C:P ratios suggest all bank sites have low P availability.

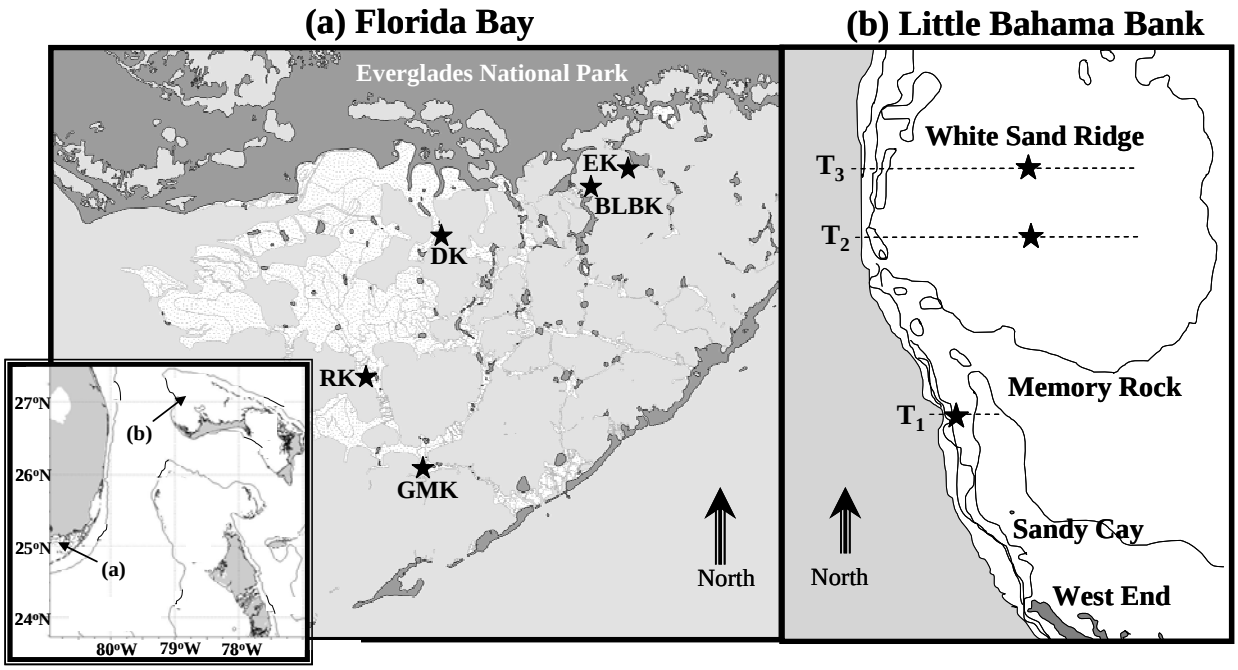

Figure 1.1. The lower left insert shows the location of our study areas (a) Florida Bay at the terminus of the south Florida peninsula and (b) the Little Bahama Bank to the north of Grand Bahama Island. The large left panel (a) identifies the five field sites in Florida Bay where in situ P*i* uptake kinetics were determined, Rabbit Key (RK) and Green Mangrove Key (GMK) along the southwestern edge of the bay bordering the Gulf of Mexico, Dump Key (DK) in the central bay, and Black Betsy Key (BLBK) and Eagle Key (EK) in the northeastern region of the bay. The right panel (b) identifies the Little Bahama Bank depicting the three cruise transects just north of Grand Bahama Island with stars depicting site locations where seagrass cores and ambient seawater was collected for shipboard P*i* uptake incubations.

1.1.2. Pi Uptake Experiments

Inorganic P kinetics were determined for three components of the ecosystem (water column, water column + sediment, and water column + sediment + seagrass) at GMK and EK in July, October, February, April of 2003-04 and at BLBK, DK, and RK in May, August, December, February of 2005-06. P*i* kinetics were determined in situ by measuring P*i* uptake until exhaustion from low-volume transparent Plexiglas chambers designed with internal baffles to

promote turbulent flow. An istotopic ^{33}P tracer approach was considered (Nielsen et al. 2006), but not employed due to concerns of isotope exchange with carbonate sediments and epiphytes. Benthic chambers (3.1 cm diameter X 15 cm height, 0.344 L internal volume including tubing) were pushed approximately 7 cm into the sediment on either bare bottom or in seagrass beds, enabling discrimination of P*i* uptake between the sediment+water column and the system (sediment+seagrass+water column). Each system chamber contained one or two shoots of *T. testudinum* (0.13 – 0.34 g dw). Uptake rates of P*i* in the water column were determined using a chamber that was closed at both ends (3.1 cm diameter X 31 cm height, 0.455 ml internal volume including tubing). Once field deployed, the chambers were connected via tubing to a high precision digitally controlled peristaltic pump located on the deck of the boat. The flow velocity inside the chambers was set to create a well-mixed water phase without disturbance to the sediment surface (personal observation) providing a chamber water turnover time of 0.43 min^{-1} and a turbulent flow rate of 0.33 cm s^{-1}.

Once the chambers were deployed, inlet tubing was placed in ambient water from the site spiked to 0.5-1.0 µmol L^{-1} PO_4^{3-} during 2003-04. Rate parameters did not change using spikes of 0.5 or 1.0 µmol L^{-1} PO_4^{3-}; therefore, the following year a spike of 0.8 µmol L^{-1} PO_4^{3-} was used. In August, 2005 a phytoplankton bloom was present at DK, resulting in sequestration of the 0.8 µmol L^{-1} PO_4^{3-} spike during the initial introduction period. Because this bloom persisted through our December 2005 and February 2006 sampling events, we increased the spike to 1.5-2.0 µmol L^{-1} PO_4^{3-}.

During chamber runs, P*i* spiked water was pumped through the chambers for 15 min allowing turnover of the water ~6.5 times. After which, the chamber was closed and sampling initiated. Samples (10 mL) were taken at 5-10 min intervals for the first 40 min and then 10-20

min intervals up to 120 min. As water sample were slowly taken from the chamber, 10 mL of in situ water was injected into the chamber at the same rate to maintain consistent chamber volume and pressure. Subsamples (5 mL) were filtered through GF/F filters, acidified (200 µl 0.4 M H_2SO_4 per sample), put on ice and brought back to the laboratory for analysis. Upon arrival to the lab, samples were frozen until analysis for P*i* (<7 d). Nitrate+nitrite (NO_x) and ammonium (NH_4^+) uptake rates were determined in 2003-04. After chamber incubations, seagrass tissue in the chamber was collected and the chambers were moved to an adjacent area within the same seagrass bed (radius 2-3 m).

Nutrient uptake experiments on the Little Bahama Bank were conducted shipboard because of depth (at some sites >10 m) and time constraints on the 5 day cruise. Four sediment cores (15 cm diameter X 20 cm height) from each site were collected by scuba divers and immediately placed in tanks with water from the site. An external flow-through water bath was used to maintain ambient temperature. Incubation chambers were placed in the center of the cores to avoid edge effects and incubations run as described above.

1.1.3. Chamber tests

Prior to the experiments, incubation chambers were tested for mixing efficiency and wall effects, as well as compared to larger chamber systems. To test the chambers for mixing efficiency, 10 mL of dye was injected into the closed system and followed spectrophotometrically over time in a water column experiment. Results showed that the water uniformly mixed after <2 min. To test for P*i* adsorption to the chamber walls a time course experiment was conducted. Closed chambers were filled with artificial seawater spiked to 0.5 and 1.0 µmol L^{-1} PO_4^{3-} and P*i* concentrations were followed for 120 min (Fig. 1.2). The

experiment showed no chamber wall adsorption as the losses of P*i* over time were accounted for by dilution with artificial seawater added as samples were taken. Finally, tests were run to compare uptake kinetic parameters S_p, the apparent first order rate constant, and C_0, the P*i* level where uptake is zero, in small (0.344 L, area 7.5 cm^2) and large volume chambers (6.2 L, area 301 cm^2). The advantages of using small volume chambers for kinetic experiments were faster mixing rates with lower flow rates limiting resuspension of fine carbonate sediments and low volume to seagrass biomass ratio, which facilitated discrimination between plant and sediment/water column P*i* uptake. Parallel incubations with small and large benthic chambers were performed at BLBK in August 2004 with the two chambers placed next to each other. The incubation was performed as described above with 5 replicates for each component. The kinetic parameters were calculated after correcting for dilution and water column uptake.

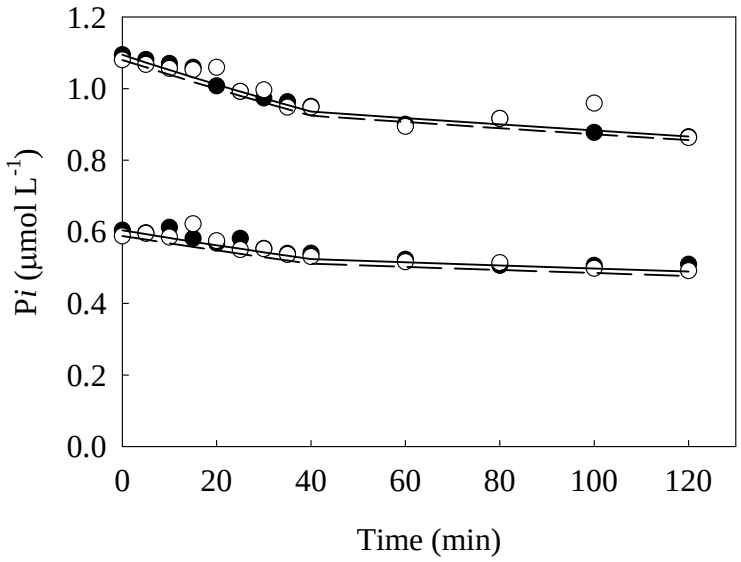

Figure 1.2. P*i* disappearance during chamber incubations filled with artificial seawater spiked with 0.5 µmol L^{-1} and 1.0 µmol L^{-1} PO_4^{3-}. Symbols represent measured values while lines are the theoretical disappearance of P*i* when corrected for dilution when sampling and replacing sampled water with non-spiked seawater. Open and closed symbols represent replicate runs at each spike level.

1.1.4. Water column P fractions

To account for P*i* sequestered by the water column biota, P uptake was fractionated by size class and the abiotic fraction elucidated by acid dissolution. During these tests, the water column biota was determined via chemotaxonomy. P*i* taken up from the spiked amendment at three sites (RK, DK, BLBK) was traced during December 2005 and February 2006. Post-incubation water was collected from chambers and ambient non-spiked water from the site (n=4). The water was divided into an unfiltered and a filtered (0.7 μm GF/F) fraction. A similar size fraction (<0.8 μm) was confirmed by microscopy to be composed primarily of bacteria in the bay (Cotner et al. 2000). The GF/F filters and the unfiltered water were kept on ice once collected and analyzed for total P. Subsamples of the filtered and unfiltered water were acidified to pH 2-3 (0.4 mmol L^{-1} H_2SO_4) and P*i* measured. P*i* was also measured in filtered and nonfiltered ambient water and chamber water samples. These data were used to operationally define three water column fractions of the added P*i* after correcting for ambient TP and P*i*: (1) phytoplankton, >0.7 μm, (2) Calcium-bound or adsorbed, >0.7 μm acidified, (3) micro-heterotrophs and picoplankton, <0.7 μm. The fractions were calculated according to the following equations:

(1) $\Delta P_{(>0.7)} = TP_{cF} - TP_{aF} - (2)$

(2) $\Delta P_{(>0.7+acid)} = (P_{cNA} - P_{cN}) - (P_{aNA} - P_{aN}) - (P_{csA} - P_{cs}) - (P_{asA} - P_{as})$

(3) $\Delta P_{(<0.7+acid)} = P_{spike} - (1) - (2)$

where: c=chamber, a=ambient, F = on filter, s=supernatant, N = not filtered, A = acidified, spike = P*i* added to chamber.

Although partitioning of P was examined in the water column at all three sites, P*i* uptake rates and phytoplankton concentrations at RK were both below detectable limits during the 2 sampling events in December, 2005 and February, 2006.

1.1.5. Nutrient Analyses

Soluble reactive phosphate (P*i*) was analyzed colorimetrically using ammonium molybdate and antimony potassium tartrate under acid conditions on an autoanalyzer (Technicon AAIII; Koroleff 1983) with a 20 nmol L^{-1} limit of detection. Total and dissolved organic P was converted to P*i* using dry oxidation according to Monaghan and Ruttenberg (1999). NO_x was measured as nitrite after reduction by a Cd-column according to the standard colorimetric sulfanilamide-naphthylene-diamine method (Grasshoff 1983a,b). Ammonium was also measured spectrophotometrically using sodium nitroprusside and salicylate in weak alkali solution (Bower and Holm-Hansen 1980). Inorganic N concentrations and uptake kinetics were only determined at GMK and EK during 2003-2004 because no net change in concentration was found during incubations.

1.1.6. Chemotaxonomy

Water samples for chemotaxonomy were collected in dark plastic bottles and placed on ice in the field. Lipophilic pigments, chlorophylls and carotenoids were separated using reverse-phase HPLC as described in Louda et al. (2002) and classified into 5 groups: diatoms, cyanobacteria, dinoflagellates, greens, and cryptophytes; however, no greens or cryptophytes were detected in any samples, thus are omitted from results.

1.1.7. Parameter Estimates and Statistics

Chamber P*i* uptake rates over time were modelled using a first-order rate constant (k) defined as $C = C_0 + ae^{-(kt)}$ where a is a constant, t is time and C_0 is the asymptotic value where no changes in concentration (C) with time is observed. For each experimental run, *k* was estimated by non-linear exponential regression. For comparison among runs, *k* was normalized to water volume (V) and the planar area of the sediment (A) and expressed as the apparent first-order rate constant for P*i*, S_p (= *k*V/A). During runs where initial uptake rates were slow and there was not a clear distinction of the asymptotic value (C_0) after 120 min, estimates of C_0 were either over- or under-estimated depending on the interpolation. In cases where C_0 was negative, values were omitted from further calculations, while overestimated C_0 values were kept, as we had no criteria to discriminate overestimated values from actual values. Thus, estimates of C_0 reported herein may be slightly overestimated.

Non-linear exponential decay regressions were performed using SigmaPlot (v9.1). The resulting P*i* uptake rate constants (S_p) were ranked, because of data non-normality, and compared using a 3-way ANOVA (site x month x ecosystem component) for data collected in 2003-2004 and 2005-2006 at EK/GMK and BLBK/RK, respectively (SAS v9.1). Multiple mean comparisons within main effects were performed using the Tukey Test with all significant differences reported at the $p < 0.05$ level (SAS v9.1). Comparisons between small and large chambers were made using a t-test (SigmaStat v3.1). Because of limited data sets, statistical comparisons of C_0 within Florida Bay, as well as comparisons of C_0 and S_p between FB and the LBB were made only in a qualitative manner.

1.2. Results

1.2.1. Pi Uptake Kinetics

In the majority of chamber experiments, P*i* concentration with time fit an exponential decay model ($R^2 > 0.92$), demonstrating that P*i* uptake is a linear function of concentration at low P*i* levels in FB and on the LBB across a range of salinity and temperature regimes (Table 1.1). There was always a net uptake of P*i* from the various ecosystem components using P*i* spikes ≤ 2.0 μmol L^{-1} (2.0, 1.5, 1.0, 0.8, or 0.5 μmol L^{-1}). In non-spiked controls, no net release of P*i* was detectable, indicating a high P*i* affinity in these carbonate systems.

Although we found rapid uptake of P*i* amended to surface waters in the bay, during incubations at GMK and EK (2003-04) with no N*i* spike dissolved inorganic nitrogen (N*i*) flux was not significantly different from zero (1 sided t-test, $p < 0.05$, data not shown). The fact that no net uptake of N*i* was found in benthic chambers could have been the result of high porewater NH_4^+ in bay sediments (range 6 to 2,400 μmol L^{-1}, median = 79); however, N*i* in the water column chambers did not change either during 120 min incubations. Nitrogen availability in the water column, evidenced by high NH_4^+ concentrations (0.6-3.3 μmol L^{-1}) and N*i*:P*i* ratios >10 may have influenced N*i* uptake rates. Longer-term incubations or N*i* spikes would probably be required to elucidated N*i* dynamics, but was not within the scope of the present study.

1.2.2. Pi uptake rate constant (S_p)

Chamber tests showed no significant difference in the system kinetic parameters S_p and C_0 between the large and small chambers, respectively, supporting the data presented herein (Table 1.2). Based on seasonal chamber P*i* uptake experiments in FB, S_p for the system was between 0 and 367 x 10^{-6} m s^{-1} for western bay sites and 115 to 661 x 10^{-6} m s^{-1} for eastern bay sites,

Table 1. Inorganic P concentrations (P*i*) and physical parameters at Green Mangrove Key (GMK), Eagle Key (EK), Rabbit Key (RK) and Dump Key (DK) in Florida Bay, and on the Little Bahamas Bank (LBB) at the time nutrient uptake experiments were conducted (n=4, ±STDEV).

Site Date	P*i* (μmol L^{-1})	Salinity (psu)	Temp (^{o}C)
Florida Bay (2003-2004)			
GMK			
July	0.108 ± 0.039	31	29.8
Oct	0.170 ± 0.028	34	25.4
Feb	0.076 ± 0.043	34	22.0
Apr	0.053 ± 0.020	38	24.3
EK			
Jul	0.116 ± 0.025	25	32.6
Oct	0.048 ± 0.019	20	24.4
Feb	0.030 ± 0.016	18	23.2
Apr	0.020 ± 0.020	28	26.5
Florida Bay (2005-2006)			
RK			
May	0.045 ± 0.015	41	25.7
Aug	0.068 ± 0.005	44	33.0
Dec	0.029 ± 0.027	32	20.6
Feb	<0.020	34	24.5
DK			
May	0.087 ± 0.009	48	27.0
Aug	nd	48	32.8
Dec	0.087 ±0.020	31	20.1
Feb	<0.020	37	24.0
BLBK			
May	0.093 ± 0.021	47	27.4
Aug	0.014 ± 0.024	34	32.0
Dec	0.177 ± 0.027	19	19.3
Feb	<0.020	27	25.4
Little Bahama Bank-June 2004			
T1	<0.020	37	27.6
T2	<0.020	37	29.2
T3	<0.020	40	29.2

Table 1.2. Apparent first order P*i* rate constants (S_p) and the P*i* concentration where net uptake is zero (C_0) for sediment and sediment + seagrass components, using large (LC, 6.5 L) and small (SC, 0.344 L) chambers deployed at Black Betsy Key in Florida Bay. Values represent mean ± SE (n=5).

	S_p (x 10^{-6} m s^{-1})		C_0 (nmol P*i* L^{-1})	
System component	LC	SC	LC	SC
Sediment	154±38	170±61	19±6.5	25±7.7
Sediment + seagrass	228±36	288±82	39±7.1	36±7.7

averaging (±SE) 171±50 and 272±66 x 10^{-6} m s^{-1}, respectively (Table 1.3). Applying these average P*i* system rate constants and the range of P*i* concentrations measured in situ (0.02 to 0.177 µmol P*i* L^{-1}; Table 1.1), we calculated system P*i* uptake rates ranging from 0.30 to 2.62 mmol P*i* m^{-2} d^{-1} at western bay sites and 0.47 to 4.16 mmol P*i* m^{-2} d^{-1} at eastern bay sites (S_p m s^{-1} X min and max water column P*i* mmol L^{-1} X 86,400 s d^{-1} X 1,000 L m^{-3}).

These results suggest a higher average P*i* uptake in the eastern versus western bay sites; however, natural seasonal and inter-annual variance in the system tempers this conclusion. For example, during 2003-2004 no significant site differences were found in S_p between eastern (EK) and western (GMK) sites, while in 2005-2006 there was a significantly higher P*i* uptake rate at the eastern bay site (BLBK, Table 1.4). The low average rate of P*i* uptake at RK in 2005-2006 was highly influenced by no P*i* uptake recorded during Dec and Feb in both the water column and sediment components, reflected in the significant season and component interactive terms in the 3-way ANOVA (Table 1.4).

Table 1.3. Apparent first order P*i* rate constants (S_p) for chambers deployed in Florida Bay at Green Mangrove Key (GMK), Eagle Key (EK), Rabbit Key (RK), Dump Key (DK), and on the Little Bahamas Bank (LBB). S_p, normalized to water volume and the planar area of the sediment, are presented for chambers with the system (water column + sediment + seagrass), sediment (water column + sediment), and water column alone. Means are presented with ± SE (n≥4). Numbers in parentheses represent % contribution of water column, sediment, and seagrass consortium to total rate for each month sampled.

S_p (x 10^{-6} m s^{-1})

Florida Bay 2003-04

	Western Bay (GMK)			Eastern Bay (EK)		
	Water	Sediment	System	Water	Sediment	System
Jul	73±7 (31)	94±17 (9)	231±30 (60)	104±38 (76)	111±28 (5)	137±31 (18)
Oct	463±92	475±192	-	167±28 (42)	211±37 (11)	397±67 (47)
Feb	101±23 (81)	117±15 (13)	125±20 (6)	78±19 (48)	158±31 (50)	162±29 (2)
Apr	99±25 (32)	121±40 (7)	313±50 (61)	51±26 (15)	298±84 (73)	337±95 (12)

Florida Bay 2005-06

	Western Bay (RK)			Central Bay (DK)			Eastern Bay (BLBK)		
	Water	Sediment	System	Water	Sediment	System	Water	Sediment	System
May	41±14 (73)	51±25 (18)	57±7 (10)	55±12 (39)	108±21 (38)	141±13 (23)	58±28 (41)	87±14 (21)	140±21 (38)
Aug	37±16 (10)	263±58 (62)	367±31 (28)	>2,800 (100)	>2,800 (0)	>2,800 (0)	257±39 (39)	427±61 (26)	661±132 (35)
Dec	0 (0)	0 (0)	32±16 (100)	>2,800 (100)	>2,800 (0)	>2,800 (0)	148±24 (66)	161±25 (6)	224±26 (28)
Feb	0 (0)	0 (0)	75±37 (100)	991±36 (98)	892±44 (0)	1,007±31 (2)	45±12 (39)	73±29 (24)	115±18 (37)

Little Bahama Bank 2004

	Bank Edge			Bank Interior		
	Water	Sediment	System	Water	Sediment	System
Jun T1	237 (100)	126±38 (0)	128±3 (0)			
Jun T2				573±8 (100)	317±80 (0)	380±90 (0)
Jun T3				881±150 (94)	940±182 (6)	769±152 (0)

(-) = missing data.

Table 1.4. Three-way ANOVA results on ranked data for the apparent first order P*i* rate constant (S_p) compared between months, ecosystem components, and eastern versus western sites in Florida Bay (a) 2003-2004 (Green Mangrove Key [GMK] vs Eagle Key [EK]) and (b) 2005-2006 (Rabbit Key [RK] vs Black Betsy Key [BLBK]). Significant differences of means within main effects are designated by different letter superscripts (Tukey Kramer, SAS v.9.1). Data from October (2003-04) were precluded from 3-way analyses as the system chamber data were not available.

(a) Florida Bay (EK & GMK) 2003-2004

Source of Variation	DF	SS	MS	F	*P*
Site (EK[a], BMK[a])	1	<1	<1	<0.01	0.98
Month (Jul[a], Feb[a], Apr[a])	2	1884	942	1.01	0.37
Component (Wat[a], Sed[b], Sys[c])	2	28077	14039	15.04	<0.01
Site x Month	2	451	225	0.24	0.79
Site x Component	2	3969	1985	2.13	0.13
Month x Component	4	6089	1522	1.63	0.17
Site x Month x Component	4	4443	1111	1.19	0.32

(a) Florida Bay (RK & BLBK) 2005-2006

Source of Variation	DF	SS	MS	F	*P*
Site (RK[a], BLBK[b])	1	20534	20534	172.15	<0.01
Month (May[a], Aug[b], Dec[a], Feb[c])	2	27643	9214	77.25	<0.01
Component (Wat[a], Sed[b], Sys[c])	2	9619	4810	40.32	<0.01
Site x Month	2	5080	1693	14.20	<0.01
Site x Component	2	455	228	1.91	0.16
Month x Component	4	2953	492	4.13	<0.01
Site x Month x Component	4	2854	476	3.99	<0.01

The lowest uptake rate across seasons was found in February during both years studied, with the exception of DK which experienced algal blooms in the winter (Table 1.3). S_p was significantly lower in February compared to spring values measured in May 2005-2006 (Table 1.4). While the inter-annual P*i* rate constant was inconsistent between sites and among seasons, there was a notable pattern that emerged across seagrass ecosystem components. During non-bloom conditions, S_p of the system was significantly higher than the water and water + sediment alone for all years and sites in FB (Table 1.4). S_p increased in the order of system > water + sediment > water (Table 1.4, Fig. 1.3).

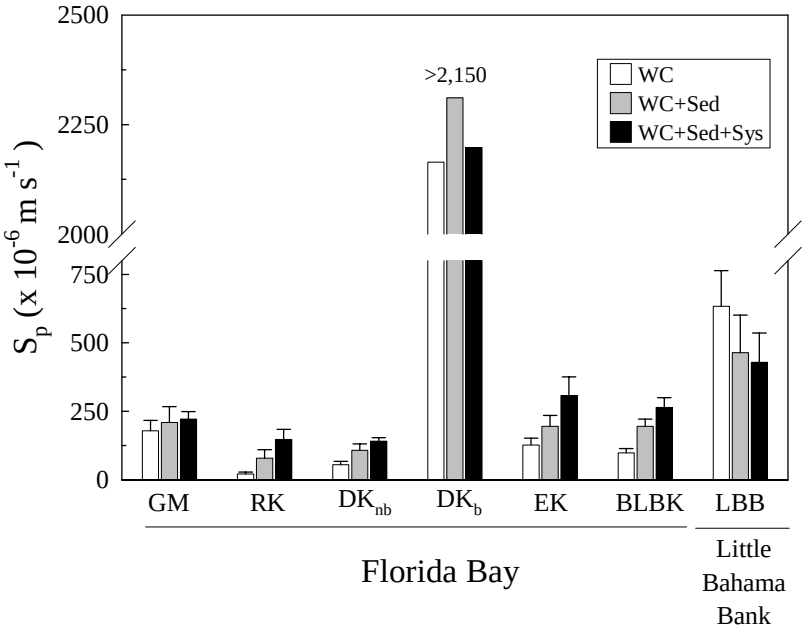

Figure 1.3. Average P*i* rate constants, S_p, for seagrass ecosystem components water column (WC), water column + sediment (WC+Sed) and system (WC+Sed+Sys) in Florida Bay and on the Little Bahama Bank. In Florida Bay, Green Mangrove Key (GMK) and Rabbit Key (RK) are western bay sites, Dump Key (DK) a central bay site, and Black Betsy Key (BLBK) and Eagle Key (EK) eastern bay sites. Dump Key S_p are given for non-bloom (DK_{nb}) and bloom (DK_b) conditions; note scale change. Averages ±SE are shown using all chamber runs for Florida Bay sites (n=15-30) with the exception of DK where DK_b n=12 and DK_{nb} n=4. On the Little Bahama Bank, the 9 replicate runs were averaged for each system component on a cruise June, 2004.

The lack of a clear increase in S_p as a function of increasing seagrass biomass (Fig. 1.3), which was higher in the chambers at western (0.29-0.34 g dw per chamber) than eastern (0.13-0.29 g dw per chamber) bay sites, suggests that small stature seagrass with their associated epiphytes may at times be important for P*i* uptake. Further, the P-limited status of the eastern bay plant-epiphyte complex, while lower in stature, and thereby surface area, may more efficiently sequester P*i*. Based on S_p, the proportion of the total system P*i* uptake (calculated above) by the seagrass-epiphyte consortium is ~27% in the eastern bay and ~52% in the western bay or 0.13 to 1.12 and 0.15 to 1.36 mmol P*i* m^{-2} d^{-1}, respectively. Normalizing these rates to seagrass biomass

from chambers in eastern (100 g m^{-2}) and western (300 g m^{-2}) sites, the mass specific uptake rate is between 0.05 to 0.47 µmol P $gdwt^{-1}$ h^{-1} and 0.02 to 0.19 µmol P $gdwt^{-1}$ h^{-1}, respectively (mmol P*i* m^{-2} d^{-1} X 1,000 µmol $mmol^{-1}$ X d 24 h^{-1} X m^2 g^{-1}).

Even though S_p was consistently higher with the contribution of the seagrass component, this was not the case on the highly oligotrophic LBB (Fig. 1.3, Table 1.3). The S_p was highest in the water column and always dominated (≥94%) P*i* uptake in the system (Table 1.3, Fig. 1.3). In fact, P*i* uptake rates were lower on average with the addition of the sediment and seagrass components, indicating a greater net efflux. Average S_p for the water column in the interior bank sites was higher than found in FB, while on the bank edge, rate constants were comparable to the bay during non-bloom conditions (Table 1.3).

During phytoplankton blooms (chl a >2 µg L^{-1}) in FB, the water column completely dominated P*i* uptake and the calculated first order rate constants were the highest found in the bay or on the bank (Fig. 1.3, Table 1.3). During the spring and summer of 2005, hot and dry conditions combined with an exceptionally active hurricane season (major tidal surge in the bay) promoted and extended a phytoplankton bloom from late summer and fall 2005, through our February 2006 sampling. In August 2005 and December 2006, the P*i* uptake was so rapid that it could not be modelled, as all the P*i* was taken up during the initial spike introduction phase of the incubation. Because of this rapid rate of P*i* uptake, only a minimum rate constant could be estimated from the DK site for these two sampling periods. This estimate of S_p was an order of magnitude higher (>2,800 x 10^{-6} m s^{-1}) than during non-bloom conditions (Table 1.3). A phytoplankton bloom was also apparent in August at BLBK, increasing the water column P*i* uptake rate constant 2 to 4-fold from previous samplings (Table 1.3).

In the absence of phytoplankton blooms, we calculated P*i* uptake rates of 17 to 149 µmol m^{-3} h^{-1} using in situ P*i* levels found in the bay during this study, 0.02 to 0.177 µmol P*i* L^{-1} and the average seasonal water column rate constant of 108 x 10^{-6} m s^{-1} (S_p m s^{-1} X 3,600 s h^{-1} X µmol P*i* L^{-1} X 1,000 L m^{-3} X 0.445 m^{-1}).

1.2.3. Threshold for Pi Uptake (C_0)

In FB and on the LBB, all components of the seagrass ecosystem reduced P*i* to nanomolar concentrations regardless of site trophic state (Table 1.5), resulting in C_0 median levels of 88 and 66 nmol L^{-1}, respectively. These median levels are similar to the range of surface water concentrations we measured in the bay, but are higher than those measured on the banks (Table 1.1). On average, the water column of the bank had a lower (< 50 nmol L^{-1}) C_0 than in the bay (<20 to 385 nmol L^{-1}), indicating its highly oligotrophic state compared to the bay (Table 1.5). While these estimates are presented, we consider this parameter to be overestimated by the model (see C_0 methods section).

1.2.4. Water column P fractions and chemotaxonomy

During the peak of the phytoplankton bloom at DK (Dec. 2005), when chl a was 16 µg L^{-1}, the majority of the P*i* spike (88%) was sequestered by phytoplankton (Fig. 1.4). Chemotaxonomy data indicate that the phytoplankton community in the bloom was completely dominated by cyanobacteria (100%, Table 1.6). A lesser amount of the P*i* spike was partitioned into the acid extractable fraction (12%), most likely as inorganic calcium bound and/or surface adsorbed P and the remaining 1% was recovered in the small size fraction <0.7 µm, attributed to heterotrophs. In February 2006, when chl a at DK dropped to 2 µg L^{-1}, although still dominated

Table 1.5. Inorganic P uptake kinetic parameter C_0, the P*i* concentration where net uptake is zero, according to model predictions based on in situ P uptake rates in chambers deployed in Florida Bay at Green Mangrove Key (GMK), Eagle Key (EK), Rabbit Key (RK), Dump Key (DK), and on the Little Bahamas Bank. C_0 parameters are presented for chamber runs with the system (water column + sediment + seagrass), sediment (water column + sediment), and water column alone. Means are presented with ± SE ($n \geq 3$). Parameter estimates are considered slightly overestimated by the model (see methods).

	C_0 (nmol L^{-1})								
Florida Bay 2003-04									
	Western Bay (GMK)						Eastern Bay (EK)		
	Water	Sediment	System				Water	Sediment	System
Jul	156±9	70±26	159±23				113±26	113±34	153±37
Oct	164±8	187±16	-				152±57	91±18	72±14
Feb	241±54	182±43	68±16				385±38	118±34	56±17
Apr	194±59	130±64	97±28				285±67	66±35	39±8
Florida Bay 2005-06									
	Western Bay (RK)			Central Bay (DK)			Eastern Bay (BLBK)		
	Water	Sediment	System	Water	Sediment	System	Water	Sediment	System
May	nd	nd	nd	<20	<20	21±5	53±53	84±44	63±19
Aug	nd	58±4	61±6	48±20	79±8	55±20	37±18	25±8	36±8
Dec	nd	nd	nd	202±44	174±25	173±34	<20	<20	<20
Feb	nd	nd	nd	21±2	22±3	20±4	nd	nd	nd
Little Bahama Bank 2004									
		Bank Edge						Bank Interior	
	Water	Sediment	System				Water	Sediment	System
Jun T1	nd	64±39	121±42						
Jun T2							48±5	61±12	103±35
Jun T3							29±4	48±22	54±11

nd = not determined because negative values were interpolated by the model.
(-) = missing data.

Table 1.6. Chlorophyll a (chl.a) and phytoplankton group percentages in the community predicted based on accessory pigment data determined from surface waters at Rabbit Key (RK), Dump Key (DK), and Black Betsy Key (BLBK) during P-fractionation experiments conducted in December 2005 and February 2006.

Site	Date	chl.a ($\mu g\ L^{-1}$)	Cyan (%)	Diat (%)
BLBK	Dec. 05	0.80	55	45
	Feb. 06	0.17	29	71
DK	Dec. 05	16.5	100	bd
	Feb. 06	2.09	100	bd
RK	Dec. 05	bd	bd	bd
	Feb. 06	0.02	bd	bd

bd = Below analytical detection

by cyanobacteria (Table 1.6), the proportion of the recovered P in the phytoplankton fraction fell from 88% to 60%, and the acid extractable pool moderately increased (Fig. 1.4). During this time, more P was recovered in the smaller heterotrophic fraction.

During a modest phytoplankton bloom at BLBK in December, 2005, P*i* uptake was also dominated (>75%) by cyanobacteria (Table 1.6, Fig. 1.4). However, when BLBK chl a fell from 0.8 to 0.2 $\mu g\ L^{-1}$ in February, 2006, the proportion of P recovered from the phytoplankton pool declined from 77 to 20%. Also at this time, phytoplankton in the community shifted to 71% diatoms and only 29% cyanobacteria. As diatoms increased, the proportion of the P accounted for by the calcium bound fraction also increased. This may have resulted from resuspension of sediments and associated benthic diatoms, a phenomenon known to occur in fine-grained carbonate systems characteristic of eastern FB. During the February sampling event at BLBK,

when phytoplankton biomass declined to levels more common in the eastern bay, the smaller heterotrophic community became more important (Fig. 1.4).

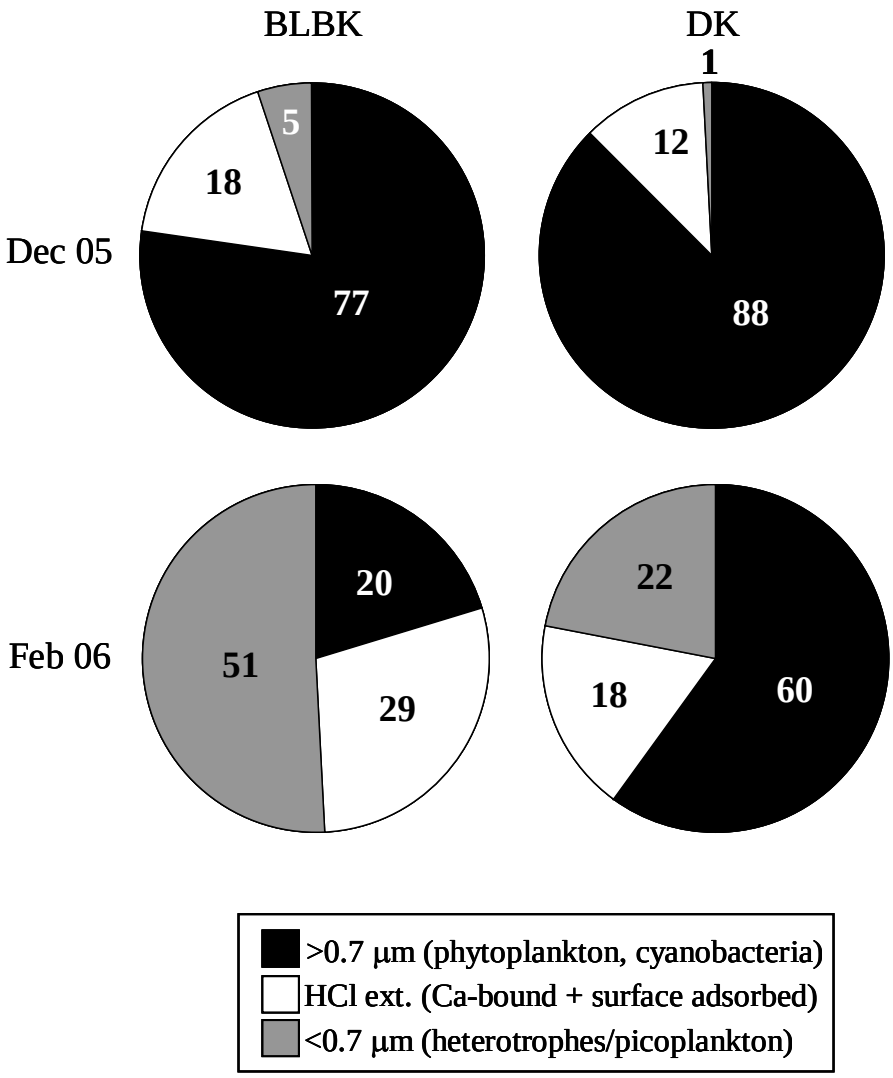

Figure 1.4. Inorganic and organic fractions of sequestered P*i* in the water column at Black Betsy Key (BLBK) and Dump Key (DK) in December, 2005 and February, 2006. Percentage of each fraction is shown in the chart above of the total amount of P*i* taken up over the 90-120 min incubation.

1.3. Discussion

First-order dependence of P*i* removal with time by all components of the FB and LBB seagrass ecosystem indicate that uptake is primarily rate-limited and not enzymatic kinetically controlled at P*i* levels <2 μmol L^{-1}. Similar rate limited uptake at low P*i* concentrations have been shown for isolated *T. testudinum* leaves and roots (Gras et al. 2003, Nielsen et al. 2006), marine bacteria and phytoplankton (Moutin et al. 2002, Thingstad et al. 2005) and coral reef ecosystems (Bilger and Atkinson 1995). The rate constants developed herein for FB seagrass compare to those reported for other shallow carbonate ecosystems under oligotrophic conditions. Steven and Atkinson (2003) determined P*i* uptake on 12 microatolls at One Tree reef lagoon in Australia over a range of seasons and environmental conditions during a three year study. They applied two nutrient loading rates that increased P*i* in the water column from 0.20 ± 0.1 μmol L^{-1} (background) to 2.3 and 5.1 μmol L^{-1} in their low and high loading rate treatments, respectively. The resulting S_p averaged 63 ± 36 x 10^{-6} m s^{-1} and 80 ± 46 x 10^{-6} m s^{-1}, falling within the lower range of our parameter estimates for FB (32 to 661 x 10^{-6} m s^{-1}). Based on average S_p for the 14 microatolls described above, and applying a background P*i* concentration of 0.2 μmol L^{-1}, Steven and Atkinson (2003) estimated uptake rates of 1.2 mmol P*i* m^{-2} d^{-1}, within the range of our areal estimates for FB, 0.30 to 4.16 mmol P*i* m^{-2} d^{-1}.

Although the microatoll study was based on mass transfer of water over the reef, as compared to our incubations in closed chambers, estimates for P*i* uptake rates were similar for these low nutrient carbonate systems. Steven and Atkinson (2003) indicated a high natural variance in rate constants, with uptake rates varying ten-fold both spatially and temporally. In some cases, variance was as high within a reef as across different atolls during sampling events. Steven and Atkinson (2003) interpreted these results to indicate that uptake rates were mass

transfer limited and differences in uptake to be attributable to significant variation in flow rates. As we used a constant turbulent flow rate in the chambers, we interpret the variance in our study to be biogeochemically controlled, rather than physically driven, but also mass transfer limited by P*i* concentration.

Seagrasses, a dominant biotic component of the FB estuary, had an estimated P*i* uptake rate between 0.02 and 0.47 µmol P $gdwt^{-1}$ h^{-1}. These field estimates of seagrass P uptake only just approach the V_{max} determined for *Thalassia* leaves using ^{33}P as a tracer and rates based on P*i* removal from closed chambers (0.58 to 3.2 µmol P $gdwt^{-1}$ h^{-1}, Stapel et al. 1996, Gras et al. 2003, Nielsen et al. 2005). However, the ranges in K_m associated with these estimates of V_{max} are at least 10-fold higher (2 to 8 µmol L^{-1}) than ambient P*i* concentrations measured in the bay. These data suggest that in oligotrophic tropical seagrass systems, P*i* concentrations may not be high enough to promote saturation, thereby limiting the applicability of V_{max} and K_m for modelling P uptake.

If we examine first order P*i* uptake kinetics of *Thalassia* leaves (Stapel et al. 1996, Gras et al. 2003, Nielsen et al. 2006), using a similar range of P*i* levels found in FB (≤ 0.26 µmol L^{-1}), uptake rates (0.0016 to 0.05 µmol P $gdwt^{-1}$ h^{-1}) fall within the range of field uptake rates measured herein, although at the lower end. The higher uptake rates calculated from the seagrass component in the field, compared to laboratory uptake experiments with seagrass leaves suggest that the epiphytic consortium is important in sequestering P*i* in these systems. This was also evidenced in the fact that only a 2-fold difference in benthic uptake was found between western and eastern sites, even though plant biomass changed 3-fold. While the seagrass epiphytic consortium and sediment-phytomicrobenthos communities were found to increase the efficiency in which P*i* was sequestered from the chambers by approximately 38% on average, P*i* uptake

was primarily controlled by the water column, particularly during phytoplankton blooms and during all incubations on the LBB.

Water column P*i* uptake rates in the bay ranged from 17 to 149 µmol m^{-3} h^{-1} in non-bloom conditions, comparing closely with rates calculated for Moreton Bay in subtropical Australia, 7 to 140 µmol m^{-3} h^{-1}, using radioisotope ($^{32}PO_4^{3-}$) assays under ambient P*i* concentrations ≤2 µmol L^{-1} (Glibert et al. 2006). In contrast, in the ultra-oligotrophic gyre in the Mediterranean Sea with extreme P limitation and ambient P*i* concentrations of only 0.002 µmol L^{-1}, a maximum P*i* uptake rate of 1.6 µmol m^{-3} h^{-1} was estimated by Thingstad et al. (2005). Maximum P*i* uptake rates of 0.2 to 0.7 µmol m^{-3} h^{-1}, close to the theoretical maximum for diffusion limitation, were estimated at ambient P*i* concentrations along a west-east transect across the Mediterranean Sea (Moutin et al. 2002). If we use the seasonal average S_p from FB and our data from the LBB, and apply the very low P*i* levels of the Mediterranean Sea (0.002 µmol L^{-1}), P*i* uptake would be 1.8 and 14 µmol m^{-3} h^{-1}, respectively. Thus, FB water column kinetics align with those from the Mediterranean, while the uptake rates on the LBB interior are quite high. A fractionation experiment in the Bahamas would be required to determine if abiotic adsorption or biotic processes were influencing these rapid rates of P*i* sequestration. The only time we found comparable rates in FB was during phytoplankton blooms dominated by cyanobacteria.

During non-bloom conditions in the bay, all components of the system (water column, sediment, and seagrass+epiphytes) contributed to P*i* uptake with phytoplankton dominating in the eastern bay and both phytoplankton and the seagrass-epiphyte consortium in the western bay. In contrast, during phytoplankton blooms, the water column completely dominated P*i* uptake with the majority of uptake being accounted for by phytoplankton. Recurrent phytoplankton blooms, primarily *Synechococcus elongatus*, a non-N_2 fixing cyanobacteria, have been

documented in the north central region of the bay (Phlips and Badylak 1996, Lavrentyev et al. 1998,Phlips et al. 1999, Cotner et al. 2000, Glibert et al. 2004). Phlips et al. (1999) traced the formation of *Synechococcus* blooms from the north-central bay into the south-central bay during a 51-month study. The periodic movement of these *Synechococcus* blooms through the bay can modify P-cycling in the system, based on this group's unique P uptake kinetics. We found cyanobacteria in the bay to have S_p constants several orders of magnitude greater than what is commonly found under non-bloom conditions. This genus has also been shown to have the ability to sequester P*i* at sub-micromolar levels (Moutin et al. 2002). Moutin et al. (2002) determined that *Synechococcus* (size fraction 0.6-2 µm) had higher maximum specific P*i* uptake rates than heterotrophic bacteria and eukaryotic algae in the Mediterranean Sea where P*i* was 0.2 to 2 nM, while heterotrophic bacteria showed the greatest increase in affinity at P*i* levels <0.5 nM. They concluded that *Synechococcus*, with a high P*i* affinity system and high rate of uptake, is competitively dominant over heterotrophic bacteria during episodic pulses of P*i* in P-limited regions of the Mediterranean. *Synechococcus* may also be poised to take advantage of pulses of P*i* in FB generated allochthonously or autochthonously via external phosphatases (Cotner and Wetzel 1992, Cotner et al. 2000, Glibert et al. 2004, Thingstad et al. 2005, Kletou and Koch, Chapter 2 this study). Heterotrophic bacteria appear to dominate in the bay when phytoplankton biomass is reduced, as was also observed by Cotner et al. (2000), perhaps related to their higher surface:volume ratio.

In FB, all components of the seagrass ecosystem reduced P*i* to nanomolar concentrations, similar to the range of surface water concentrations measured in situ, suggesting a redundancy in the system to sequester P*i*. Efficient uptake of P*i* by several system components (Fig. 1.5) probably explains the observation of consistently low water column P*i* concentrations in

carbonate-dominated seagrass ecosystems in the tropics and subtropics (Patriquin 1972; Morse et al. 1987; Fourqurean et al. 1993; Jensen et al. 1998; Koch et al. 2001) including FB (long-term median 0.04 μmol L^{-1}, Boyer et al. 1997, 1999) even across a sediment nutrient gradient. This may be controlled by P-limited biota rapidly scavenging P*i* from the water column and carbonate sediments sequestering P over the long-term into solid-phase pools such as fluorapatite (Ruttenberg and Berner 1993, Jensen et al. 1998, Koch et al. 2001, Zhang et al. 2004). Although the sediment is a major sink for P in carbonate-dominated estuaries (Koch et al. 2001, Zhang et al. 2004), on average P*i* sequestered across the sediment-water interface was limited to 15 to 27% during this study (Fig. 1.5). The potentially slower process of P incorporation into solid-phase inorganic sediment pools, as well as higher porewater P*i*, may have accounted for lower net P*i* sequestration at the sediment-water interface based on P*i* uptake kinetics.

We propose that in carbonate-dominated seagrass systems, P*i* is primarily taken up by the water column biota, particularly when driven by cyanobacteria with extremely rapid P*i* uptake rates (Fig. 1.5). In the absence of algal blooms, suspended sediments and heterotrophs in the water column, as well as the benthos (seagrass ≥ sediment) become more important; although in highly oligotrophic systems, such as on the interior of the LBB, P*i* uptake appears to always be controlled by the water column, even in the absence of phytoplankton blooms. Once sequestered by the water column, P is remineralized/hydrolyzed in the water column or settles to the benthos where it is incorporated into the sediment solid phase pools and can be remineralized or dissolved into porewater and subsequently support benthic primary production (Fig. 1.5).

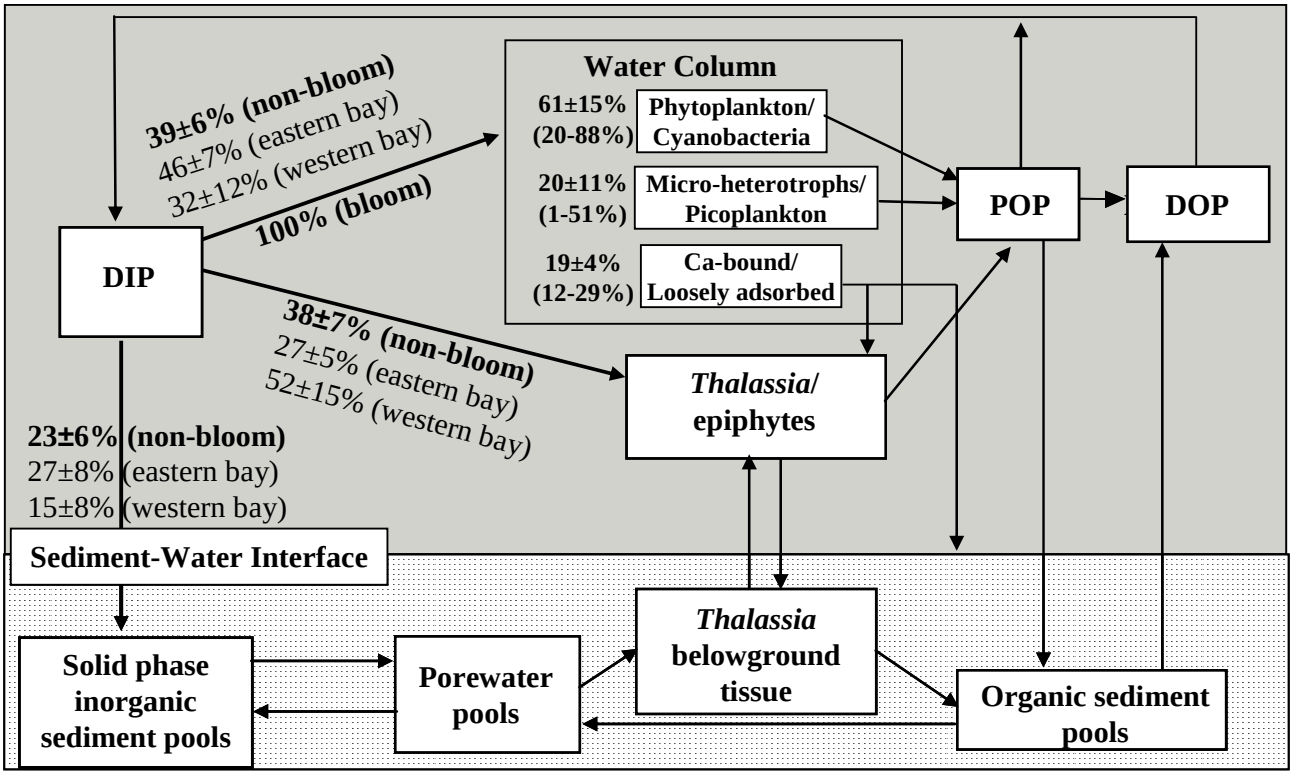

Figure 1.5. Conceptual model illustrating the dominant pathways through which P*i* is cycled in Florida Bay. Data are based on the S_p of each system component for P*i* uptake from the water column. We estimated the relative contribution (mean%±stderr) of the components of the seagrass ecosystem during non-bloom and bloom conditions and for eastern and western sites in the bay based on seasonal averages (see Table 1.3). Compartmentalization of P taken up by the water column (average±SE, ranges) is based on fractionation of biota into size class and acid dissolution (see methods).

1.4. Literature cited

Atkinson, M. J. 1987. Rates of Phosphate Uptake by Coral Reef Flat Communities. Limnology and Ocenography 32(2):426-435.

Bilger, R. W. and M. J. Atkinson. 1995. Effects of nutrient loading on mass-transfer rates to a coral-reef community. Limnology and Ocenography 40(2):279-289.

Bower, C. E. and T. Holm-Hansen. 1980. A salicylate-hypochlorit method for determining ammonia in seawater. Canadian Journal of Fisheries and Aquatic Sciences 37:794-798.

Boyer, J. N., J. W. Fourqurean, and R. D. Jones. 1997. Spatial characterization of water quality in Florida Bay and Whitewater Bay by multivariate analysis: Zones of similar influence. Estuaries 20:743-758.

Boyer, J. N., J. W. Fourqurean, and R. D. Jones. 1999. Seasonal and long-term trends in water quality in Florida Bay (1989-1997). Estuaries 22:417-430.

Cotner, J. B., H. Bootsma, T. Johengen, J. F. Cavaletto, and W. S. Gardner. 2000. Nutrient limitation of heterotrophic bacteria in Florida Bay. Estuaries 23:611-620.

Cotner, J. B. and R. G. Wetzel. 1992. Uptake of dissolved inorganic and organic phosphorus-compounds by phytoplankton and bacterioplankton. Limnology and Ocenography 37:232-243.

Currie, D. J. and J. Kalff. 1984. A comparison of the abilities of freshwater algae and bacteria to acquire and retain phosphorus. Limnology and Oceanography 29:298-310.

De Kanel, J. and J. W. Morse. 1978. The chemistry of orthophosphate uptake from seawater on to calcite and aragonite. Geochimica et Cosmochimica Acta 42:1335-1340.

Falkner, G. R. Falkner, and A. J. Schwab. 1989. Bioenergetic characterization of transient state phosphate uptake by the cyanobacterium *Anacystis nidulans*. Archives of Microbiology 152:353-361.

Fourqurean, J. W., R. D. Jones, and J. C. Zieman. 1993. Processes influencing water column nutrient characteristics and phosphorus limitation of phytoplankton biomass in Florida Bay, FL, USA: interferences from spatial distributions. Estuarine, Coastal and Shelf Science 36:295-314.

Fourqurean, J. W., J. C. Zieman, and G. V. N. Powell. 1992*a*. Phosphorus limitation of primary production in Florida Bay – evidence from C-N-P ratios of the dominant seagrass *Thalassia testudinum*. Limnology and Oceanography 37:162-171.

Fourqurean, J. W., J. C. Zieman, and G. V. N. Powell. 1992*b*. Relationships between porewater nutrients and seagrasses in subtropical carbonate environments. Marine Biology 114:57-65.

Glibert, P. M., C. A. Heil, D. Hollander, M. Revilla, A. Hoare, J. Alexander, and S. Murasko. 2004. Evidence for dissolved organic nitrogen and phosphorus uptake during a cyanobacterial bloom in Florida Bay. Marine Ecology Progress Series 280:73-83.

Glibert, P. M., C. A. Heil, J. M. O'Neil, W. C. Dennison, and M. J. H. O'Donohue. 2006. Nitrogen, phosphorus, silica, and carbon in Moreton Bay, Queensland, Australia: Differential Limitation of Phytoplankton Biomass and Production. Estuaries and Coasts 29:209-221.

Gras, A. F., M. S. Koch, and C. J. Madden. 2003. Phosphorus uptake kinetics of a dominant tropical seagrass *Thalassia testudinum*. Aquatic Botany 76:299-315.

Grasshoff, K. 1983*a*. Determination of nitrite, p. 139-142. *In*: Grasshoff, K., M. Ehrhardt, and K. Kremling. Methods of seawater analysis. Verlag Chemie, Weinheim.

Grasshoff, K. 1983*b*. Determination of nitrate, p. 143-150. *In*: Grasshoff, K., M. Ehrhardt, and K. Kremling. Methods of seawater analysis. Verlag Chemie, Weinheim.

Howarth, R. W. 1988. Nutrient limitation of net primary production in marine ecosystems. Annual Review of Ecology and Systematics 19:89-110.

Jensen, H. S., K. J. McGlathery, R. Marino and R. W. Howarth. 1998. Forms and availability of sediment phosphorus in carbonate sand of Bermuda seagrass beds. Limnology and Oceanography 43:799-810.

Kitano,Y., M. Okumura, and M. Idogaki. 1978. Uptake of phosphate ions by calcium carbonate. Geochemical Journal 12:29-37.

Koch M. S., R. E. Benz and D. T. Rudnick. 2001. Solid-phase phosphorus pools in highly organic carbonate sediments of Northeastern Florida Bay. Estuarine, Coastal and Shelf Science 52:270-291.

Koroleff, F. 1983. Determination of phosphorus, p 125-139. *In*: Grasshoff, K., M. Ehrhardt, and K. Kremling (eds.). Methods of seawater analysis. Verlag Chemie, Weinheim.

Lavrentyev, P. J., H. A. Bootsma, T. H. Johengen, J. F. Cavaletto, and W. S. Gardner. 1998. Microbial plankton response to resource limitation: insight from community structure and seston stoichiometry in Florida Bay, USA. Marine Ecology Progress Series 165:45-57.

Louda, J. W., L. Liu, and E. W. Baker. 2002. Senescence- and death-related alteration of chlorophylls and carotenoids in marine phytoplankton. Organic Geochemistry 33:1635-1653.

McGlathery, K. J., R. Marino, and R. W. Howarth. 1994. Variable rates of phosphate uptake by shallow marine carbonate sediments: Mechanisms and ecological significance. Biogeochemistry 25:127-146.

Millero, F. J., F. Huang, X. Zhu, X. Liu, and J. Z. Zhang. 2001. Adsorption and desorption of phosphate on calcite and aragonite in seawater. Aquatic Geochemistry 7:33-56.

Monaghan, E., and K. Ruttenberg. 1999. Dissolved organic phosphorus in the coastal ocean: Reassessment of available methods and seasonal phosphorus profiles from the Eel River Shelf. Limnology and Oceanography 44:1702-1714.

Morse, J. W., J. J. Zullig, R. L. Iverson, G. R. Choppin, A. Mucci, and F. J. Millero. 1987. The influence of seagrass beds on carbonate sediments in the Bahamas. Marine Chemistry 22:71-83.

Moutin, T., T. F. Thingstad, F. V. Wambeke, D. Marie, G. Slawyk, P. Raimbault, and H. Claustre. 2002. Does competition for nanomolar phosphate supply explain the predominance of the cyanobacterium *Synechococcus*? Limnology and Oceanography 47(5):1562-1567.

Nielsen, O. I., M. S. Koch, H. S. Jensen, and C. J. Madden. 2006. *Thalassia testudinum* phosphate uptake kinetics at low in situ concentration using a ^{33}P radioisotope technique. Limnology and Oceanography 51:208-217.

Patriquin, D. G. 1972. The origin of nitrogen and phosphorus for growth of marine angiosperm *Thalassia testudinum*. Marine Biology 15:33-46.

Phlips, E. J. and S. Badylak. 1996. Spatial variability in phytoplankton standing crop and composition in a shallow inner-shelf lagoon, Florida Bay, Florida. Bulletin of Marine Science 58:203-216.

Phlips E. J., S. Badylak, and T. C. Lynch. 1999. Blooms of the picoplankton cyanobacterium *Symechococcus* in Florida Bay, a subtropical inner-shelf lagoon. Limnology and Oceanography 44:1166-1175.

Powell, G. V. N., W. J. Kenworthy, and J. W. Fourqurean. 1989. Experimental evidence for nutrient limitation of seagrass growth in a tropical estuary with restricted circulation. Bulletin of Marine Science 44:324-340.

Rudnick, D. T., Z. Chen, D. L. Childers, J. N. Boyer, and T. D. Fontaine III. 1999. Phosphorus and nitrogen inputs to Florida Bay: the importance of the Everglades watershed. Estuaries 22:398-416.

Ruttenberg, K. C. and R. A. Berner. 1993. Authigenic apatite formation and burial in sediments from non-upwelling, continental-margin environments. Geochimica et Cosmochimica ACTA 57:991-1007.

Short, F. T., W. C. Dennison, and D. G. Capone. 1990. Phosphorus-limited growth of the tropical seagrass *Syrengodium filiforme* in carbonate sediments. Marine Ecology Progress Series 62:169-174.

Stapel, J., T. L. Aarts, B. H. M. van Duynhoven, J. D. de Groot, P. H. W. van den Hoogen, and M. A. Hemminga. 1996. Nutrient uptake by leaves and roots of the seagrass *Thalassia hemprichii* in the Spermonde Archipelago, Indonesia. Marine Ecology Progress Series 134:195-206.

Steven, A. D. L. and M. J. Atkinson. 2003. Nutrient uptake by coral-reef microatolls. Coral Reefs 22:197-204.

Thingstad, T. F., M. D. Krom, R. F. C. Mantoura, G. A. F. Flaten, S. Groom, B. Herut, N. Kress, C. S. Law, A. Pasternak, P. Pitta, S. Psarra, F. Rassoulzadegan, T. Tanaka, A. Tselepides, P. Wassmann, E. M. S. Woodward, C. Wexels Riser, G. Zodiatis, T. Zohary. 2005. Nature of phosphorus limitation in the ultraoligtrophic eastern Mediterranean. Science 309:1068-1071.

Zhang, J. - Z., C. J. Fisher, and P. B. Ortner. 2004. Potential availability of sedimentary phosphorus to sediment resuspension in Florida Bay. Global Biogeochemical Cycles 18: GB4008. doi:10.1029/2004GB002255.

CHAPTER 2

ALKALINE PHOSPHATASE ACTIVITY OF SEAGRASS AND WATER COLUMN FRACTIONS IN FLORIDA BAY

2.0. Introduction

In P depleted open ocean systems with high rates of N_2 fixation (Karl et al., 2001; Ammerman et al., 2003), and in coastal estuaries with high nitrogen availability (Boyer et al., 2006), satisfying the P-nutrition of phytoplankton and bacteria is dependent on the availability of both dissolved organic P (DOP) and enzymes such as alkaline phosphatase (AP) (Hernández et al., 1996a; Vidal et al., 2003; Glibert et al., 2004). AP attached to organisms, as cellular surface -bound enzymes or freely dissolved in the water column from cell lysis or excretion (Li et al., 1998), can hydrolyze a wide variety of organic phosphomonoesters or PMEs (Shan et al., 1994). Upon enzyme hydrolysis, PMEs release inorganic phosphate (P*i*) to the water that is available to planktonic as well as benthic organisms in shallow marine systems (Cembella et al., 1984; Hernández et al., 2000). APA has been identified and measured in all major groups of eukaryotic algae (Lapointe et al., 1992; Lapointe et al., 1994; Lapointe 1997; Hernández et al., 1997; Hernández et al., 1999), cyanobacteria (Ray et al., 1991, Yelloly and Whitton, 1996, Glibert et al., 2004; Williams and Jochem, 2006), heterotrophic bacteria (Martinez et al., 1996) and seagrass and macroalgae (Pérez and Romero, 1993; Lapointe et al., 1994; Hernández et al., 1994b; Touchette, 1999). Due to the widespread occurrence of AP in aquatic plants and microbes from oligotrophic systems, it is generally presumed that AP promotes organic P hydrolysis and recycling of P in these systems (Taft et al., 1977; Kobori and Taga, 1979; Vidal et al., 2003; Boyer et al., 2006).

Coastal marine environments frequently have high dissolved organic matter efflux from land-margin ecosystems (Meybeck, 1993), particularly in the tropics where fringing mangrove and shallow seagrass communities dominate (Fourqurean et al., 1993; Rudnick et al., 1999). These systems are known to export a large amount of dissolved organic matter, although the

organic chemistry and bioavailability of these nutrient sources are not well understood (Clark et al., 1998; Suzumura et al., 1998; Boyer et al., 2006). While some plankton utilize various forms of organic P, such as *Trichodesmium* in the open ocean (Dyhrman et al., 2006), the majority of aquatic primary producers and bacteria are limited to the hydrolysis of PMEs (Cembella et al., 1984). Karl and Yanagi (1997) in the oligotrophic north Pacific ocean, used UV decomposition to distinguish between two chemically distinct DOP pools: UV-labile phosphorus (primarily PMEs) made up 51% of the total dissolved phosphorus (TDP) pool and UV-stable phosphorus (primarily nucleotide di- and tri-phosphates, nucleic acids and other compounds that are resistant to UV treatment) made up 26% of the TDP. In coastal areas of Tokyo Bay, Suzumura et al. (1998) used 2 phosphohydrolytic enzymes to demonstrate the presence of 3 forms of high molecular weight (HMW) DOP: easily hydrolyzable mono- and diesters and unhydrolyzable nonreactive DOP. The nonreactive DOP made up a significant fraction (up to 67%) of the HMW DOP pool. In marine systems a variable percentage of DOP is constituted of PMEs ranging from negligible values up to 70% (Shan et al., 1994; Karl and Yanagi, 1997; Huang and Hong, 1999; Hernández et al., 2000; Labry et al., 2005); thus, the availability of the hydrolyzable fraction (primarily PMEs) of the DOP pool is very site specific and dynamic.

Few phosphorus (P) depleted coastal marine ecosystems have been examined for their capacity to hydrolyze phosphomonoesters (PMEs), and no studies to date have simultaneously examined water column and benthic APA. Benthic studies of APA have primarily focused on macroalgae and seagrass, using PME substrate levels several orders of magnitude higher than DOP levels found in the field, as many of these studies primarily used APA as an indicator of P-limitation (Pérez and Romero, 1993; Lapointe et al., 1992; Lapointe, 1997; Touchette and Burkholder, 2000). In the present study, we investigated AP activities of several ecosystem

components in a seagrass-dominated highly oligotrophic coastal estuary, Florida Bay, across a well established P-gradient (Zieman et al., 1989; Fourqurean et al., 1992a, b; Zhang et al., 2004; Nielsen et al., 2006). AP activities were examined at the lower range of PME concentrations equating to DOP levels found in situ (0.05 to 2.0 µmol L^{-1} MUF-P). Seasonal determinations were made for AP activities of the water column community based on size fractions, phytoplankton (>1.2 µm), bacteria (<1.2 and > 0.2 µm) and freely dissolved enzymes (<0.2 µm). The influence of cell surface enzymes on leaves and associated epiphytes of *Thalassia testudinum*, a dominant tropical seagrass of the tropical Atlantic-Caribbean region, on water column AP activity was also examined. The P-gradient across the bay was hypothesized to significantly influence water column and seagrass AP enzyme activity in this P-limited estuary. Further, we suggest that *T. testudinum* would contribute significantly to water column PME enzyme hydrolysis, particularly with the attached epiphytic consortium.

2.1. Materials and Methods

2.1.1. *Study Sites*

Florida Bay is a large (2200 km^2), shallow (mean depth <2 m) (Corbett et al., 1999), seagrass-dominated (Fourqurean et al., 2001), semi-enclosed lagoon that has a sediment P gradient from west (high P) to east (low P) across the Bay (Zhang et al., 2004), although P*i* levels are relatively low in surface waters across the bay (0.03 ± 0.01 µM; Fourqurean et al., 1993). This sediment P gradient, which leads to a high seagrass biomass in the western bay, relative to the eastern bay, is a result of P inputs from the Gulf of Mexico into the western regions of the bay and the P-limited Everglades marsh flowing into the eastern bay (Rudnick et

al., 1999). The three Florida Bay sites chosen for this study (Fig. 2.1) span this nutrient gradient with a site in the western bay, Rabbit Key (RK; 24°58’50”N/80°50’11”W), in the northeastern bay, Black Betsy Key (BLBK; 25°08’23”N/80°38’51”W), and in the northcentral bay, Dump Key (DK; 25°06’40”N/80°46’15”W).

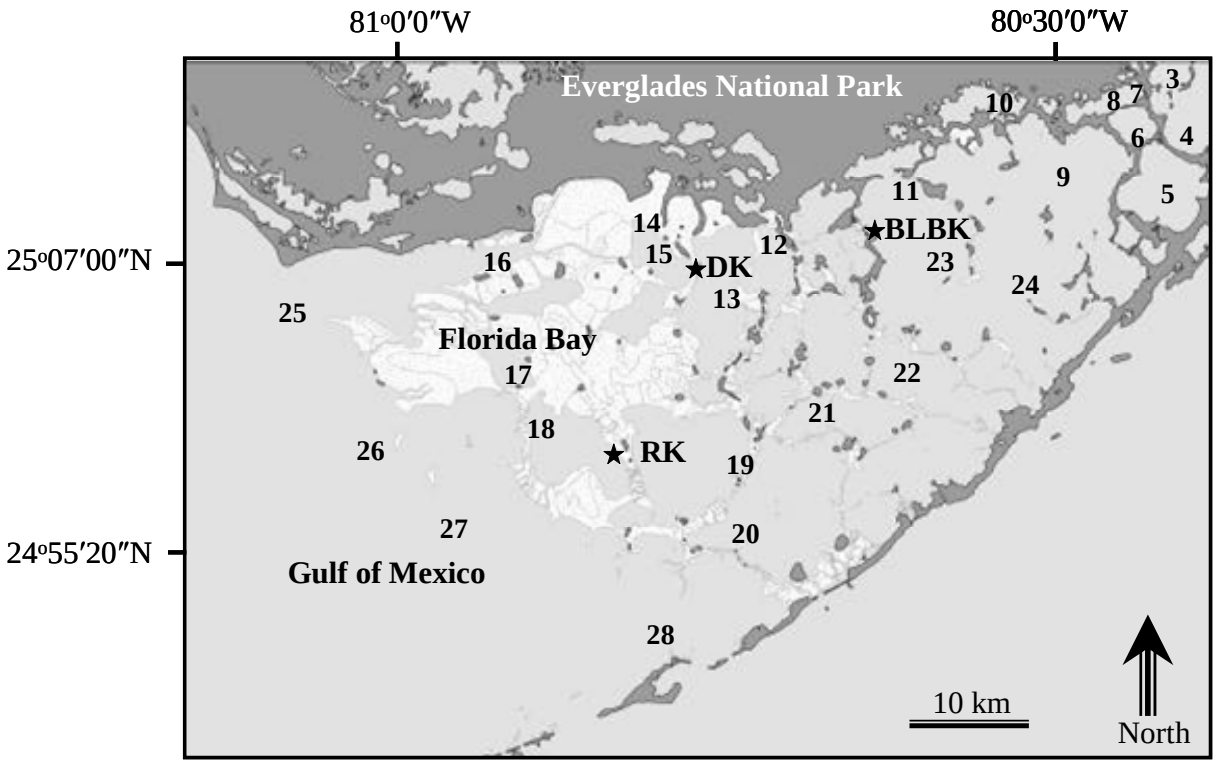

Figure 2.1. Three APA study sites in Florida Bay indicated by a star, at the southern terminus of the south Florida peninsula: Black Betsy Key (BLBK) in the northeast, Dump Key (DK) in the northcentral, and Rabbit Key (RK) in the western region of the Bay. The 28 long-term monitoring sites by Boyer et al. (1999, 1995) where PMEs were measured are also shown. Numerous mangrove islands are can be seen in the bay and the Florida Keys to the south and Everglades mangroves and marsh to the north in dark gray.

2.1.2. Sampling and APA Analysis

APA was determined for size-fractionated water column components (Labry et al., 2005) and seagrass (*Thalassia testudinum*) leaves with and without epiphytes during 2006-2007 (August, November, January, April). The five system components tested were (1) non filtered ambient water, representing water column phytoplankton, particle-associated bacteria and freely dissolved AP, (2) ambient water filtered through 1.2 µm filters, representing free-living bacteria and freely dissolved AP, (3) ambient water filtered through 0.2 µm filters, representing the freely dissolved AP, (4) *Thalassia testudinum* leaves + epiphytes, and (5) *Thalassia testudinum* leaves alone without epiphytes. All leaves were incubated in non filtered ambient water to estimate the relative importance of seagrass versus water column hydrolysis.

APA was evaluated using the fluorogenic substrate analogue 4-methylumbelliferyl phosphate (MUF-P) (Hoppe, 1983) for each of the above components within 5-10 h after collection. APA was determined as an increase in fluorescence of methylumbelliferone (MUF) cleaved from MUF-P over time (nmol P L^{-1} h^{-1}). A stock solution of 4-methylumbelliferyl phosphate (MUF-P) $C_{10}H_7Na_2O_6P$ was prepared to an initial concentration of 100 µM using artificial seawater (ASW) of negligible P concentration (previously tested on a Technicon AA3) adapted from Kalle (1945). Since the fluorescent substrates are light sensitive, incubations and all processing were carried out in the dark. The stock solution (100 µM) was diluted (using site-specific in situ water) to the range of MUF-P substrate levels examined (0 (blank), 0.05, 0.1, 0.25, 0.5, 0.75, 1.0, 1.5, and 2.0 µM), encompassing the DOP concentrations found in the bay (Boyer et al., 1999). Fluorescence was measured at field temperatures using a 2-h incubation time, also used by Boyer et al. (1999, 2006) in an ongoing bay-wide water quality monitoring program. Using this 2 h incubation time, hydrolysis rates were linear for all system components

at 2 µM MUF-P; however, at lower substrate concentrations, hydrolysis may have saturated during some seasonal incubations and PME hydrolysis rates at lower substrate levels may have been underestimated. Therefore, in this study we present APA kinetic data using a hyperbolic model and estimate V_{max}, but K_m is not reported. We are reexamining water column APA kinetics at low level substrates (<1 µM) in a subsequent study using shorter incubation times (30 min) and time course (every 3 min) experiments (Koch unpublished data).

2.1.3. Field Collections and Incubations

Water was collected from the field in large carboys (10 L) and immediately transported to the lab for filtration and APA incubations. *Thalassia testudinum* leaves were collected in the field by cutting the short shoot with scissors and allowing leaves to float into plastic bags which were immediately placed in a cooler with ice packs for transportation to the lab (3-5h). While precautions were taken not to disturb epiphytes, some epiphytes were dislodged from the leaves in transport (personal observation). During each sampling event, surface water temperature, salinity and pH were recorded from each site.

In the lab, leaves were immediately sectioned into 5 cm segments with and without epiphytes (removed by gently sliding leaf between two gloved fingers) and placed into low-P ASW for 10 min. The area of the leaves varied across the bay reflecting the P gradient with RK leaves having the largest average surface area (7.4 ± 0.09 cm^2) followed by DK (7.0 ± 0.08 cm^2) and BLBK (5.2 ± 0.06 cm^2) (n = 144 for each site). Incubations were run in duplicate using black 15 mL centrifuge tubes filled with substrate medium, either non-filtered or filtered water from each site. During incubations, tubes were gently shaken every 20-30 min to allow efficient mixing of the contents and optimize substrate flow around leaves. After the incubation, 80 µL

aliquots of the assay medium were pipetted into a 384-well microplate (2 replicates for each sample) and read at 25°C with a spectrofluorometer (SpectraMax Gemini XPS) at 360 nm excitation and 450 nm emission wavelengths. Duplicate (n=2) tubes for all MUF-P level (n=9) by system component (n=5) combinations were run for each of the three sites (total treatment # tubes run = 270). Replicate blanks were also run for each MUF-P level along with one set amended with alkaline phosphatase used in PME determinations in the field (described below) to ensure ~100% recovery.

Fluorescence units were calibrated with 12 MUF standard concentrations (0, 0.025, 0.05, 0.075, 0.10, 0.15, 0.25, 0.5, 0.75, 1.0, 1.5 and 2.0 µM) using 4-methylumbelliferone sodium salt (M1508-10G) and in situ water. Stock solution of 100 µM MUF was prepared using ASW. Standards were prepared using site-specific ambient water, as tests had shown that the standard curve varied slightly using water from different sites; all standard curves were highly linear (R^2 >0.99).

2.1.4. Water column TP, TDP, Pi and PME analyses

During each sampling trip, surface water was also collected (2 L, n = 4) from each site, subsamped into 20 mL scintillation vials for the later determination of TP (unfiltered), DOP, P*i* and PMEs (GFF and 0.2 µm millipore filters). PME concentrations were determined as the difference between P*i* levels before and after exhaustive hydrolysis with calf intestinal mucosa AP (Hernández et al., 1993; Huang and Hong, 1999). At each site 1 mL of enzyme solution (1,000 units of bovine intestinal mucosa in 100 mL ASW; 10 units mL^{-1} , Sigma P-6772) was added to 20 mL of seawater in the field and further incubated in a water bath at in situ temperature for 4 h once samples were brought back to the lab. In addition to measuring PMEs,

we evaluated the phosphodiester concentration in the same way described above with *Crotalus atrox* phosphodiesterase (Sigma P4506; Pant et al., 2002). These data are not reported; however, as the enzyme (PDEase) produced a high background P*i* concentration (blanks varied between 5.7-7.3 µmol P*i* L^{-1}).

All nutrient samples were placed in a cooler and kept cold on ice in transport. Alkaline phosphatase assays were completed within 10 h of collection and nutrient determinations within 1 to 10 d. Nutrients were analyzed using an autoanalyzer with a digital colorimeter (Technicon AA3) following a low P*i* seawater analysis protocol (Bran Luebbe Inc.) after Murphy and Riley (1962). TP and TDP were determined using a high temperature ashing/hydrolysis method after Monaghan and Ruttenberg (1999) and dissolved organic phosphorus (DOP) calculated by subtracting P*i* from TDP.

To investigate the spatial representation of PME concentrations in the bay, in support of our seasonal data from 3 sites across the bay, we also measured PME levels at 28 long-term water quality sites (Fig. 2.1; Boyer et al. 1997, 1999) September, 2006, applying the same methodology as above.

2.1.5. Data Analyses

Kinetic data on MUF-P hydrolysis were graphed using the Michaelis and Menten equation ($v = V_{max}[S]/K_m+[S]$) and V_{max} determined. We also compared rates of hydrolysis at 2 µmol L^{-1} among water column fractions (using ranked data) and NF water column with leaves and leaves with epiphytes across sites and seasons using a repeated measure (season) multivariate analysis (MANOVA, Wilks Lambda statistic; SAS v 9.1). Mean comparisons for

APA across sites, seasons and system components were analyzed using a Tukey-Kramer test. Statistical differences are reported at the $p < 0.05$ level unless otherwise stated.

2.2. Results

2.2.1. Seasonal Patterns of APA

Based on repeated measures analysis, APA in the bay showed both site and size fraction differences in PME hydrolysis rates over time using 2 µmol L^{-1} MUF-P (Table 2.1).

Table 2.1. Seasonal APA at 2 µmol L^{-1} MUF-P in the water column with sequential size fractions added and with 5 cm sections of *T. testudinum* leaves (L) and leaves with epiphytes (LE) added to 15 mL of non-filtered (NF) water from each site: Black Betsy Key (BLBK), Dump Key (DK) and Rabbit Key (RK). Chlorophyll normalized APA for NF water column fraction.

		nmol P L^{-1} h^{-1}					nmol P Chl. a^{-1} h^{-1}
Date	Site	<0.2 µm	<1.2 µm	NF	NF+L	NF+LE	NF
Aug 06	BLBK	518	559	686	648	691	1,500
Nov 06	BLBK	190	275	359	476	451	3,000
Jan 07	BLBK	62	64	137	157	221	667
Apr 07	BLBK	121	237	254	321	518	1,250
Aug 06	DK	370	660	748	750	734	412
Nov 06	DK	190	1,135	951	1,108	953	70
Jan 07	DK	251	306	673	647	709	438
Apr 07	DK	248	246	408	782	1,012	1,242
Aug 06	RK	308	318	390	555	751	415
Nov 06	RK	346	437	603	771	751	455
Jan 07	RK	353	334	1,220	915	1,075	83
Apr 07	RK	387	509	790	796	723	356
Site Averages(±SE)							
	BLBK	223±102	284±103	359±118	401±105	470±97	1,604±497
	DK	265±38	587±204	695±112	822±100	852±76	541±248
	RK	349±16	399±45	751±176	759±75	825±84	327±84

APA was significantly ($p < 0.01$) affected by season, season x fractions, and season x site x fractions, indicating a complex pattern of APA across sites in the bay. These dynamics were primarily driven by the water column biota, as seasonal shifts in enzyme activity were clearly not controlled by changes in temperature, salinity or pH (Tables 2.1, 2.2, Figs. 2.2, 2.3).

Table 2.2: Salinity (S), temperature (T), pH, total phosphorus (TP), total dissolved phosphorus (TDP), inorganic soluble reactive phosphorus (P*i*) and phospho-monoester (PME) concentrations in the water column at Black Betsy Key (BLBK), Dump Key (DK) and Rabbit Key (RK) during APA determinations.

Date	Site	S (psu)	T (^{o}C)	pH	TP (µM)	TDP (µM)	P*i* (µM)	PME (µM)
Aug 06	BLBK	31	31	-	0.57±0.05	0.43±0.04	0.071±0.004	0.064
Nov 06	BLBK	29	22	8.2	0.49±0.02	0.43±0.02	0.047±0.007	bd
Jan 07	BLBK	28	20	8.2	0.52±0.04	0.44±0.05	0.036±0.003	bd
Apr 07	BLBK	31	25	8.0	0.43±0.05	0.30±0.09	0.070±0.018	bd
Aug 06	DK	37	31	-	1.62±0.28	0.27±0.10	0.277±0.020	0.033
Nov 06	DK	33	21	8.5	1.77±0.07	0.35±0.04	0.330±0.005	bd
Jan 07	DK	34	20	8.3	1.06±0.06	0.59±0.02	0.062±0.011	bd
Apr 07	DK	35	25	8.4	0.53±0.06	0.37±0.03	0.107±0.024	bd
Aug 06	RK	36	31	-	0.72±0.02	0.53±0.07	0.365±0.009	bd
Nov 06	RK	39	22	8.3	0.72±0.04	0.48±0.05	0.315±0.017	bd
Jan 07	RK	38	21	8.4	1.48±0.04	0.50±0.02	0.289±0.016	0.001
Apr 07	RK	32	25	8.3	0.74±0.06	0.48±0.05	0.204±0.014	bd

bd=below detection; - = missing data.

At the northeastern and most P-limited site in the bay (BLBK), APA from ambient non-filtered water was significantly lower across seasons, particularly in January, 137 nmol P L^{-1} h^{-1}, compared to the western (RK) and central (DK) bay sites where the lowest AP activities measured were 408 and 390 nmol P L^{-1} h^{-1}, respectively (Table 2.1; Fig. 2.2). The highest AP activities at BLBK were recorded in the summer (686 nmol P L^{-1} h^{-1}) associated with peaks in

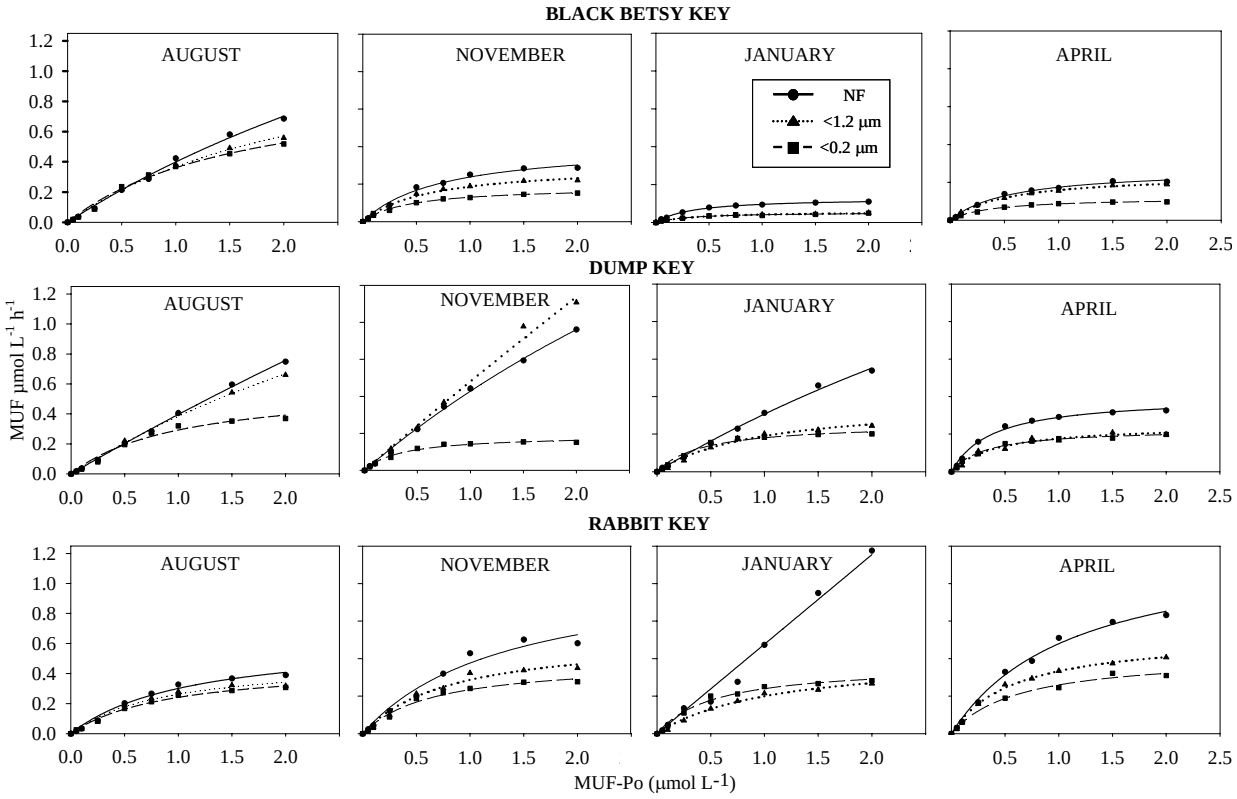

Figure 2.2. Seasonal alkaline phosphatase enzyme kinetics using the Michaelis-Menten hyperbolic model for non-filtered (NF), <1.2 µm, and <0.2 µm size fractionated water column at three sites in the bay (Black Betsy Key, northeastern Bay; Dump Key, northcental Bay; Rabbit Key, western Bay) during August and November, 2006 and January and April, 2007.

phytoplankton biomass. During August at BLBK, Chl. a in the water column was 2-3 times higher than during fall, winter or spring (Table 2.3). The higher Chl.a was accounted for by an increase in cyanobacteria in the water column, evidenced by chemotaxonomic analysis of the phytoplankton community (Table 2.3). Phosphomonoester concentrations were also detectable in the water column during this time and P*i* and TP levels were relatively high (Table 2.2).

In contrast to the low APA levels found at BLBK, unfiltered water at DK and RK approached or were greater than hydrolysis rates of 1,000 nmol L^{-1} P h^{-1} at 2.0 µmol L^{-1} MUF-P,

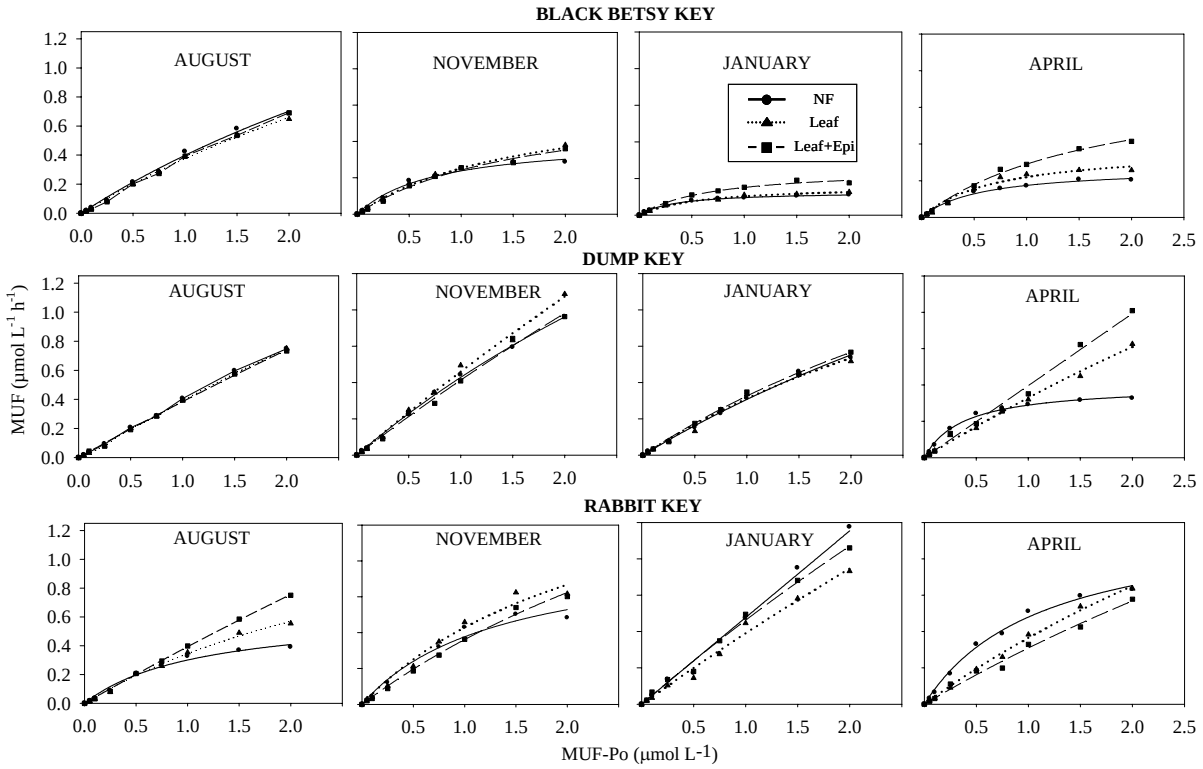

Figure 2.3. Seasonal alkaline phosphatase enzyme kinetics using the Michaelis-Menten hyperbolic model for non-filtered (NF) water and NF water with 5 cm leaf segments of *Thalassia testudinum* both with and without epiphytes at three sites in the Bay (Black Betsy Key, northeastern Bay; Dump Key, northcental Bay; Rabbit Key, western Bay) during August and November, 2006 and January and April, 2007.

influenced by algal bloom initiation (Table 2.1, 2.3). Chl.a levels at these two sites were an order of magnitude (14-15 µg L^{-1}) higher than was found at BLBK during the study. While algal booms occurred at the central and western sites, the timing of the phytoplankton blooms was different. At RK, the bloom peaked during January, 2007 shifting from diatoms to cyanobacteria dominance, concomitant with Chl. a increasing from 1 to 15 µg L^{-1} (Table 2.3) and TP concentrations increasing 2-fold (Table 2.2). The bloom at DK peaked in November, but before the initiation and during the fall bloom, TP and P*i* levels were 2-5 times higher relative to the winter and spring sampling periods. Also, PMEs were detectable in August at DK; however, at

very low concentrations (0.03 μmol P L^{-1}, Table 2.2). The cycles of these major algal blooms that have the capacity to influence APA in the bay were approximately 6 months from initiation, bloom, to residual conditions based on Chl. a and APA during this one-year study (Fig. 2.2, Tables 2.1, 2.3). While peaks in APA always corresponded to cyanobacterial blooms, fractionation of the APA in the water column suggested both direct and indirect controls of these blooms on potential rates of PME hydrolysis.

Table 2.3. Water column chlorophyll a (Chl. a) and phytoplankton group dominance based on chemotaxonomy at Rabbit Key (RK), Dump Key (DK) and Black Betsy Key (BLBK) during the time of seasonal APA determinations.

Site	Date	Chl.a (μg L^{-1})	Cyan (%)	Diat (%)	Crypt (%)	Dino (%)
BLBK	Aug 06	0.46±0.07	100±<1	bd	bd	bd
	Nov 06	0.12±0.04	bd	100±<1	bd	bd
	Jan 07	0.21±0.03	13±7	87±7	bd	bd
	Apr 07	0.20±0.06	bd	67±3	bd	33±3
DK	Aug 06	1.82±0.12	75±2	9±1	16±1	bd
	Nov 06	13.64±2.44	100±<1	bd	bd	bd
	Jan 07	1.53±0.62	88±2	12±2	bd	bd
	Apr 07	0.33±0.07	19±3	35±5	15±8	31±<1
RK	Aug 06	0.94±0.15	13±<1	87±<1	bd	bd
	Nov 06	1.32±0.10	90±3	10±3	bd	bd
	Jan 07	14.75±2.34	99±<1	1±<1	bd	bd
	Apr 07	2.22±0.69	86±4	4±<1	6±2	5±1

bd = Below analytical detection.

2.2.2. Size Fractionated APA

Even though APA maximums were coincident with high phytoplankton biomass in the water column, the <0.2 μm dissolved free phase contributed the most to APA. Comparisons

made in the water column fractions at the 2 µM substrate level using MANOVA indicated that the <0.2 µm fraction was statistically lower than NF water in all seasons; however free enzyme activity was more stable and consistent across seasons and sites, and had an average contribution of ~50% to the total APA by the water column at 2 µmol L^{-1} (Tables 2.1, 2.4). A noted exception

Table 2.4. Percent (%) APA contribution to total APA (at 2 µmol L^{-1} MUF-P) in the water column by each size fraction averaged across seasons for each site: Black Betsy Key (BLBK), Dump Key (DK) and Rabbit Key (RK). Contribution of *T. testudinum* leaves (L) and leaves with epiphytes (LE) was calculated as the percent increase in APA with a 5 cm leaf section added to 15 mL of unfiltered water column.

	Water column fraction (µm)				
Site	<0.2	>0.2 - <1.2	>1.2	L	LE
BLBK	55±7	19±10	26±10	15±5	27±11
DK	42±9	28±15	26±12	16±11	16±15
RK	54±10	8±4	38±11	13±8	29±11
Average	50±4	18±6	30±4	14±1	20±4

was at BLBK where the dissolved fraction was variable, having both the highest (518 nmol L^{-1} P h^{-1}) and lowest (62 nmol L^{-1} P h^{-1}) activities measured during summer and winter, respectively (Table 2.1). The next dominant fraction of APA in the water column was the phytoplankton (>1.2 µm) which contributed ~30% on average to the total activity (Table 2.4), but as discussed above, was highly variable on any particular sampling date influenced by phytoplankton blooms (Tables 2.1, 2.3). Typically under phytoplankton bloom conditions, this fraction would be much greater than that attributed to the microbial size fraction; however, at DK in November, the

bloom appeared to stimulate heterotrophs and they became the most important size fraction for APA in the water column (Table 2.1, Fig. 2.2). These data suggest that the presence of cyanobacteria can have an indirect effect on microbial APA in the water column. Because of the difficulty in filtering these small size fractions when Chl. a. is >10 µg L^{-1}, some of the APA in the smaller fraction could have been cyanobacteria; however, there was no stimulation in the dissolved APA pool to suggest a problem with cell lyses by filtration (Sala et al. 2001). Also, the microbial APA dominance over the phytoplankton size class can be seen initiating in August at DK (Fig. 2.2). It is interesting that in January at DK and RK, a similar stimulation of APA during cyanobacterial blooms did not stimulate heterotrophic enzyme activity. On average, the contribution of the bacterial size class APA was 8 and 19% at RK and BLBK, but at DK, as a result of the greater microbial APA, was 28%, on par with phytoplankton (Table 2.4).

In addition to the water column, we determined if cell surface enzymes of seagrass leaves and/or their associated epiphytes would stimulate water column PME hydrolysis. Leaves modestly stimulated PME hydrolysis of the unfiltered water column by approximately 14%, while including the epiphytic consortium, enhanced rates 20% (Table 2.4). Thus, the water column is very efficient at hydrolyzing PMEs with seagrass and their associated epiphytic consortium only contributing moderately to the total APA and acquiring a more significant role in PME hydrolysis when water column enzyme activities were low (Fig. 2.3). However, local PME hydrolysis may be important, as the seagrasses themselves and the epiphytic consortium can be a source of organic P.

2.2.3. Alkaline Phosphatase Kinetics

Florida Bay water column AP hydrolysis rates as a function of MUF concentration up to 2 µmol MUF-P approached saturation or saturated during the majority of incubations (Figs. 2.2, 2.3). For AP in the dissolved phase, enzyme hydrolysis saturated within the 2 µmol L^{-1} range during most of the incubations. In the second size fraction, attributable to the microbial community, V_{max} also showed similar ranges across seasons and sites (700±210; median 490 nmol L^{-1} h^{-1}), approximately 20% higher than the dissolved fraction, with the exception of DK in November. During November at DK, the PRESS statistic and high parameter error terms, as well as the clearly non-saturating characteristic of the curve fit of the data (Fig. 2.2), indicate that the hydrolysis rates did not saturate up to 2 µmol L^{-1}, and therefore the MM model is not applicable. In the phytoplankton size fraction, only kinetics in August at RK, November at BLBK, January at BLBK, and April at BLBK and DK fit the hyperbolic model, based on low parameter error terms and a low PRESS statistic (Table 2.5), resulting in a median V_{max} of 500 nmol L^{-1} P h^{-1} for the water column as a whole. During these times, Chl. a. (µg L^{-1}) was at a minimum within each site: 0.94 at RK, 0.33 at DK, and 0.12 to 0.21 at BLBK. Thus, water column V_{max} would be considered the maximum hydrolysis rate without the influence of a major algal bloom. Comparing the water column with leaves and epiphytes (Fig. 2.2), it is clear that the water column dominated the hydrolysis; however adding the leaves and epiphytes linearized the rates even further, also shown in the high PRESS statistic (Table 2.5). Only at BLBK in August, January and April was V_{max} adequately predicted by the MM model, resulting in a median rate of 470 and 800 nmol L^{-1} h^{-1} of the water column with leaves and leaves with epiphytes, respectively.

Table 2.5. Seasonal alkaline phosphatase enzyme hydrolysis kinetic parameter, V_{max} (µmol P L^{-1} h^{-1}) at Black Betsy Key (BLBK), Dump Key (DK) and Rabbit Key (RK) in Florida Bay defined based on substrates up to 2.0 µmol L^{-1} MUF-P (see Figs. 3,4). Parameters (± SE) are shown for various size fractions in the water column: phytoplankton + bacteria + free enzymes (non-filtered, NF), bacteria + free enzymes (<1.2 µm filtered), and free enzymes (<0.2 µm filtered) and with the addition of 5 cm segments of *Thalassia testudinum* leaves in NF water with (LE) and without (L) epiphytes. The 2-parameter hyperbolic model fits by the PRESS statistic (PRESS x 10^3) where lower values represent a better fit to the model.

Date/Site	Fraction	V_{max} ± SE	PRESS
Aug 06			
BLBK	<0.2 µm	0.96±0.10*	3.50
BLBK	<1.2 µm	1.28±0.16	4.90
BLBK	NF	2.94±0.77	9.90
BLBK	L	2.69±0.47	4.00
BLBK	LE	5.01±1.79	2.00
DK	<0.2 µm	0.59±0.07*	8.30
DK	<1.2 µm	2.56±0.54	4.30
DK	NF	8.50±3.71	4.20
DK	L	16.58±12.43	1.80
DK	LE	10.00±5.40	2.90
RK	<0.2 µm	0.47±0.03*	1.70
RK	<1.2 µm	0.49±0.05*	6.60
RK	NF	0.64±0.07*	5.40
RK	L	1.63±0.28	6.50
RK	LE	9.56±4.03	1.50
Nov 06			
BLBK	<0.2 µm	0.23±0.01*	0.50
BLBK	<1.2 µm	0.38±0.03*	2.40
BLBK	NF	0.52±0.04*	4.40
BLBK	L	0.81±0.10*	7.80
BLBK	LE	0.80±0.09*	3.90
DK	<0.2 µm	0.24±0.01*	1.40
DK	<1.2 µm	23.09±43.30	67.60
DK	NF	4.26±0.77	2.70
DK	L	11.08±8.01	20.30
DK	LE	9.13±6.48	27.60
RK	<0.2 µm	0.49±0.04*	5.50
RK	<1.2 µm	0.65±0.07*	10.50
RK	NF	1.10±0.19	44.40

RK	L	1.87±0.45	73.30
RK	LE	2.86±0.71	22.70
Jan 07			
BLBK	<0.2 µm	0.07±<0.01*	0.10
BLBK	<1.2 µm	0.07±<0.01*	0.07
BLBK	NF	0.16±<0.01*	0.07
BLBK	L	0.21±0.01*	0.40
BLBK	LE	0.32±0.02*	2.40
DK	<0.2 µm	0.32±0.02*	2.90
DK	<1.2 µm	0.47±0.05*	3.10
DK	NF	3.45±0.94	10.30
DK	L	2.35±0.70	17.10
DK	LE	2.72±0.48	2.40
RK	<0.2 µm	0.46±0.03*	3.40
RK	<1.2 µm	0.52±0.04*	1.50
RK	NF	ns	26.20
RK	L	10.68±14.10	30.30
RK	LE	9.25±6.53	18.20
Apr 07			
BLBK	<0.2 µm	0.15±<0.01*	0.10
BLBK	<1.2 µm	0.30±0.01*	0.20
BLBK	NF	0.34±0.02*	1.40
BLBK	L	0.47±0.05*	8.00
BLBK	LE	0.98±0.09*	4.10
DK	<0.2 µm	0.29±0.01*	0.90
DK	<1.2 µm	0.31±0.03*	4.10
DK	NF	0.50±0.02*	2.10
DK	L	5.10±2.80	17.60
DK	LE	ns	13.50
RK	<0.2 µm	0.53±0.04*	3.80
RK	<1.2 µm	0.66±0.03*	2.10
RK	NF	1.28±0.09	11.30
RK	L	3.68±0.95	12.20
RK	LE	4.31±2.65	14.30

(ns) = not saturating-V_{max} > 100.
(*) = V_{max} estimates with low error terms and PRESS statistic fits to the MM model.

2.3.4. PME Levels in Florida Bay

Although APA kinetics were linked to biological activity in the water column and potential rates were high, PME levels measured in the bay during this study fell below the limits of detection 75% of the time and when detectable were between 0.001 and 0.064 µmol L^{-1} (Table 2.2). Sampling 28 sites throughout the entire bay (Fig. 2.1) also resulted in non-detectable PME levels 47% of the time, and when detectable, ranged between 0.001 and 0.061 µmol L^{-1}, less than or equal to P*i* concentrations (Table 2.6). While PMEs are likely a transient pool in a highly P-limited system, such as Florida Bay, even the total DOP pools (TDP) were <0.59 µmol L^{-1} during this study across study sites and seasons (Table 2.2).

Table 2.6. Soluble reactive phosphorus (P*i*) and phosphomonoester (PME) concentrations measured at Boyer's Florida Bay long-term monitoring sites (see Fig. 1) September, 2006.

Site (number)	Latitude	Longitude	µmol L^{-1}	
			P*i*	PME
Card Sound Bridge (1)	25°16.42'	80°22.48'	0.281±0.049	0.045
Middle Key (2)	25°17.10'	80°23.70'	0.212±0.028	0.035
Manatee Bay (3)	25°15.06'	80°24.91'	0.213±0.027	bd
Barnes Sound (4)	25°13.30'	80°23.30'	0.292±0.030	bd
Blackwater Sound (5)	25°10.44'	80°25.39'	0.131±0.028	0.006
Little Blackwater Sound (6)	25°12.40'	80°26.42'	0.192±0.003	bd
Highway Creek (7)	25°15.22'	80°16.65'	0.044±0.007	bd
Long Sound (8)	25°13.64'	80°27.70'	0.108±0.009	0.044
Duck Key (9)	25°10.62'	80°29.49'	0.061±0.017	0.003
Joe Bay (10)	25°13.47'	80°32.20'	0.048±0.003	bd
Little Madeira Bay (11)	25°10.51'	80°37.62'	0.020±0.004	0.023
Terrapin Bay (12)	25°08.42'	80°42.97'	0.226±0.005	0.046
Whipray Basin (13)	25°05.49'	80°45.29'	0.376±0.018	bd
Garfield Bight (14)	25°09.03'	80°48.55'	0.221±0.046	0.044
Rankin Lake (15)	25°07.28'	80°48.17'	0.194±0.001	bd
Murray Key (16)	25°07.10'	80°56.38'	0.272±0.022	bd
Johnson Key Basin (17)	25°02.55'	80°54.89'	0.107±0.017	0.061
Rabbit Key Basin (18)	25°00.15'	80°54.01'	0.195±0.015	bd
Twin key Basin (19)	24°58.66'	80°45.21'	0.317±0.042	0.001
Peterson Keys (20)	24°55.77'	80°45.03'	0.429±0.013	bd

Porpoise Lake (21)	25°00.40'	80°40.88'	0.450±0.039	0.037
Captain Key (22)	25°02.41'	80°36.84'	0.216±0.004	0.017
Park Key (23)	25°07.08'	80°35.98'	0.011±0.010	0.012
Butternut Key (24)	25°06.11'	80°31.88'	0.105±0.004	bd
East Cape (25)	25°05.02'	81°04.84'	0.126±0.021	0.036
Oxfoot Bank (26)	24°58.64'	81°00.10'	0.138±0.007	bd
Sprigger Bank (27)	24°55.12'	80°56.09'	0.122±0.001	0.047
Old Dan Bank (28)	24°52.03'	80°48.43'	0.079±0.010	bd

bd = below detection.

2.3 Discussion

Alkaline phosphatase activities in the surface waters of Florida Bay were extremely high, averaging 356, 695 and 751 nmol P L^{-1} h^{-1} in northeastern, northcentral and western bay sites, respectively (2 µmol L^{-1} MUF-P). Long term decadal monitoring studies in Florida Bay (Boyer et al. 1997, 1999) also consistently reported high APA in unfiltered surface waters, using a similar fluorescent PME substrate (methylfluorescein phosphate at 2 µmol L^{-1}). Boyer et al. (1999), in a summary of long-term water quality data in the bay from 1989 to 1997, showed median APA values of 400, 1,950 and 240 nmol P L^{-1} h^{-1} from the east, central and western basins of the bay, respectively. In Boyer et al. (2006), APA in the bay ranged from 100 to 4,500 nmol P L^{-1} h^{-1} within the 95 percentile of the mean (Table 2.7a), comparable to AP activities in the interior mangrove zones of the southwest Florida coast in Whitewater Bay, within the largest contiguous mangrove forest in North America. However, in the south Florida estuaries with greater tidal exchange and more open coastal zones, AP peak activities are about an order of magnitude lower than in Florida Bay or Whitewater Bay interior. For example, in the southwestern Florida coastal mangrove creeks (Whitewater Bay coastal region; Boyer, 1997), with moderate tidal influence (~1 m) and in Biscayne Bay, Rookery Bay and along the southwest Florida shelf, AP activities had average values ranging from 100 to 190 nmol P L^{-1} h^{-1} (Boyer

2006, Table 2.7a). Cotner et al. (2000) and Glibert et al. (2004) in their experimental studies on nutrient dynamics and phytoplankton blooms in Florida Bay also support our results and those of Boyer (et al., 1997; et al., 1999; 2006) with ranges of APA from 30 to 2,350 nmol L^{-1} h^{-1} (Table 2.7a). Thus, interior estuaries associated with the Everglades ecosystem appear to possess some of the highest potential rates for PME hydrolysis among coastal estuaries in south Florida and other marine systems (Table 2.7a).

Comparing our PME hydrolysis rates to other estuaries and coastal zones using similar fluorescent substrates, only a few studies had AP activities within the range we estimated for Florida Bay. These included APA rates for the relatively P-limited Bay of Biscay, the Mississippi plume in the Gulf of Mexico, Hudson River estuary and Baltic Sea (Table 2.7b), all of which are high in organic carbon and primary productivity. In contrast to these relatively high APA systems, those reported for open oceans represent the other extreme end member. APA reported for the Indian Ocean and northeast Atlantic, as well as the highly P-limited Mediterranean Sea, had rates of enzyme hydrolysis of PMEs that were extremely low, orders of magnitude lower than those determined for Florida Bay and other estuaries (Table 2.7c). These lower open ocean estimates for APA may be attributable to the fact that these systems maintain extremely low numbers of organisms (Sebastián et al., 2004) that could act as substrates for microbial production of AP. In addition, APA has been shown to increase, sometimes >10-fold, with depth (Hoppe and Ullrich, 1999) up to 4,000 m, suggesting that AP fluxes from the surface to the deep ocean via rapidly sinking particles further limit the potential for PME hydrolysis in surface waters (Koike and Nagata 1997).

Table 2.7. Literature comparisons of APA in marine ecosystems comparing reported activities from a) south Florida estuaries, b) other estuarine/shelf systems, and c) open ocean systems based on studies using fluorescent substrates.

$P_{substrate}$ (µM)	APA_{vol} (nmol L^{-1} h^{-1})	Fraction (µm)	Location	Source
a) South Florida Estuarine Systems				
-	<100-1,600 (400)	NF	Florida Bay (Western)	Boyer et al. 1997*
-	100-2,000 (500)	NF	Florida Bay (Eastern)	Boyer et al. 1997
-	500-4,500 (3,000)	NF	Florida Bay (Northcentral)	Boyer et al. 1997
-	250-2,600 (600)	NF	Whitewater Bay (Interior/mangroves)	Boyer et al. 1997
-	<100-400 (100)	NF	Whitewater Bay (Coastal/creeks)	Boyer et al. 1997
1.0	33-2,352	NF	Florida Bay (East to West)	Cotner et al. 2000
-	100-1,800	NF	Florida Bay (East to West)	Glibert et al. 2004
1-200	61-1,022	NF	Florida Bay	Williams & Jochem 2006
2.0	137-1,219	NF	Florida Bay (East to West)	This study
-	135 (190)	NF	Biscayne Bay	Boyer, 2006**
-	58 (141)	NF	Ten Thousand Islands (Coastal)	Boyer, 2006
-	46 (53)	NF	Rookery Bay	Boyer, 2006
-	44 (172)	NF	Florida SW Shelf	Boyer, 2006
2.0	246-1,135	<1	Florida Bay (East to West)	This study
2.0	62-353	<0.2	Florida Bay (East to West)	This study
b) Other Estuarine/Shelf Systems				
0.1-10	200-500	NF	Gulf of Mexico (Mississippi plume)	Ammerman & Glover 2000
0.5-250	2-477	NF	Bay of Biscay	Labry et al., 2005
~50	15-158	NF	Palmones River Estuary	Hernàndez et al. 2000
20	1-125	NF	Hudson River Estuary	Taylor et al.2003
250	10-550	NF	Baltic Sea (River Plume) Summer	Nausch 1998
250	5-85	NF	Baltic Sea (River Plume) Fall	Nausch 1998
200	0-108	NF	North Adriatic Sea (Coastal)	Zaccone & Caruso 2002
-	2-20	NF	Tokyo Bay	Kobori & Taga 1979
-	0.3-2	NF	Sagami Bay (Coastal)	Kobori & Taga 1979
-	0.3-4.3	NF	Suruga Bay (Coastal)	Kobori & Taga 1979

0.5-250	18-321	>1	Bay of Biscay	Labry et al., 2005
0.5-250	26-30	0.2-1	Bay of Biscay	Labry et al., 2005
0.5-250	<1-126	<0.2	Bay of Biscay	Labry et al., 2005
c) Open Ocean Systems				
10	0-48	NF	Central Atlantic	Vidal et al. 2003
100-150	0.2-1.5	NF	Central Pacific	Koike & Nagata 1997
250	0.2-0.6	NF	Indian Ocean	Hoppe & Ullrich 1999
250	2.3-3.1	NF	Indian Ocean (Upwelling)	Hoppe & Ullrich 1999
-	1.4-2.7	NF	Sargasso Sea	Cotner et al. 1997
0.025-1	0.6-12.9	NF	Mediterranean Sea (Open Sea)	Van Wambeke et al. 2000
0.025-25	0.25-2.1	NF	Northeast Atlantic	Sebastián et al. 2004
10	0-29	>0.8	Central Atlantic	Vidal et al. 2003
10	0-9	0.2-0.8	Central Atlantic	Vidal et al. 2003
10	0-19	<0.2	Central Atlantic	Vidal et al. 2003

*-ranges 95 percentile with (mean) monthly sampling.
**-median (average) monthly sampling Biscayne Bay 93-06, Rookery Bay 99-06, Shelf 95-06, Ten Thousand Isl. 94-06 (n=2,000 – 4,000 samples).

In contrast, Florida Bay is shallow (~2m) with numerous mud banks and mangrove islands with a benthos dominated by seagrass, all of which continually release organics to the water column (Brylinsky, 1977). In addition, freshwater from the Everglades marshes pulse organic rich nutrients into the northern bay during the rainy season and tropical storms (Rudnick et al., 1999). This results in chronic, as well as episodic organic nutrient inputs into the bay, and seeding of cyanobaceria from northern ecotone ponds (Louda, personal communication) that in turn stimulate phytoplankton and microbial populations in the water column. Phytoplankton blooms, indicated by 10-fold higher levels of Chl. a (1 to 15 µg L^{-1}) than background (<1 µg L^{-1}), were primarily dominated by cyanobacteria in this study. In Florida Bay, these blooms have become recurrent, particularly in the northcentral and western regions, and identified as primarily *Synechococcus elongatus* (Lavrentyev et al., 1998, Phlips et al., 1999, Glibert et al., 2004). As a group, cyanobacteria are known to possess very high cell-specific AP activities, approximately 33 times higher than other phytoplankton, including diatoms (Giraudet et al., 1997) and repeatedly show the capability to sequester organic P through enzyme hydrolysis of mono- and diesters (Glibert et al., 2004, Cotner et al., 2000). In Florida Bay, low APA per Chl. a was found at RK in August when diatoms dominated, a group known for relatively low AP activities (Nicholson et al., 2006), in comparison to cyanobacteria.

Recent molecular evidence also suggests that at least some marine strains of *Synechococcus* have the capacity to sequester what has been considered non-labile organic P pools such as phosphonates (Palenik et al., 2003; Moore et al., 2005; Dyhrman et al., 2005), a potentially large fraction of TP in seawater (Clark et al., 1998, Karl and

Björkman, 2002). *Synechococcus* also has solute-binding proteins for urea (Palenik et al., 2003) and has been shown to take up this form of organic nitrogen in Florida Bay (Glibert et al., 2004). Organic N, APA and organic C have also emerged as a principle component in multivariate analysis of water quality data from Florida Bay and Whitewater Bay (Boyer et al., 1997, Boyer, 2006), although Chl. a clustered with TP and turbidity. Thus, the combination of organic nitrogen utilization, in parallel with rapid organic P hydrolysis, would allow for nutrient sequestration under pulsed organic nutrient loads from the Everglades as well as sediment and seagrass communities in the benthos, which primarily efflux organic material to the water column (Velimirov, 1986; Bugden et al., 1998). Once the organic P is hydrolyzed by free AP in the water column, cyanobacteria, with also a high affinity for inorganic P, can rapidly sequester phosphate (Scanlan et al., 1993; Su et al., 2003; Moore et al., 2005, Nielsen et al., in press). These nutrient cycling processes may promote rapid formation and maintenance of cyanobacterial blooms even as they move across the bay driven by wind, a noted occurrence (Phlips et al., 1999; Boyer et al., 1999; Glibert et al., 2004).

While maximum rates of PME hydrolysis were found in our study during cyanobacteria blooms, the dissolved AP pool accounted for the majority of enzyme hydrolysis, based on the water column fractioned to <0.2 µm. Thus, normalizing APA to Chl a. might be misleading in Florida Bay, where most of the APA appears to be contributed by the microbial and free dissolved AP. During blooms, some of this activity may have been from cell lyses during filtration (Sala et al., 2001); however, we also found high APA in the dissolved fraction when Chl. a. levels were low. We estimated that freely dissolved enzymes can be major contributors to the total APA (20-76% at 2

µM MUF-P) in the water column of Florida Bay. Significant contributions of dissolved AP (42-74%; 13-44%) to the total activity (150 nmol L^{-1} h^{-1}; 400 nmol P L^{-1} h^{-1}) have also been observed in coastal waters of the northern Red Sea (Li et al. 1998) and in the estuarine waters in the Bay of Biscay (Labry et al. 2005). In the central Atlantic APA has also shown to be dominated by the free fraction (40-100%, Vidal et al., 2003). In fresh water systems, free dissolved activity contribution to total activity (50 nmol L^{-1} h^{-1}) was also found to be high (71-83%) (Hernandez et al., 2000) and correlated with bacteria and phytoplankton with a maxima in the zone where cell biotic lyses is high (4-5 m) (Reichardt et al., 1967). Sloppy feeding by zooplankton on algal cultures is known to release dissolved AP (Boavida and Heath, 1984), and these dissolved forms of AP can be stable for >40 days (Li et al., 1998). In Florida Bay, decomposing algae and bacteria during and post-blooms, which in this study lasted for months, probably release unassociated free AP. Glibert et al. (2004) also showed a strong relationship between cyanobacteria, bacteria counts, and APA indicating the strong association among biotic components and PME hydrolysis. Once freely dissolved APases are released, they would tend to accumulate in Florida Bay because of its long hydraulic residence time, particularly in interior basins with restricted flow from numerous mud banks and mangrove islands (Smith, 1984; Nuttle, 2000).

While most of the APA was accounted for by the <0.2 µm fraction, particularly at low PME concentrations, the other fractions added to the total activity. In the northeastern bay (BLBK), Chl. a normalized APA (1,604 nmol P Chl. a^{-1} h^{-1}) was 3-4 times higher than the central and western sites, also where Cotner et al. (2000) determined the highest bacteria:phytoplankton ratios. Thus bacteria, also with extremely

high potentials for PME hydrolysis, accounted for significant portion of APA found in the northeastern bay, and normalizing APA to Chl. a at this site is not applicable. APA contributions by bacteria were also high in the central bay at DK prior to and post algal blooms, suggesting that bacterial AP activities may be associated with cyanobacterial blooms in the bay. This is not surprising, as cyanobacteria produce copious amounts of organic polymers and mucilage which can act as substrates for microbial heterotrophs. Seagrass leaves may also support heterotrophs in the water column by releasing nutrients during decomposition, and may themselves contribute to enzyme hydrolysis of PMEs. However, in this study we only found modest increases in the APA (14-20%) of the water column with the addition of seagrass leaves. This APA may be locally important, but is not as significant as dissolved, microbial, and cyanobacteria in defining the Florida Bay estuary as a high end member for APA in marine systems (Table 2.7).

The high APA observed in different ecosystem fractions of the bay may be an adaptation to respond to high turnover rates of natural PME substrates in this P-limited estuary; however, very little is known about the forms and availability of DOP in Florida Bay (Boyer et al., 2006) as well as other oligotrophic marine systems (Clark et al., 1998; Suzumura et al., 1998; Karl and Björkman, 2002). While characteristics of organic P in the bay are unknown, there is a high percentage of TP represented by the DOP fraction. We observed the highest concentration of DOP and percentage of DOP:TP at BLBK (~0.34 µmol L^{-1}, 70 %) in the northeastern bay, followed by DK and RK (~0.20 µmol L^{-1}/ 18 and 30%) in the northcentral and southwestern bay, respectively, explained by the fact that DOP enters the bay primarily from the Everglades on the northeastern margin of the bay (Suzumura et al., 1998; Rudnick et al., 1999). Monthly determinations for 6 years

have also shown high DOP constituting 88% of TP (0.49 µmol L^{-1}) (Boyer et al., 1997) in Florida and Whitewater Bay. High proportions of DOP in the TP pool also result from high biological uptake of inorganic P by the water column (Nielsen et al., in press) and binding to carbonate sediments (Kitano et al., 1978, Zhang et al. 2004). Total DOP, however, does not provide an indicator of organic P availability, as many of the organic P fractions exported from terrestrial sources are refractory (Suzumura et al., 1998). Easily hydrolyzed DOP (PMEs) were undetectable 75% of the time from our three sites over the year, and when detectable, were between 0.001 and 0.064 µmol L^{-1}. We also measured PMEs across 28 sites throughout the bay with PMEs detectable 47% of the time, ranging from 0.001-0.061 µmol L^{-1}. In Florida Bay other organic substrates such as phosphodiesters may be important, as was reported for the freshwater Everglades (71% of DOP, Pant et al., 2002). However, based on the extremely active APA we found in the bay, it is unlikely that labile organic compounds will accumulate in a large measurable pool. In a dynamic system like Florida Bay where algal, microbial and benthic organisms compete for P and the microbial loop is active (Lavrentyev et al., 1998; Boyer et al., 2006), APA in the water column probably accounts for the negligible PME concentrations measured in this study.

We conclude that in shallow highly P-limited seagrass-dominated systems like Florida Bay, where DOP availability is high, hydrolysis of organic compounds may be a major pathway for P*i* regeneration and is mostly driven by the water column, particularly during cyanobacteria blooms. During non-bloom conditions, free dissolved APA is high enough in the system to saturate enzyme hydrolysis in the range of DOP concentrations found in the field. Hydrolysis rates of PMEs in this coastal estuary are in the upper range

of those reported for marine ecosystems, probably a function of the close association of the benthos (seagrass and sediment) and wetlands (mangroves and marsh) with the shallow water column, providing organic substrates and nutrients, which can support high microbial and algal activities with high APA (Cotner et al., 2000; Boyer et al., 2006).

2.4. References

Ammerman, J.W., Glover, W.B., 2000. Continuous underway measurement of microbial ectoenzyme activities in aquatic ecosystems. Marine Ecology Progress Series 201, 1-12.

Ammerman, J.W., Hood, R.R., Case, D.A., Cotner, J.B., 2003. Phosphorus deficiency in the Atlantic: An emerging paradigm in oceanography. Eos Transactions, American Geophysical Union 84, 165-170.

Boavida, M.J., Heath, R.T., 1984a. Phosphatase activity of *Chlamydomonas acidophila* Negoro (Volvocales, Chlorophyceae). Phycologia 25, 400–404.

Boyer, J.N., Fourqurean, J.W., Jones, R.D., 1997. Spatial characterization of water quality in Florida Bay and Whitewater Bay by multivariate analyses: zones of similar influence. Estuaries 20, 743-758.

Boyer, J.N., Fourqurean, J.W., Jones, R.D., 1999. Seasonal and long-term trends in the water quality of Florida Bay (1989-1997). Estuaries 22, 417-430.

Boyer, 2006. South Florida Coastal Water Quality Monitoring Network. Southeast Environmental Research Center, Florida International University, Miami, FL 33199. http://serc.fiu.edu/wqmnetwork/SFWMD-CD/index.htm.

Boyer, J.N., Dailey, S.K., Gibson, P.J., Rogers, M.T., Mir-Gonzalez, D., 2006. The role of dissolved organic matter bioavailability in promoting phytoplankton blooms in Florida Bay. Hydrobiologia 569, 71-85.

Brylinsky, M., 1977. Release of dissolved organic matter by some marine macrophytes. Marine Biology 39, 213-220.

Bugden, J.B.C., Guerrero, M.A., Jones, R.D., 1998. Spatial and temporal variation of marine bacterioplankton in Florida Bay, USA. Journal of Coastal Research 14, 1304-1313.

Cembella, A.D., Antia, N.J., Harrison, P.J., 1984. The utilization of inorganic and organic phosphorous compounds as nutrients by eukaryotic microalgae: A multidisciplinary perspective. Critical Reviews Microbiology 2,13–81.

Clark, L., Ingall, E., Benner, R., 1998. Marine phosphorus is selectively remineralized, Nature 393, 426.

Corbett, D.R., Chanton, J., Burnett, W., Dillon, K., Rutkowski, C., Fourqurean, J.W., 1999. Patterns of groundwater discharge into Florida Bay. Limnology and Oceanography 44, 1045-1055

Cotner, J.B., Ammerman, J.W., Peele, E.R., Bentzen, E., 1997. Phosphorus-limited bacterioplankton growth in the Sargasso Sea. Aquatic Microbial Ecology 13, 141-149

Cotner, J.B., Sada, R.H., Bootsma, H., Johengen, T., Cavaletto, J.F., Gardner, W.S., 2000. Nutrient limitation of heterotrophic bacteria in Florida Bay. Estuaries 23, 611-620.

Dyhrman, S.T., Chappell, P.D., Haley, S.T., Moffett, J.W., Orchard, E.D., Waterbury, J., Webb, E.A., 2005. Phosphonate utilization by the globally important marine diazotroph *Trichodesmium.* Nature 439, 68-71.

Dyhrman, S.T., Chappell, P.D., Haley, S.T., Moffett, J.W., Orchard, E.D., Waterbury, J., Webb, E.A., 2006. Phosphonate utilization by the globally important marine diazotroph *Trichodesmium*. Nature 439, 68-71.

Fourqurean, J.W., Zieman, J.C., Powell, G.V.N., 1992a. Relationships between porewater nutrients and seagrasses in a subtropical carbonate environment. Marine Biology 114, 57-65.

Fourqurean, J.W., Zieman, J.C., Powell, G.V.N., 1992b. Phosphorus limitation of primary production in Florida Bay: evidence from the C:N:P ratios of the dominant seagrass *Thalassia testudinum*. Limnology and Oceanography 37, 162-171.

Fourqurean, J.W., Jones, R.D., Zieman, J.C., 1993. Processes influencing water column nutrient characteristics and phosphorus limitation of phytoplankton biomass in Florida Bay, FL, USA: inferences from spatial distributions. Estuarine Coastal and Shelf Science 36, 295–314.

Fourqurean, J.W., Willsie, A., Rose, C.D., Rutten, M.L., 2001. Spatial and temporal pattern in seagrass community composition and productivity in south Florida. Marine Biology, 138, 341-354.

Giraudet, H., Berthon, J.L., Buisson, B., 1997. Comparison of the daily alkaline phosphatase activity of a cyanobacterium (*Microcystis aeruginosa*) and a diatom (*Synedra capitata*). Comptes rendus de l'Académie dea sciences. Série III, Sciences de la vie 320, 451-458.

Glibert, P.M., Neil, C.A., Hollander, D., Revilla, M., Hoare, A., Alexander, J., Murasko, S., 2004. Evidence for dissolved organic nitrogen and phosphorus uptake during a cyanobacterial bloom in Florida Bay. Marine Ecology Progress Series 280, 73-83.

Hernández, I., Fernández, J.A., Niell, F.X., 1993. Influence of phosphorus status on the seasonal variation of alkaline phosphatase activity in *Porphyra umbilicalis* (L.) Kützing. Journal of Experimental Marine Biology and Ecology 173, 181–196.

Hernández, I., Niell, F.X., Fernández, J.A., 1994b. Alkaline phosphatase activity in marine macrophytes. Study of its localization in some widespread species in southern Spain. Marine Biology 120, 501–509.

Hernández, I., Niell, F.X., Fernández, J.A., 1996a. Alkaline phosphatase activity of the red alga *Corallina elongata* Ellis et Solander. Sci. Mar. 60, 297–306.

Hernández, I., Christmas, M., Yelloly, J., Whitton, B.A., 1997. Factors affecting surface alkaline phosphatase activity in the brown alga *Fucus spiralis* at a North Sea intertidal site (Tyne Sands, Scotland). Journal of Phycology 33, 569–575.

Hernández, I., Andría, J.R., Christmas, M., Whitton, B.A., 1999. Testing the allometric scaling of alkaline phosphatase activity to surface/volume ratio in benthic marine macrophytes. Journal of Experimental Marine Biology and Ecology 241, 1–14.

Hernández, I., Pérez-Pastor, A., Pérez-Lloréns, J.L., 2000. Ecological significance of phosphomonoesters and phosphomonoesterase activity in a small Mediterranean river and its estuary. Aquatic Ecology 34, 107–117.

Hoppe, H.G. 1983. Significance of exoenzymatic activities in the ecology of brackish water: Measurements by means of methylumbelliferyl-substrates. Marine Ecology Progress Series 11, 299–308.

Hoppe, H.G., Ullrich, S., 1999. Profiles of ectoenzymes in the Indian Ocean: phenomena of phosphatase activity in the mesopelagic zone. Aquatic Microbial Ecology 19, 139-148.

Huang, B., Hong, H., 1999. Alkaline phosphatase activity and utilization of dissolved organic phosphorus by algae in subtropical coastal waters. Marine Pollution Bulletin 39, 205–211.

Kalle, K., 1945. In: Chemical Oceanography Vol. II, J.P. Riley and G. Skirrow (eds.), p.601. 1975. Academic Press, London.

Karl, D.M., Yanagi, K., 1997. Partial characterization of the dissolved organic phosphorus pool in the oligotrophic North Pacific Ocean. Limnology and Oceanography 42, 1398–1405.

Karl, D.M., Björkman, K.M., Dore, J.E., Fujieki, L., Hebel, D.V., Houlihan, T., Letelier, R.M., Tupas, L.M., 2001. Ecological nitrogen- to-phosphorus stoichiometry at station ALOHA. Deep-Sea Research II 48, 1529–1566

Karl, D.M., Björkman, K.M., 2002. Dynamics of DOP. In: Hansell DA, Carlson CA (eds) Biogeochemistry of marine dissolved organic matter. Academic Press, San Diego, p 249–366.

Kitano, Y., Okumura, M., Idogaki, M., 1978. Uptake of phosphate ions by calcium carbonate. Geochemistry Journal 12, 29-37.

Kobori, H., Taga, N., 1979. Occurrence and distribution of phosphatase in neritic and oceanic sediments. Deep-Sea Research 26, 799-808.

Koike, I., Nagata, T., 1997. High potential activity of extracellular alkaline phosphatase in deep waters of the central Pacific. Deep Sea Research II 44, 2283-2294.

Labry, C., Delmas, D., Herblandi, A., 2005. Phytoplankton and bacterial alkaline phosphatase activities in relation to phosphate and DOP availability within the

Gironde plume waters (Bay of Biscay). Journal of Experimental Marine Biology and Ecology 318, 213–225.

Lapointe, B.E., Clark, M.W., 1992. Nutrient inputs from the watershed and coastal eutrophication in the Florida Keys. Estuaries 15, 465–476.

Lapointe, B.E., Tomasko, D.A., Matzie, W.R., 1994. Eutrophication and trophic state classification of seagrass communities in the Florida Keys. Bulletin of Marine Science 54, 696–717.

Lapointe, B.E., 1997. Nutrient thresholds for bottom-up control of macroalgal blooms on coral reefs in Jamaica and Southeast Florida. Limnology and Oceanography 45, 1119–1131.

Lavrentyev, P. J., Bootsma, H.A., Johengen, T.H., Cavaletto, J.F., Gardner, W.S., 1998. Microbial plankton response to resource limitation: insights from the community structure and seston stoichiometry in Florida Bay, USA. Marine Ecology Progress Series 165, 45-57.

Li, H., Veldhuis, M.J.W., Post, A.F., 1998. Alkaline phosphatase activities among planktonic communities in the northern Red Sea. Marine Ecology Progress Series 173, 107-115.

Martinez, J., Smith, D.C., Steward, G.F., Azam, F., 1996. Variability in ectohydrolytic enzyme activities of pelagic marine bacteria and its significance for substrate processing in the sea. Aquatic Microbial Ecology 10, 223-230.

Meybeck, M., 1993. C, N, P and S in rivers: from sources to global inputs. In Interactions of C, N, P and S Biogeochemical Cycles and Global Change, ed. R. Wollast, F.T. Mackenzie, L. Chou, pp. 163-93. Berlin: Springer-Verlag.

Monaghan, E., Ruttenberg, K., 1999. Dissolved organic phosphorus in the coastal ocean: Reassessment of available methods and seasonal phosphorus profiles from the Eel River Shelf. Limnology and Oceanography 44, 1702-1714.

Moore, L.R., Ostrowski, M., Scanlan, D.J., Feren, K., Sweetsir, T., 2005. Ecotypic variation in phosphorus-acquisition mechanisms within marine picocyanobacteria. Aquatic Microbial Ecology 39, 257-269.

Murphy, J., Riley, J.P., 1962. A modified single solution method for the determination of phosphate in natural waters. Anal. Chim. Acta 27, 31 36.

Nausch, M., 1998. Alkaline phosphatase activities and the relationship to inorganic phosphate in the Pomeranian Bight southern Baltic Sea. Aquatic Microbial Ecology 16, 87–94.

Nicholson, D., Dyhrman, S., Chavez, F., Paytan, A., 2006. Alkaline phosphatase activity in the phytoplankton communities of Monterey Bay and San Francisco Bay. Limnology Oceanography 51, 874-883.

Nielsen, O.I., Koch, M.S., Jensen, H.S., Madden, C.J., 2006. *Thalassia testudinum* phosphate uptake kinetics at low in situ concentration using a ^{33}P radioisotope technique. Limnology and Oceanography 51, 208-217.

Nuttle, W.K., Fourqurean, J.W., Cosby, B.J., Zieman, J.C., Robblee, M.B., 2000. Influence of net freshwater supply on salinity in Florida Bay. Water Resources Research 36, 1805-1822.

Palenik, P., Brahamsha, B., Larimer, F.W., Land, M., Hauser, L., Chain, P., Lamerdin, J., Regala, W., Allen, E.E., McCarren, J., Paulsen, I., Dufresne, A., Partensky, F., Webb, E.A., Waterbury, J., 2003. The genome of a motile marine *Synechococcus.* Nature 424, 1037-1042.

Pant, K.H., Reddy, K.R., Dierberg F.E., 2002. Bioavailability of organic phosphorus in a submerged aquatic vegetation-dominated treatment wetland. Journal of environmental quality 31, 1748-1756.

Pérez, M., Romero, J., 1993. Preliminary data on alkaline phosphatase activity associated with Mediterranean seagrasses. Botanica Marina 36, 499-502.

Phlips, E.J., Badylak, S., Lynch, T.C., 1999. Blooms of the picoplanktonic cyanobacterium Synechococcus in Florida Bay, a subtropical inner-shelf lagoon. Limnology and Oceanography 44, 1166-1175.

Reichardt, W., Overbeck, J., Steubing, L., 1967. Free Dissolved Enzymes in Lake Waters. Nature 216, 1345-1347.

Ray, J.M., Bhaya, D., Block, M.A., Grossman, A.R., 1991. Isolation, transcription, and inactivation of the gene for an atypical alkaline phosphatase of Synechococcus sp. strain PCC 7942. Journal of Bacteriology 173, 4297-4309

Rudnick, D.T., Chen, Z., Childers, D.L., Boyer, J.N., Fontaine, T.D., 1999. Phosphorus and nitrogen inputs to Florida Bay: The importance of the Everglades watershed. Estuaries 22, 398-416.

Sala, M.M., Karner, M., Arin, L., Marrase, C., 2001. Measurement of ectoenzyme activities as an indication of inorganic nutrient imbalance in microbial communities. Aquatic Microbial Ecology 23, 301-311.

Scanlan, D.J., Mann, N.H., Carr, N.G., 1993. The response of the picoplanktonic marine cyanobacterium *Synechococcus* species WH 7803 to phosphate starvation involves a protein homologous to the periplasmic phosphate-binding protein of *Escherichia coli.* Molecular Microbiology 10, 181–191.

Sebastián, M., Aristegui, J., Montero, M.F., Niell, F.X., 2004. Kinetics of alkaline phosphatase activity, and effect of phosphate enrichment: a case study in the NW African upwelling region. Marine Ecology Progress Series 270, 1-13.

Shan, Y., McKelvie, I.D., Hart, B.T., 1994. Determination of alkaline phosphatase hydrolyzable phosphorus in natural water systems by enzymatic flow injection. Limnology Oceanography 39, 1993–2000.

Smith, S.V., 1984. Phosphorus vs. nitrogen limitation in the marine environment. Limnology and Oceanography 29, 1149-1160.

Su, Z., Dam, P., Chen, X., Olman, V., Jiang, T., Palenik, B., Xu, Y., 2003. Computational inference of regulatory pathways in microbes: an application to phosphorus assimilation pathways in *Synechococcus* sp. WH8102. Genome Informatics 14, 3-13.

Suzumura, M., Ishikawa, K., Ogawa, H., 1998. Characterization of dissolved organic phosphorus in coastal seawater using ultrafiltration and phosphohydrolytic enzymes. Limnology and Oceanography 43, 1553–1564.

Taft, J. L., Loftus, M. E., Taylor, R. W., 1977. Phosphate uptake from phosphomonoesters by phytoplankton in Chesapeake Bay. Limnology and Oceanography 22, 1012-21.

Taylor, G.T., Way, J., Yu, Y., Scranton, I., 2003. Ectohydrolase activity in surface waters of the Hudson River and western Long Island Sound Estuaries. Marine Ecology Progress Series 263, 1-15.

Touchette, B.W., 1999. Physiological and Developmental Responses of Eelgrass (*Zostera marina* L.) to Increases in Water-Column Nitrate and Temperature. Ph.D. dissertation. North Carolina State University, Raleigh, NC.

Touchette, B.W., Burkholder, J.M., 2000. Review of nitrogen and phosphorus metabolism in seagrasses. Journal of Experimental Marine Biology and Ecology. 250, 133-167.

Van Wambeke, F., Christaki, U., Giannakourou, A., Moutin, T., Souvemerzoglou, K., 2002. Longitudinal and vertical trends of bacterial limitation by phosphorus and carbon in the Mediterranean Sea. Microbial Ecology 43, 119–133.

Velimirov, B., 1986. DOC dynamics in a Mediterranean seagrass system. Marine Ecology Progress Series 28, 21-41.

Vidal, M., Duarte, C.M., Agusti, S., Gasol, J.M., Vaque, D., 2003. Alkaline phosphatase activities in the central Atlantic Ocean indicate large areas with phosphorus deficiency. Marine Ecology Progress Series 262, 43–53.

Yelloly, J.M., Whitton, B.A., 1996. Seasonal changes in ambient phosphate and phosphatase activities of the cyanobacterium *Rivularia atra* in intertidal pools at Tyne Sands, Scotland. Hydrobiologia 325, 201–212.

Williams., C. J., Jochem, F.J., 2006. Ectoenzyme kinetics in Florida Bay: Implications for bacterial carbon source and nutrient status. Hydrobiologia 569, 113-127

Zaccone, R., Caruso, G., 2002. Microbial hydrolysis of polysaccharides and organic phosphates in the northern Adriatic Sea. Chemistry and Ecology 18, 85-94.

Zhang, J.Z., Fisher, C.J., Ortner, P.B., 2004. Potential availability of sedimentary phosphorus to sediment resuspension in Florida Bay. 600 Global Biogeochemical Cycles 18: GB4008. doi:10.1029/2004GB002255.

Zieman, J.C., Fourqurean, J.W., Iverson, R.L., 1989. Distribution, abundance and productivity of seagrasses and macroalgae in Florida Bay. Bulletin of Marine Sciences 44, 292-311.

CHAPTER 3

SEAGRASS (*THALASSIA TESTUDINUM*) NUTRIENT RECYCLING IN FLORIDA BAY, A CARBONATE-DOMINATED SHALLOW ESTUARY

3.0. Introduction

Seagrasses have high rates of primary production in coastal marine ecosystems worldwide (Hemminga and Duarte 2000). The resulting biomass serves as a direct food source to grazers or is transferred to the detrital and/or microbial food web (Larkum et al. 1989). High rates of primary production, however, require adequate nutrients, particularly for tropical seagrasses in oligotrophic estuaries and coastal lagoons. These benthic autotrophs reside in open systems with detrital export; thus, nutrients associated with biomass production can be lost from the system (Hemminga et al. 1991). Tropical seagrass communities with modest terrestrial nutrient loads are dependent on recycling of nutrients in situ and therefore may be prone to nutrient-limitation (Erftemeijer and Middelburg 1995). To offset these losses, efficient nutrient recycling by plants may occur by means of resorption, in which nutrients are transferred from senescent to growing tissue, an ecological process well established in the terrestrial plant literature (Chapin 1980; Chapin and Kedrowski 1983; Aerts 1996). Nutrient resorption is commonly reported in terms of efficiency, defined as the difference between the nutrient content of senescent versus young actively growing leaves (Van Heerwaarden et al. 2003). In seagrasses, leaching of nutrients from leaves to the water column may also contribute to a loss of nutrients over time. However, previous resorption studies disregard leaching affects, considering this flux to be relatively insignificant (<10%) based on work with the temperate seagrass *Zostera marina* (Borum et al. 1989). Average seagrass resorption efficiencies from previous studies have been estimated to be 15 to 40% for nitrogen (N) and 21 to 22% for phosphorus (P) (Borum et al. 1989; Pedersen and Borum 1993; Stapel and Hemminga 1997; Hemminga et al. 1999; Stapel et al. 2001; Lepoint et al. 2002).

However, high variance in nutrient resorption efficiencies has been found between and within species attributed to the trophic state at a particular site.

Resorption has been shown to increase with decreasing nutrient availability in terrestrial (Pugnaire and Chapin 1993; Van Heerwaarden et al. 2003) and wetland plants (Shaver and Melillo 1984; Rejmankova 2005), yet few studies have examined the effect of nutrient availability on seagrass resorption. Stapel and Hemminga (1997) calculated resorption efficiencies for several seagrass species (*Thalassia hemprichii, Enhalus acoroides, Cymodocea rotundata, Thalassodentron ciliatum, Posidonia oceanica,* and *Zostera marina*) from tropical (Indonesia and Kenya), Mediterranean (Spain), and temperate (Netherlands) areas and did not detect a difference in the resorption efficiencies between species with high and low leaf nutrient concentrations, which were used as an indicator of nutrient availability. When comparisons were made within particular species, *E. acoroides* and *T. hemprichii*, however, leaf nutrient resorption increased in plants with a high leaf nutrient concentration, indicating a positive relationship between resorption and nutrient availability (Stapel and Hemminga 1997). Pedersen and Borum (1993) calculated greater rates of N resorption in the seagrass *Z. marina* during seasons in which nutrient availability declined. Due to varying nutrient efficiencies reported for seagrass in the literature and the fact that no known study has examined nutrient resorption in the dominant tropical Atlantic seagrass species, *Thalassia testudinum*, often found growing in nutrient-depleted carbonate environments, *T. testudinum* nutrient resorption in Florida Bay was examined across a well established nutrient gradient (Fourqurean et al. 1992*ab*; Fourqurean et al. 1993).

Resorption not only reduces a plants dependence on external nutrients, but also influences the nutrient content of tissues, which can affect senescent leaf and below-ground tissue decomposition rates (Harrison 1989). High nutrient availability has also been shown to increase rates of decomposition in aquatic plants (Valiela et al. 1985; Xie 2004; Debusk and Reddy 2005), yet nutrient effects on seagrass decomposition have not been well established. Leaves of *Ruppia cirrhosa* under brackish conditions were found to decompose faster with the addition of either N or P (Menendez et al. 2003). Weight loss of decomposing *Z. marina* roots was also greater in sediment with a higher N content (Kenworthy and Thayer 1984). Nutrient additions to *P. oceanica* beds have been shown to significantly increase bacterial activity while simultaneously decreasing sediment organic matter, which indicated increased bacterial decomposition of seagrass detritus (Lopez et al. 1998). However, Fourqurean and Schrlau (2003) did not detect a difference in decomposition rates of the tropical seagrass *T. testudinum* among sites across a nutrient gradient in Florida Bay. It is clear that additional studies are required to better understand the link between nutrient availability and decomposition kinetics of seagrass for both above- and below-ground tissues, as these represent a large component of the labile nutrient pool in shallow seagrass-dominated estuaries.

In the present study, leaf nutrient resorption and decomposition rates of leaf, root and rhizome tissue were simultaneously examined in the dominant Caribbean/tropical Atlantic seagrass species, *T. testudinum*, across a nutrient gradient in Florida Bay, a carbonate-dominated P-limited shallow estuary. It was hypothesized that leaf nutrient resorption efficiencies, particularly for P, would decrease as nutrient availability increased across the trophic gradient, while senescent leaf, root and rhizome decay rates

(*k*) would increase. In addition, the quantitative importance of seagrass nutrient flux to the water column and sediment through decomposition processes in the bay was estimated.

3.1 Materials and Methods

3.1.1. Site Description

Decomposition and nutrient resorption experiments of the dominant tropical seagrass *Thalassia testudinum* were conducted at three sites in Florida Bay, a shallow (< 3 m) semi-enclosed estuary located at the southern tip of Florida (Fig. 3.1). A well established P gradient exists in the bay with the highest levels of P input in the western bay margin from the Gulf of Mexico and low P inputs in the eastern bay, as this region primarily receives fresh water from the P-limited freshwater Everglades marsh (Zieman et al. 1989; Fourqurean et al. 1992*ab*; Zhang et al. 2004; Nielsen et al. 2006). Three sites were chosen that encompass the east-west P gradient in the bay: Black Betsy Key (BLBK, N 25º 8.380', W 80º 38.848'), Dump Key (DK, N 25º 6.673', W 80º 46.251'), and Rabbit Key (RK, N 24° 58.830', W 80° 50.187') in the northeastern, northcentral, and western regions of the bay, respectively.

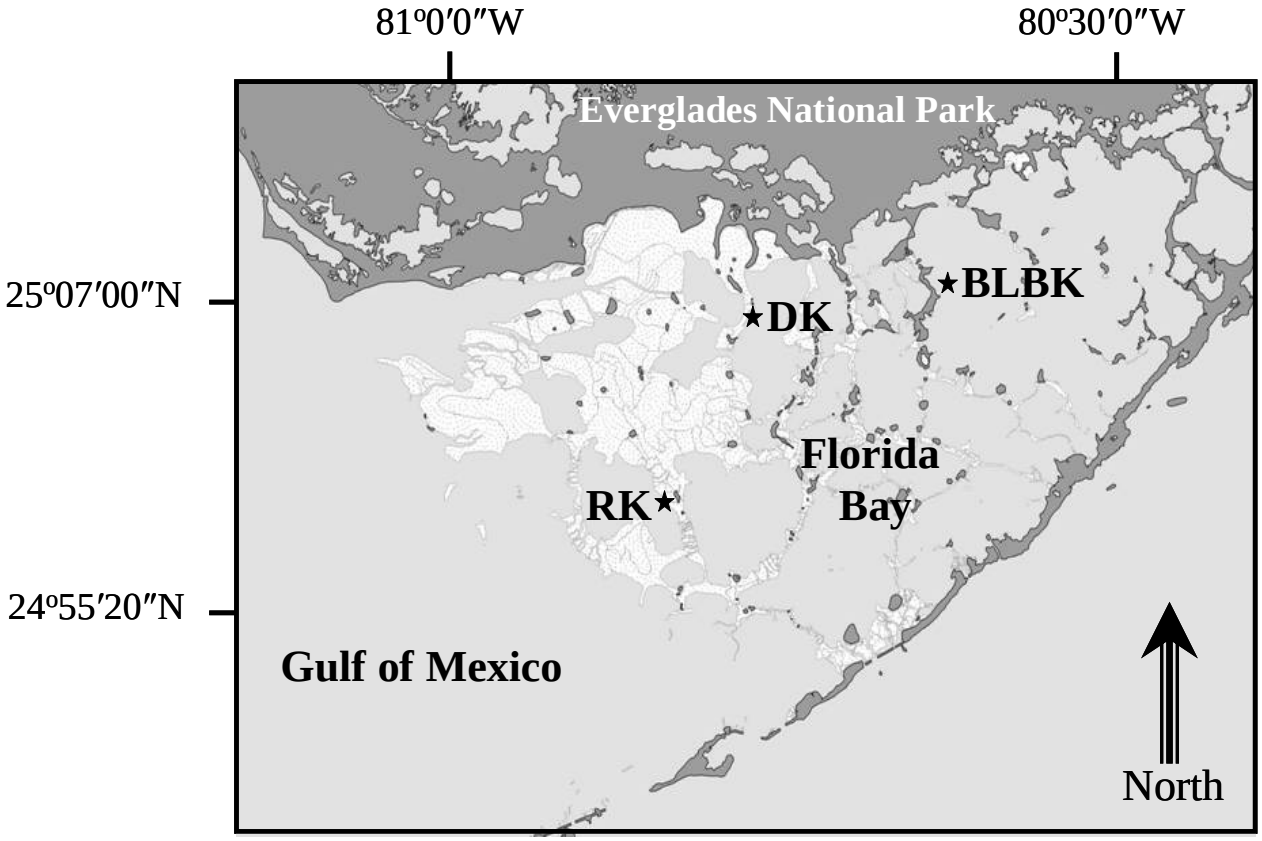

Figure 3.1. Study sites: Black Betsy Key (BLBK), Dump Key (DK), and Rabbit Key (RK) in Florida Bay, a semi-enclosed estuary at the southern terminus of the Florida peninsula bounded to the north by the fresh water Everglades marsh and to the south by the Florida Keys. Numerous mangrove islands (dark gray) and shallow mud banks (light gray) are noted.

3.1.2. Leaf Nutrient Resorption Study

3.1.2.1. Resorption Experiment

In order to calculate N and P resorption by *T. testudinum* leaves, nutrient changes between new and senescent leaves on short shoots were determined in May, August, October, and December 2006. During each sampling, between ten and twenty *T. testudinum* short shoots from each site were collected and cable-tied together to prevent detachment of senescent leaves upon sampling. The newest fully emergent leaf and terminal senescent leaf were rinsed with deionized (DI) water, and the attached epiphytes removed by gently sliding the surface of the leaf between two gloved fingers. Each leaf was oven dried at 80-90ºC until constant weight, weighed, and ground in liquid N_2. Depending on site and collection time, 2-4 leaves were pooled to obtain enough tissue for analyses (n = 4-7). Ground samples were analyzed for total carbon (TC) and total nitrogen (TN) using a CNS analyzer (Carlo Erba NA1500 Series 2) with a detection limit of 0.176% for TC and 0.044% for TN. Total phosphorus (TP) was determined by perchloric acid digestion followed by spectrophotometric analysis (EPA 365.2; method detection limit of 10 mg kg^{-1}). Leaf nutrient (N and P) resorption efficiencies, as % nutrient decline, were calculated using the following equation (Stapel and Hemminga 1997; Van Heerwaarden et al. 2003):

$$\text{\% nutrient decline} = \frac{L_{nfe} - L_{ts}}{L_{nfe}} * 100\%$$

where L_{nfe} is the nutrient concentration in the newest fully emergent leaf and L_{ts} is the nutrient concentration in the terminal senescent leaf.

3.1.2.2. Senescent Leaf Decomposing Tissue

Since the terminal senescent leaves between and within sites varied in the amount of decomposing tissue on the leaf, defined as brown tissue that was clearly in a state of decomposition, the area of this tissue was estimated to the nearest 10% before the leaf was processed for weight and nutrients, as described above. In addition, senescent leaves from each site were examined in December 2006 to determine the difference in tissue TN and TP between the upper decomposing brown tissue and lower yellowing section (10-24 leaves were pooled to obtain enough tissue for analysis; n = 2 sets of pooled leaves).

3.1.2.3. Leaf Biomass and Nutrient Production

During seasonal resorption studies (May, August, October, and December 2006), new leaf productivity was also measured and TN and TP production rates calculated. At each site, 10-20 short shoots were marked with a hypodermic needle at the base of each shoot, which produced a small visible scar on each leaf (Zieman 1974). Marked shoots were collected after 14 to 16 d, and the new growth determined and weighed. The number of shoots pooled together for TN and TP analysis varied (1-14 shoots) because of differences in new biomass allocation among sites and seasons, depending on net productivity rates. Seasonal leaf biomass production rates (g dwt m^{-2} d^{-1}; n = 5-16) were calculated from the percent of new growth each season and leaf biomass density at each site. Nutrient production rates (mmol TN or µmol TP m^{-2} d^{-1}) were calculated by multiplying leaf biomass production rates with the TN or TP concentration in new growth.

3.1.3. Decomposition Study

3.1.3.1. Litterbag Experiments

Decomposition experiments were initiated in February and August, 2006, allowing for the determination of decomposition and nutrient loss rates from *T. testudinum* leaves, roots, and rhizomes in the winter and summer. For leaves, ~200 terminal senescent leaves still attached to the shoots were collected, while cores (five 20 cm diameter) were taken to collect live root and rhizome tissue. Below-ground biomass measurements were also used to estimate total flux rates of nutrients based on decomposition rates and site-specific biomass (see calculations below). *T. testudinum* tissue was collected and transported in a cooler and immediately prepared for redeployment within 24 hours. Each tissue type was rinsed of sediment, wet weight determined, and divided amongst 30 litterbags, including 3 initial bags retained for initial nutrient content. Leaf epiphytes were not removed, because this would have changed the in situ microflora and carbonate epiphytes would have to be dissolved with acid, significantly influencing tissue and biotic composition. Replicate litterbags at each site contained approximately equal tissue biomass, however, due to variations in shoot size and biomass density among sites, initial wet weight for leaf, root and rhizome tissue ranged between 2-5, 2-4 and 6-15 g, respectively. Litterbags (10 cm x 20 cm) were constructed from vinyl-coated polyester mesh (1 x 2 mm pore size) and sewn together with monofilament (6 lb test). Leaf bags were placed at the sediment surface in the plant canopy, and roots and rhizomes buried at 10 cm, the depth observed to be the zone of maximum decomposition for *T. testudinum* root and rhizome tissue (Kenworthy and Thayer 1984). Nine bags of each tissue type were attached to nylon twine staked by PVC,

and three replicate lines were deployed totaling 27 bags of each tissue type per site. For the winter deployment, litterbags were collected at day 8, 20, 34, 60, 76, 105, 143, 194, and 238, while for the summer deployment, bags were collected at day 8, 18, 37, 51, 81, 109, 139, 164, and 185. A total of 486 litterbags were deployed during the decomposition study.

When sampled, litterbags were transported in a cooler to the laboratory within 24 h and all visible macrofauna removed. Tissue was carefully rinsed free of sediment in DI water, dried to constant weight at 80-90°C and weighed. Dried tissue was ground and analyzed for TC, TN, and TP as stated above in the resorption experiment. Resulting leaf decomposition rates may be slight overestimates due to attached epiphytes; however this was only a problem at RK where carbonate epiphytes dominated and an increase in mass over time occurred over the first 60 days during the 238 d decomposition study; thus, leaf decay rates in the winter at RK were not determined.

3.1.3.2. Decomposition and Nutrient Loss Calculations

Using the initial (W_0) and final (W_t) dry weight of each litterbag (corrected for wet:dry wt ratios) and nutrient content of the tissue, the proportion of original biomass (W_t/W_0) and total mass of nitrogen and phosphorus (TMN_t/TMN_0 and TMP_t/TMP_0) remaining was calculated at each time interval. Rates of biomass loss over time for each tissue type, over the sites and seasons sampled, were determined using a two parameter exponential decay model (Sigma Plot v. 9.0) with the following equation:

$$\frac{W_t}{W_0} = a * e^{-kt}$$

where W_0 is the initial dry weight, W_t is the dry weight at time *t*, *a* is the y-intercept, and *k* is the exponential decay constant.

Changes in N and P content via decomposition of each tissue type were also determined during both winter and summer decomposition experiments at every site. Rates of the total mass of nutrient loss were determined according to:

$$TMN_t \text{ or } TMP_t = \frac{W_t\ (TN_t \text{ or } TP_t)}{W_0\ (TN_0 \text{ or } TP_0)}$$

where TMN_t or TMP_t is the total mass of original N or P remaining, TN_t or TP_t is the tissue nutrient content remaining at time *t*, W_t is the dry weight at time *t*, W_0 is the initial dry weight, and TN_0 or TP_0 is the initial concentration of nutrients in the tissue. Subsequently, the total relative mass of nutrients over time was fit to an exponential decay equation, as above, for each tissue type, site, and season.

3.1.4. Site Temperature, Salinity, and O_2 Dynamics

During the resorption and decomposition study, water column temperature and salinity were recorded (YSI 85). Also, in August and November 2006 a series of diurnal O_2 measurements were taken (10-15 min intervals) using in situ data recorders (YSI 600 XLM) placed horizontally in the seagrass bed ~5 cm above the sediment surface. Ecosystem net production (9 hr d^{-1}) and respiration (24 hr d^{-1}) rates (µmol O_2 L^{-1} d^{-1}) were calculated from the linear regression slopes of oxygen flux for three consecutive days (n = 3).

3.1.5. Statistical Analyses

A 2-way ANOVA followed by the Holm-Sidak multiple comparison test (Sigma Stat v. 3.1) was used for site and seasonal comparisons of nutrient concentrations (TN and TP) in newly emergent leaves, TN declines between senescent and fully emergent leaves, tissue decay constants (senescent leaf, root, and rhizome), and O_2 production rates. Respiration rates were ranked prior to performing a 2-way ANOVA. TP declines between senescent and fully emergent leaves were compared among sites using the Kruskal-Wallis test on ranks followed by the Tukey's mean comparison test. TN concentrations between brown and yellowing tissue on senescent leaves were analyzed using a t-test, and a Mann-Whitney Rank Sum test for TP. Comparisons of leaf biomass production rates among sites were made using a 1-way ANOVA for the winter and Kruskal-Wallis for the remaining three seasons, followed by Tukey's test or Dunn's method (for unequal group size).

3.1.6. Calculation of Bay-wide Nutrient Fluxes

Because of the high component of leaf nutrient loss as live leaves senesced in this study, to determine rates of leaf nutrient release into the water column, resorption efficiencies for the tropical Indonesian seagrass *T. hemprichii* (31% P and 23% N; Stapel and Hemminga 1997) were subtracted from the average nutrient declines in senescent leaves in this study. Estimates of resorption in *T. hemprichii* were used because they represent the best independent estimate for resorption in *T. testudinum* and are slightly higher than the average seagrass resorption efficiencies reported in a literature review by Hemminga et al. 1999 (22% P; 20% N), and thus provide a conservative estimate for

rates of nutrient release into the water column through decomposition while still attached to the short shoots. The average bay-wide leaf standing crop of *T. testudinum* from 107 sites across Florida Bay (46 g dwt m^{-2}; Hall et al. 1999), the average P (0.095%) and N (2.20%) content of leaves from 50 sites in the bay (Fourqurean et al. 1992*a*), the leaf turnover rate of *T. testudinum* (2.19% d^{-1}; Zieman et al. 1989), and the average percent of leaf nutrients released into the water column (site and season) were used to calculate rates of nutrient release (mmol or µmol m^{-2} d^{-1}) from attached seagrass leaves on a bay-wide scale.

To determine rates of nutrient release from detached senescent leaves at each site, the senescent leaf nutrient content, rate of senescent leaf nutrient decline, based on decomposition experiments, and leaf biomass at each site, as well as the leaf turnover rate of *T. testudinum* in Florida Bay (2.19% d^{-1}; Zieman et al. 1989) were used.

To calculate rates of nutrient release from decaying rhizomes, average rhizome nutrient contents and nutrient decay rates from this study, as well as minimum and maximum reported *T. testudinum* rhizome productivity values (0.099 g dwt m^{-2} d^{-1}, Van Tussenbroek 1998; 1.76 g dwt m^{-2} d^{-1}, Patriquin 1973), were used. Nutrient decay rates from roots were calculated in the same way, however root productivity was estimated from rhizome productivity times the root:rhizome biomass ratio from this study (0.29), comparable to a previous estimate of 0.35 by Fourqurean and Zieman (1991).

3.2. Results

3.2.1. Resorption Study

3.2.1.1. Leaf Nutrient Retention

Changes in the N and P content of leaves senescing on *T. testudinum* short shoots elicited a complex pattern across sites which affected our ability to establish a true estimate of leaf nutrient resorption. The decline in leaf tissue nutrient concentration during senescence, the index used to calculate nutrient resorption, appeared to be significantly influenced by either nutrient loss by decomposition or leaching of nutrients to the water column. Tissue nutrient loss as leaves changed from a fully emergent to a senescent state was high, even though the senescent leaf typically followed the newly fully emergent leaf in a senescence sequence. Mean nutrient loss was 65% for P and 36% for N; however, it was also highly variable ranging from 29-95% and 14-55% for P and N, respectively, with significant site effects for both P and N ($p < 0.01$) and seasonal effects for N ($p < 0.01$; Fig. 3.2). At RK, the western bay site, senescent leaves had significantly lower

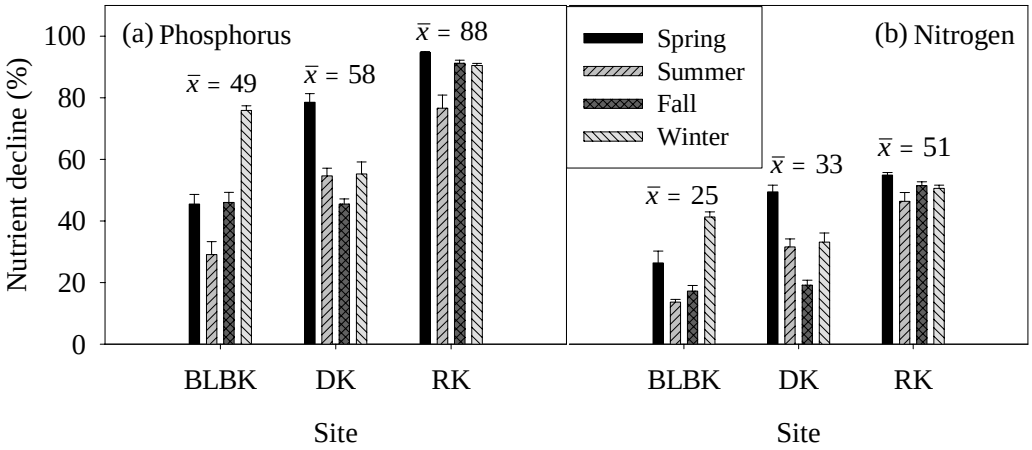

Figure 3.2. Seasonal senescent leaf phosphorus (a) and nitrogen (b) leaf decline as they senesced on the short shoot at three sites across Florida Bay: Black Betsy Key (BLBK), Dump Key (DK), and Rabbit Key (RK). Mean ± SE; n = 4-7 (10-21 pooled leaves). Values above bars represent the mean of all seasons for each site (n = 23).

retention of nutrients across all seasons compared to BLBK and DK, and averaged only 12 and 49% remaining leaf P and N, respectively, compared to fully emergent photosynthetically active leaves (Fig. 3.2). Overall BLBK had approximately 10% greater retention of both P and N compared to DK, although DK was greater in winter and both sites had similar retention in the fall for both N and P. While the difference in nutrient content between emergent and senescent leaves is frequently attributed to nutrient resorption, extremely low nutrient retention by seagrass leaves suggests that in Florida Bay leaf nutrient loss on the short shoot may be primarily accounted for by tissue leaching and/or decomposition.

3.2.1.2. Senescent Leaf Decomposing Tissue

This loss of nutrients on the shoot is evidenced by the fact that the difference in nutrient concentration between brown decomposing and yellowing tissue on the same senescent leaves were significantly different for both P ($p < 0.01$) and N ($p < 0.05$) with mean nutrient declines of 68% and 24%, respectively, across sites (Table 3.1). Due to the significantly lower nutrient content of decomposing tissue, the proportion of brown tissue on senescent leaves influenced site differences in nutrient declines between senescent and fully emergent leaves. Although these brown leaf segments of the leaves on live shoots lost a significant amount of nutrients, the total biomass of live green and senescent leaves were relatively similar, indicating that the decomposition associated with nutrient loss on the shoot enhanced nutrient leakage, rather than causing direct loss of tissue.

Table 3.1. Decline in *Thalassia testudinum* total phosphorus (TP) and total nitrogen (TN) from yellowing to decomposing tissue on the same senescent leaves at three sites across Florida Bay: Black Betsy Key (BLBK), Dump Key (DK), and Rabbit Key (RK, collected December 2006). Mean ± SE; n = 2 (from 10-24 pooled leaves).

Site	TP (% decline)	TN (% decline)
BLBK	72.4±0.7	30.2±3.3
DK	58.9±8.2	26.8±5.7
RK	73.5±4.4	15.8±9.2

3.2.1.3. *Nutrient Declines versus Percent Decomposing Tissue*

The relationship between tissue decomposing and percent nutrient decline showed some consistent site and seasonal patterns (Fig. 3.3). BLBK had the lowest decline in %P as a function of percent decomposing tissue compared to DK and RK, even when leaves showed 100% decomposing tissue in the fall (Fig. 3.3). In contrast, DK had a high % loss

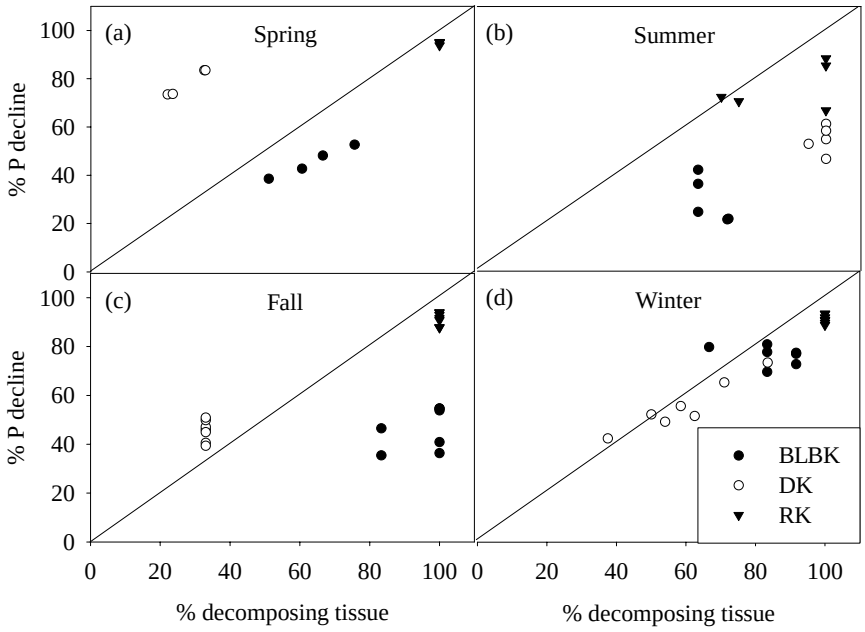

Figure 3.3. Relationship between decomposing tissue on senescent leaves, as estimated by area of brown tissue clearly in a state of decomposition, and the P decline between senescent and new fully emergent leaves on intact short shoots of *Thalassia testudinum* at Black Betsy Key (BLBK), Dump Key (DK) and Rabbit Key (RK) during (a) May, (b) August, (c) October, and (d) December, 2006.

of P, relative to the percent decomposing tissue and RK senescent leaves were almost always completely decomposed. RK retained very little P despite having on average only 0.3 leaves between senescent and the newest fully emergent leaf, slightly greater than the number between leaf pairs for BLBK (0.1) and DK (0.0). All sites contained on average less than 1 leaf between leaf pairs, suggesting that the greater nutrient decline at RK, relative to the other two sites, cannot be accounted for by a difference in the number of leaves between those which were senescent and newly fully emergent.

During the winter sampling, % P decline and decomposition of tissue were close to unity for all sites when growth rates were at a minimum (Fig. 3.3; Table 3.2) indicating that during other seasons, leaf growth patterns or shifts in decomposition may have changed the trajectory of nutrient conservation as leaves senesced on the short shoots. These seasonal patterns of leaf % P decline (Fig. 3.3) would also hold for % N loss,

Table 3.2. *Thalassia testudinum* leaf biomass, total phosphorus (TP), and total nitrogen (TN) production at Black Betsy Key (BLBK), Dump Key (DK) and Rabbit Key (RK). Biomass was extrapolated to m^{-2} using 41, 118 and 153 g dwt m^{-2} for BLBK, DK and RK, respectively. Mean ± SE; n = 5-16 for biomass production and n = 1-5 for TP and TN production, depending on the amount of biomass available for analyses.

Site	Spring	Summer	Fall	Winter
I. Biomass Production (g dwt m^{-2} d^{-1})				
BLBK	1.2±0.1	1.0±<0.1	1.3±0.1	0.6±0.2
DK	2.4±0.1	3.4±0.4	2.3±0.4	1.1±0.2
RK	2.9±0.2	3.3±0.4	2.4±0.2	0.7±0.1
II. TP Production (µmol TP m^{-2} d^{-1})				
BLBK	42±3	26±3	52±3	16
DK	90±3	126±13	116±13	55±<3
RK	90±10	100±13	103±13	26
III. TN Production (mmol TN m^{-2} d^{-1})				
BLBK	2.49±0.10	2.24±0.17	2.61±0.24	1.13
DK	4.52±0.19	7.02±0.74	4.88±0.61	2.71±0.26
RK	4.27±0.32	4.62±0.42	3.65±0.35	1.13

as there was a strong linear relationship between P and N loss in *T. testudinum* leaves from newly emergent to senescent leaves across sites (Fig. 3.4). The close relationship between % N and P decline across sites further suggests that seagrass leaf nutrients, a large pool of nutrients in the bay, are being turned over in the water column, prior to leaves detaching from the short shoot probably through decomposition and/or leaching.

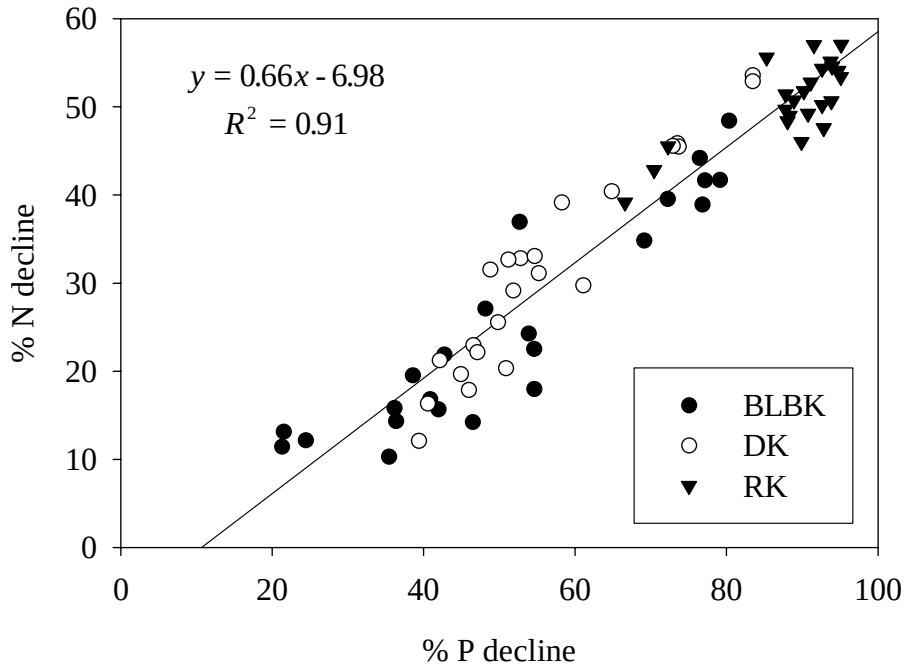

Figure 3.4. Linear relationship between leaf tissue N and P loss (%) as leaves senesced on the short shoots at Black Betsy Key (BLBK), Dump Key (DK) and Rabbit Key (RK), including all seasonal measurements.

3.2.1.4. Leaf Nutrient Content

The stoichiometry of leaf tissue nutrients, while frequently used as an indicator of site trophic state, and may influence plant tissue decomposition once in the detrital pool, was not as predicted across the established P gradient in the bay (Table 3.3). DK, the northcentral bay site, possessed significantly higher leaf TP concentration than the other two sites ($p < 0.01$). In fact, RK the most western bay site had statistically similar levels of TP in fully emergent new leaf tissues as BLBK in the eastern bay ($p = 0.95$). Even the C:P ratios were more similar between eastern and western bay sites than the central bay site. While this stoichiometry does not agree with the established P gradient in the bay, the anomaly is explained by dilution of P through growth. Growth rates at RK were significantly higher than those at BLBK ($p < 0.05$) by up to 3-fold, with the exception of winter when all growth rates were low (Table 3.2). The total amount of P sequestered by new leaf tissue was also 2-3 times higher at RK than BLBK during the growing season (Table 3.2).

Leaf tissue nutrient content at the RK site also indicated potential N limitation in comparison to the other two sites. RK had the lowest leaf TN content ($p < 0.01$) and thus the highest C:N ratio during all seasons (Table 3.3). This mismatch between TP and TN resulted in a similar N:P ratio between DK and RK, separating these two sites from BLBK; however, these ratios are not strictly a result of P limitation. Nitrogen allocation to leaves is clearly highest in the northcentral site at DK, particularly after the initial growth phase in spring, even though leaf biomass production is equivalent to RK (Table 3.2).

Table 3.3. Seasonal differences in total nitrogen (TN) and total phosphorus (TP) concentration and molar ratios of carbon (C), nitrogen (N), and phosphorus (P) in newly fully emergent and senescent leaves of *Thalassia testudinum* at three sites across Florida Bay: Black Betsy Key (BLBK), Dump Key (DK) and Rabbit Key (RK) in May, August, October, and December, 2005. Mean ± SE; n = 4-7 from 10-21 pooled leaves.

Site	Season	TN (g kg^{-1})	TP (mg kg^{-1})	C:N	C:P	N:P
I. Newest Fully Emergent Leaf						
BLBK						
	Spring	27±0.2	747±69	16±0.2	1,335±145	82±8
	Summer	30±0.7	788±70	15±0.3	1,342±150	87±8
	Fall	31±0.5	919±36	15±0.3	1,102±46	74±
	Winter	30±0.5	885±33	15±0.2	1,131±43	75±2
DK						
	Spring	27±0.3	901±47	16±0.2	1,037±53	67±3
	Summer	25±1.1	1,414±85	18±0.9	723±52	39±1
	Fall	30±0.6	1,388±77	14±0.2	706±40	49±3
	Winter	30±0.5	1,342±39	15±0.2	716±19	49±1
RK						
	Spring	22±0.4	1,125±49	19±0.3	808±39	43±3
	Summer	16±0.5	680±23	25±0.7	1,349±53	53±3
	Fall	20±0.4	784±35	20±0.4	1,144±53	56±2
	Winter	21±0.7	740±19	20±0.6	1,219±34	62±3
II. Senescent Leaf						
BLBK						
	Spring	20±1.0	411±53	22±1.2	2,494±388	110±11
	Summer	26±0.6	552±47	18±0.4	1,910±175	106±7
	Fall	25±0.5	494±31	18±0.4	2,091±130	115±5
	Winter	17±0.4	214±16	25±0.5	4,665±339	185±11
DK						
	Spring	14±0.5	191±21	29±1.0	4,778±552	162±14
	Summer	17±0.2	636±33	26±0.3	1,558±76	60±2
	Fall	24±0.5	758±53	18±0.5	1,344±91	73±4
	Winter	20±0.7	594±46	21±0.9	1,644±143	76±4
RK						
	Spring	10±0.2	60±5	42±0.7	15,507±1,386	372±38
	Summer	9±0.3	161±31	48±1.2	6,934±1,667	145±35
	Fall	10±0.2	68±7	41±0.8	13,379±1,383	327±32
	Winter	10±0.4	71±5	39±1.1	13,001±898	334±28

In situ loss of acquired nutrients from newly emergent leaves (Fig. 3.2) is seen in the nutrient concentrations and stoichiometry of senescent leaves (Table 3.3). At RK, leaves had the highest loss rate of both N and P, giving rise to almost an order of magnitude greater C:P ratio and 2-fold higher C:N ratio in senescent leaves compared to BLBK and DK. Interestingly, while the N:P ratio of photosynthetic leaves was lowest at RK, suggesting N limitation by the plant, the decomposing senescent leaves displayed the highest N:P ratio indicating a preferential loss of P. In all cases, the loss of nutrients in terms of total amount of nutrients and/or concentration is significantly lower in the senescent leaves compared to photosynthetic fully emergent leaves, resulting in a significant amount of nutrient loss on the short shoots. The relative differences among the loss rates of leaf nutrient content at the various sites subsequently had an impact on the decomposition rates of senescent leaves as detrital material on the sediment surface.

3.2.2. Decomposition Experiment

3.2.2.1. *Seasonal Effect on Decay Constants*

Water column respiration rates were 2.5 to 7-fold higher ($p < 0.01$) in August than November (Table 3.4), indicating an increase in heterotrophic activity at the initiation of the summer decomposition experiment when temperatures were on average ~5°C higher than winter incubations (Fig. 3.5). Senescent leaf decay constants (*k*) were also at a maximum in summer ($p < 0.01$; Table 3.5), and despite the shorter incubation period, significantly less senescent leaf biomass remained at all sites in summer compared to winter ($p < 0.05$; Fig. 3.6). On average, 90% of the senescent leaf biomass was decomposed over the summer deployment compared to 75% following winter

deployment. Root tissue also had significantly faster decay constants ($p < 0.01$) during the summer months (Fig. 3.7, Table 3.5), resulting in 70% loss rates in the summer compared to only 50% following winter deployments. Rhizomes, which generally decayed slower than senescent leaves or roots, had decay rates that were independent of season deployed ($p = 0.93$). The average rhizome biomass loss at all sites was only 54% after winter and 41% after summer deployment (Fig. 3.8).

Table 3.4. Net production and respiration at each site: Black Betsy Key (BLBK), Dump Key (DK), and Rabbit Key (RK). Rates calculated from linear regression slopes of oxygen fluxes over three consecutive days (n = 3).

		Net Production ($\mu mol\ O_2\ L^{-1}\ d^{-1}$)		Respiration ($\mu mol\ O_2\ L^{-1}\ d^{-1}$)	
Month	Site	Mean ± SE	R^2	Mean ± SE	R^2
August	BLBK	124.9±43.2	0.93-0.99	174.0±16.7	0.98-0.99
	DK	242.4±12.7	0.98-0.99	724.5±83.3	0.97-0.98
	RK	256.5±27.0	0.98-0.99	571.5±63.7	0.98-0.99
November	BLBK	36.6±6.5	0.96-0.98	70.5±10.5	0.95-0.97
	DK	101.3±10.3	0.98-0.99	100.5±18.8	0.96-0.99
	RK	70.9±1.9	0.98-0.99	177.0±8.4	0.99-0.99

3.2.2.2. Site Effects on Decay Constants

Decomposition of *T. testudinum* senescent leaves also significantly differed across sites ($p < 0.01$) with DK decay constants 2-3 times higher than BLBK and RK (Table 3.5). The slow leaf decay rates at BLBK in winter resulted in 40% of leaf biomass remaining after 238 d. Although RK kinetic data are not presented, because of epiphytes confounding weight loss of tissues, the final remaining biomass (26%) in winter was lower than at BLBK. In contrast, 90% of the senescent leaf biomass was decomposed at

DK even during winter months (Fig. 3.6). During the summer at DK, leaf senescent biomass loss increased to 97% with RK and BLBK also showing significant biomass declines, 87 and 95%, respectively. Comparing among sites, DK had the highest decay constants among sites in the summer (Table 3.5) corresponding to the highest respiration rates among sites during this period (Table 3.4).

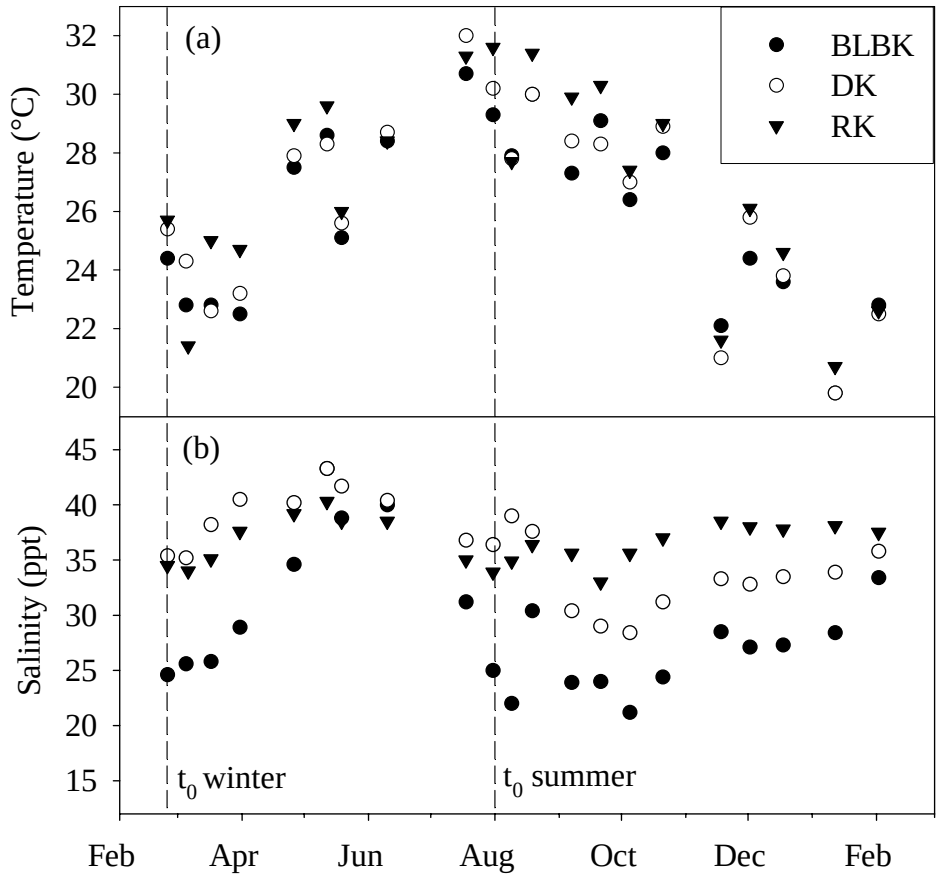

Figure 3.5. Temperature (a) and salinity (b) in the water column at each site: Black Betsy Key (BLBK), Dump Key (DK), and Rabbit Key (RK) over the study period. Time of winter and summer deployment of litterbags (t_0) is indicated by vertical dotted bars.

Table 3.5. Decay rate constants (k ± SE) for loss of plant tissue biomass and total mass of P (TMP) and N (TMN) over time at Black Betsy Key (BLBK), Dump Key (DK) and Rabbit Key (RK) using a 2-parameter exponential decay model. Model fit is described by the R^2 and the predicted residual error sum of squares (PRESS); the smaller the PRESS the better the model fit to data.

Site	Tissue Type	Winter Deployment			Summer Deployment		
		k x 10^{-4} (d^{-1})	R^2	PRESS	k x 10^{-4} (d^{-1})	R^2	PRESS
I. Biomass							
BLBK	Leaf	33±9	0.65	0.18	91±12	0.93	0.09
	Root	29±6	0.80	0.09	42±13	0.59	0.23
	Rhizome	34±3	0.95	0.03	36±7	0.77	0.10
DK	Leaf	82±2	0.81	0.24	129±17	0.94	0.10
	Root	40±7	0.83	0.10	65±7	0.93	0.06
	Rhizome	30±4	0.91	0.05	33±8	0.71	0.12
RK	Leaf	nd			78±13	0.88	0.13
	Root	35±5	0.87	0.09	66±8	0.91	0.08
	Rhizome	30±1	0.99	0.01	23±4	0.77	0.05
II. TMP							
BLBK	Leaf	35±37	0.08	0.91	144±14	0.97	0.06
	Root	60±18	0.67	0.30	27±11	0.46	0.22
	Rhizome	105±24	0.84	0.27	84±13	0.89	0.17
DK	Leaf	60±28	0.48	0.57	348±72	0.90	0.23
	Root	38±8	0.79	0.14	26±8	0.58	0.14
	Rhizome	63±18	0.72	0.32	704±167	0.88	0.24
RK	Leaf	nd			<1±17	<0.01	0.76
	Root	20±9	0.42	0.31	25±12	0.34	0.26
	Rhizome	66±11	0.88	0.13	85±15	0.85	0.15
III. TMN							
BLBK	Leaf	58±12	0.81	0.17	88±11	0.93	0.07
	Root	29±12	0.43	0.29	21±15	0.21	0.34
	Rhizome	93±20	0.81	0.22	45±11	0.71	0.17
DK	Leaf	64±16	0.76	0.24	141±31	0.85	0.26
	Root	34±10	0.62	0.20	30±12	0.47	0.23
	Rhizome	51±8	0.87	0.11	64±25	0.48	0.44
RK	Leaf	nd			55±11	0.81	0.16
	Root	19±6	0.59	0.14	27±10	0.48	0.19
	Rhizome	35±5	0.88	0.06	39±11	0.62	0.20

nd = not determined due to epiphytes increasing biomass.

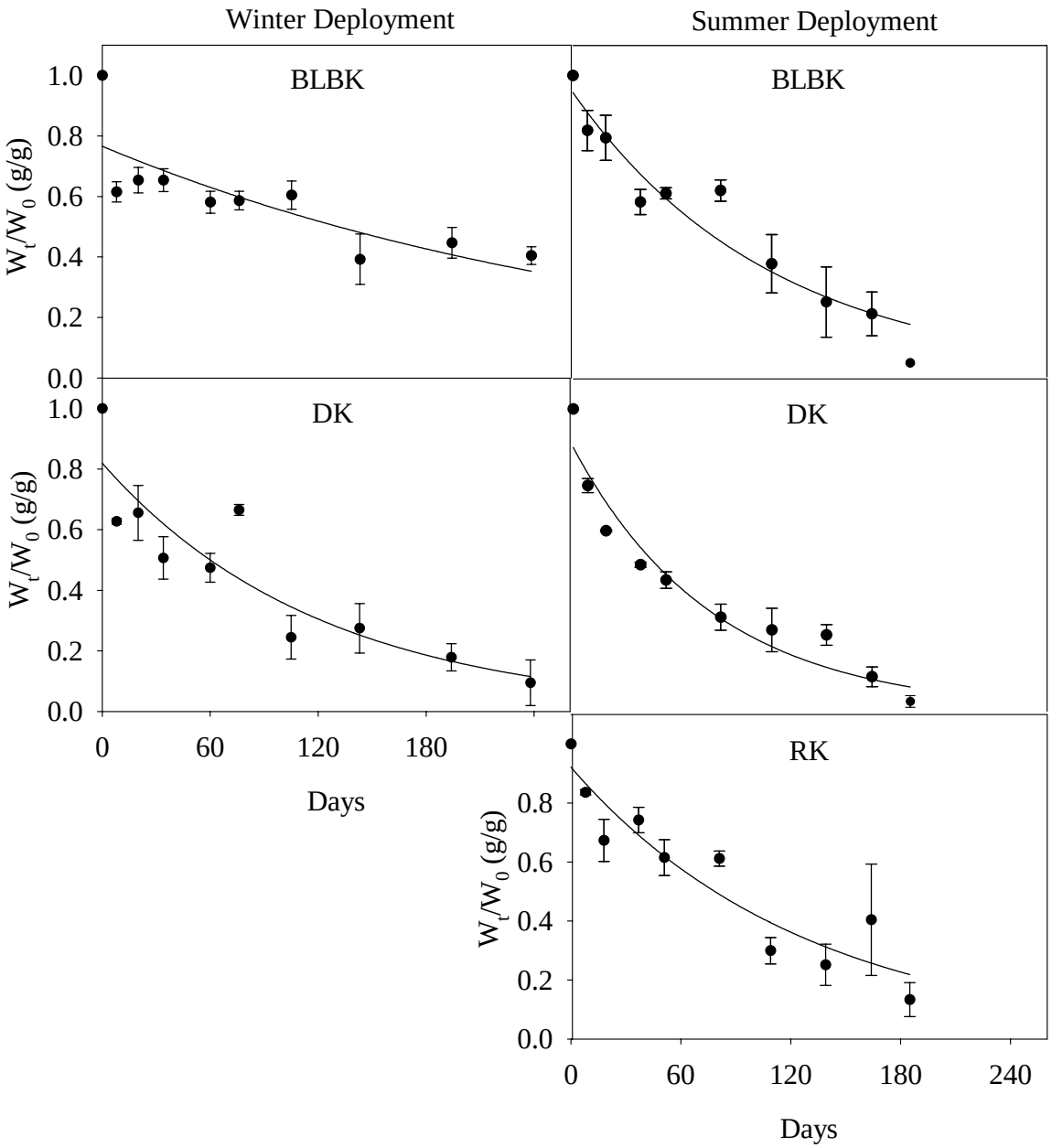

Figure 3.6. Proportional loss of senescent leaf biomass (mean ± SE; n = 3) deployed at each site in litterbags at Black Betsy Key (BLBK), Dump Key (DK), and Rabbit Key (RK) fit over time for each site and season with a 2-parameter exponential decay model. Winter deployment began in February, and summer deployment began in August.

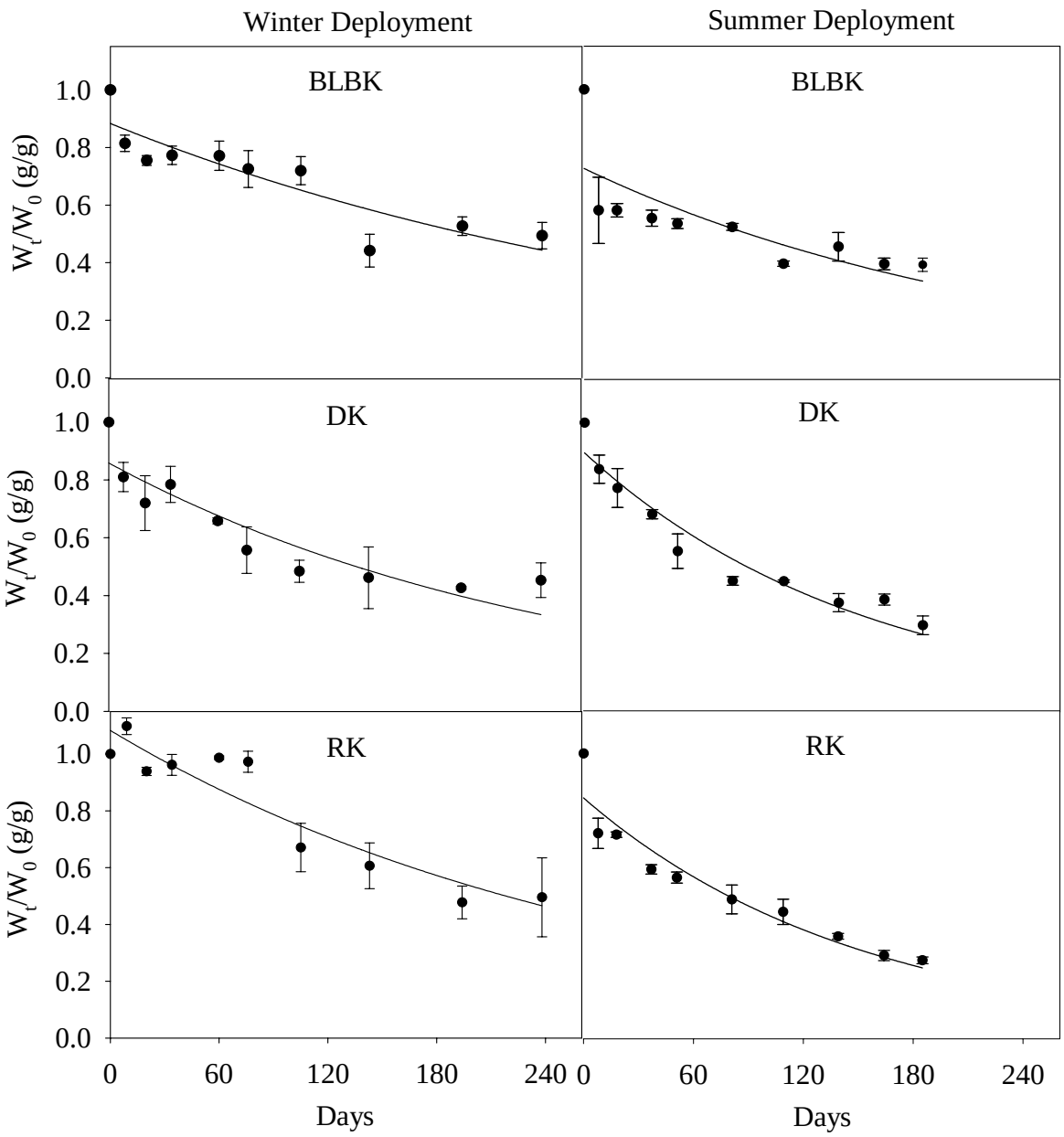

Figure 3.7. Proportional loss of root biomass (mean ± SE; n = 3) deployed at each site in litterbags at Black Betsy Key (BLBK), Dump Key (DK), and Rabbit Key (RK) fit over time for each site and season with a 2-parameter exponential decay model. Winter deployment began in February, and summer deployment began in August.

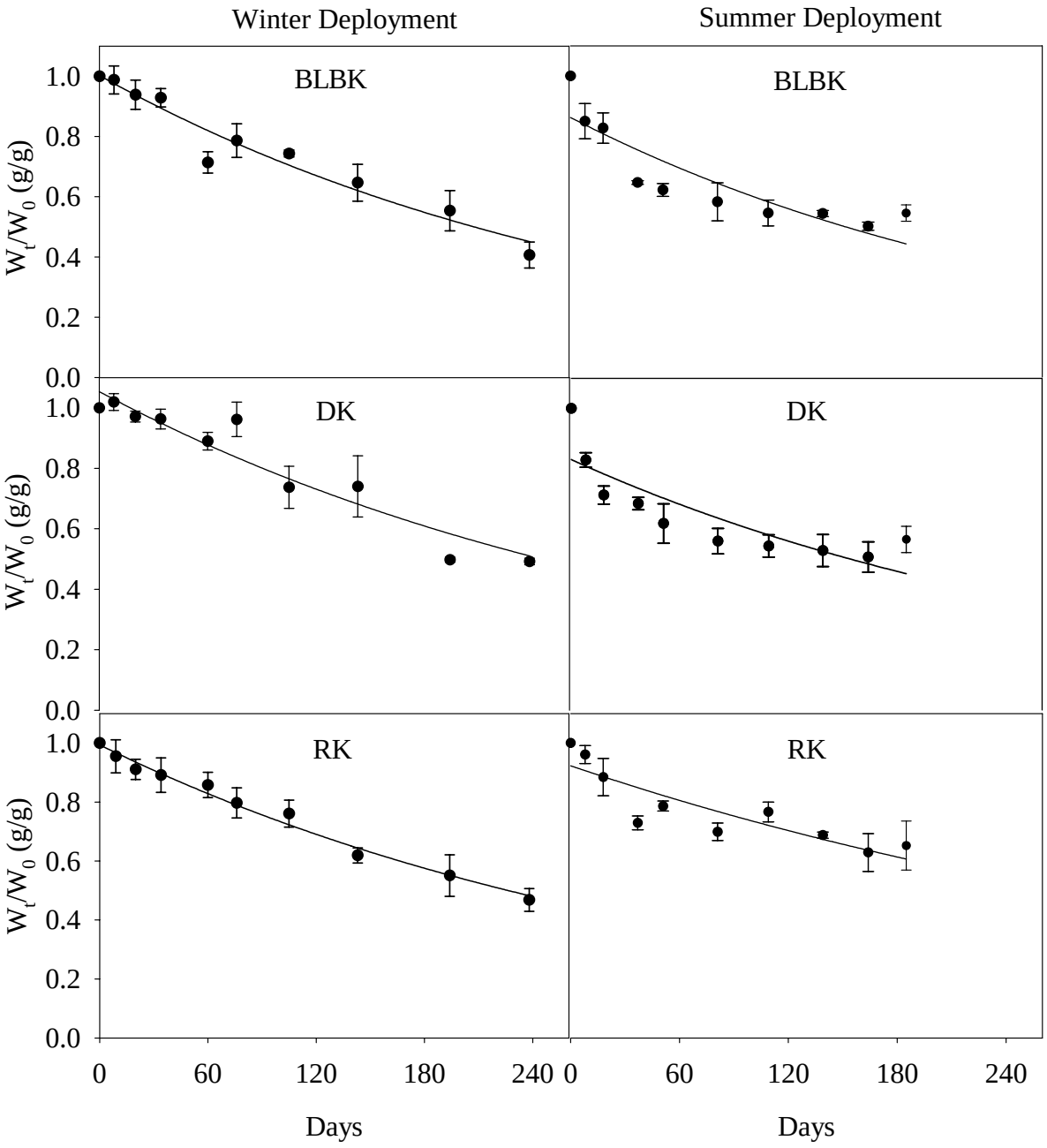

Figure 3.8. Proportional loss of senescent rhizome biomass (mean ± SE; n = 3) deployed at each site in litterbags at Black Betsy Key (BLBK), Dump Key (DK), and Rabbit Key (RK) fit over time for each site and season with a 2-parameter exponential decay model. Winter deployment began in February, and summer deployment began in August.

Root decay constants were also significantly different among sites ($p < 0.01$), with the slowest root decay rates observed at BLBK compared to DK and RK. While decay constants differed in the water column for senescent leaves between DK and RK sites, no significant difference in root decay rates were found during winter or summer months. Rhizomes were the only tissue type that had decay constants that were uniform across all three sites in the bay ($p = 0.20$; Table 3.5).

3.2.2.3. Seagrass Tissue Nutrient Loss Rates

The N and P in seagrass tissue declined during decay due to both biomass losses and changes in nutrient stoichiometry over time (Figs. 3.9 and 3.10), resulting in site and seasonal differences in the total mass of P (TMP) and total mass of N (TMN) decay constants (Table 3.5). The fact that decay constants of TMP ≥ TMN indicate a preferential or equivalent loss of P compared to N. Senescent leaf TMP and TMN decay constants also reflect trends in biomass loss; higher at DK and during the summer deployment. Root TMP decay constants were similar at all sites during the summer but greatest at BLBK during winter. The highest root TMN decay constants were found at DK, however each site had high standard errors of the decay constant parameter and a relatively poor fit to the exponential decay model ($R^2 = 0.2\text{-}0.6$). Both rhizome TMP and TMN constants were greatest during the summer except at BLBK. Highest rhizome TMP and TMN decay constants were found at BLBK during the winter but at DK during the summer. Despite the site and seasonal variations, the proportion of original N and P lost through decomposition was significant. Following winter deployment, an average of

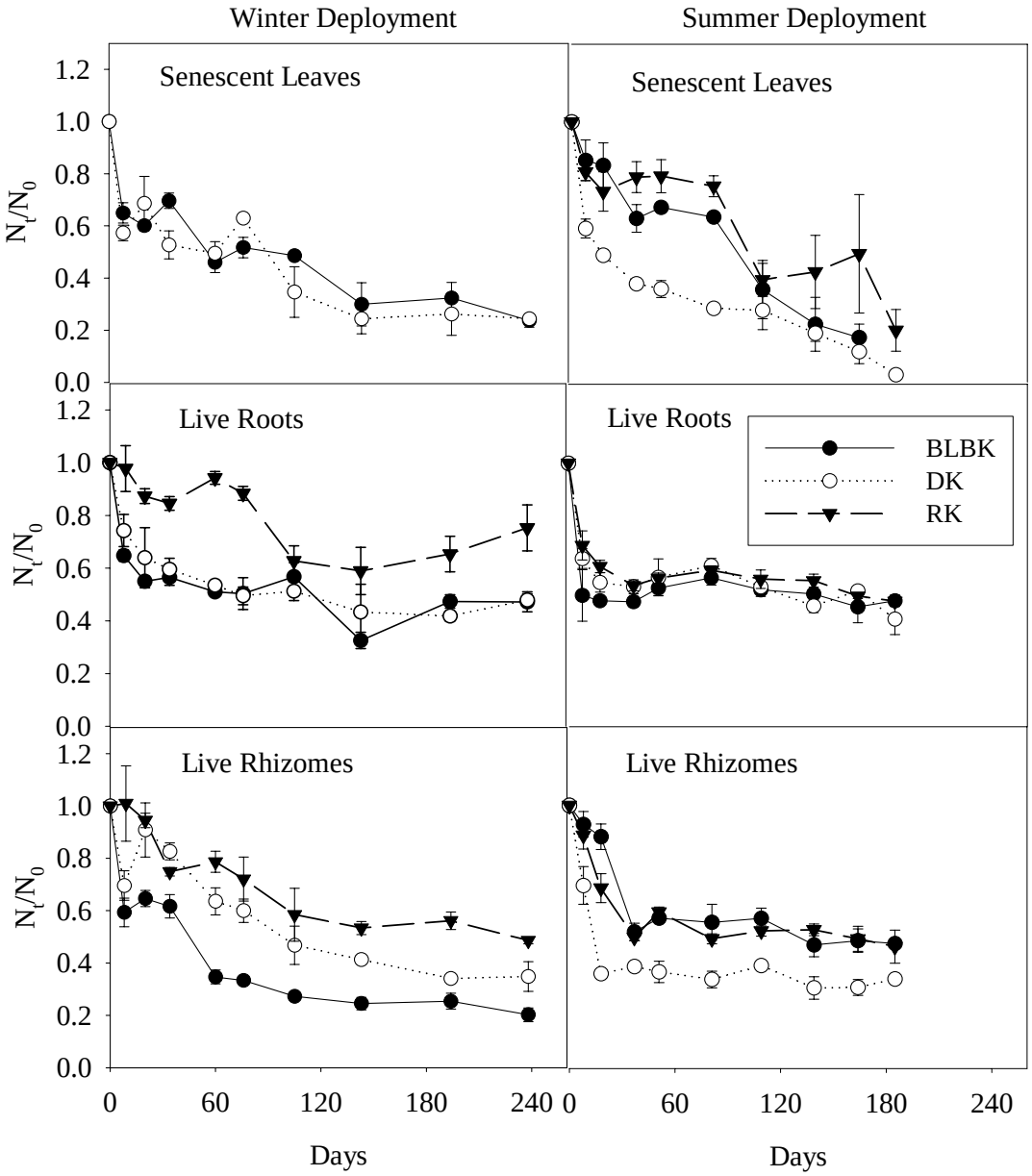

Figure 3.9. Proportion of original N remaining (N_t/N_0; mean ± SE) over time for all tissue types following winter and summer deployment at Black Betsy Key (BLBK), Dump Key (DK), and Rabbit Key (RK). Senescent leaves at RK during the winter are not included due to increasing biomass from heavily encrusting epiphytes.

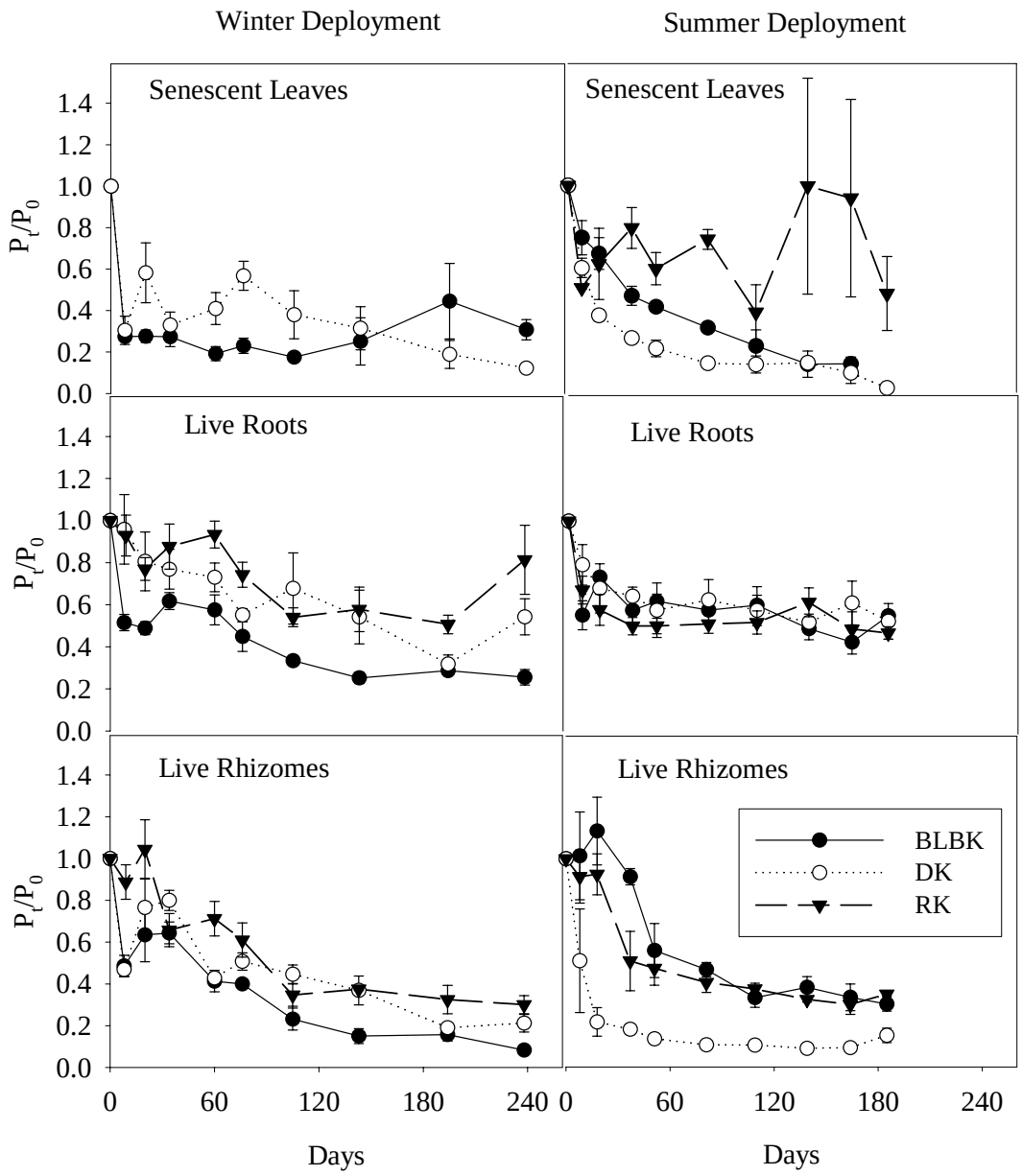

Figure 3.10. Proportion of original P remaining (P_t/P_0; mean ± SE) over time for all tissue types following winter and summer deployment at Black Betsy Key (BLBK), Dump Key (DK), and Rabbit Key (RK). Senescent leaves at RK during the winter are not included due to increasing biomass from heavily encrusting epiphytes.

approximately 78%, 43%, and 65% of N and 76%, 46%, and 86% of P was lost in senescent leaves, roots, and rhizomes, respectively. Following the summer deployment, approximately 88%, 54%, and 57% of N and 78%, 48%, and 73% of P was lost in senescent leaves, roots, and rhizomes, respectively.

3.3. Discussion

Nutrient cycling within seagrass-dominated systems is thought to occur primarily through seagrass detritus; however, this study indicates that a large proportion of seagrass nutrients in Florida Bay were released into the water column during leaf senescence on short shoots, with the magnitude of this flux significantly influenced by site trophic state. Senescent *T. testudinum* leaves still attached to the shoots had 29-95% and 14-55% lower TP and TN, respectively, compared to newly fully emergent leaves. Major losses of nutrients by seagrass leaves in the water column suggest that seagrasses can function as a nutrient pump, transferring inorganic nutrients from the porewater into the water column while still attached to the short shoot. While it has been documented that seagrass leaves can sequester nutrients from the water column, the primary nutrient source is the sediments through root uptake (Fourqurean et al. 1992*b*; Hemminga 1998). Preferential root uptake of nutrients by seagrass in Florida Bay is primarily driven by a low concentration of inorganic phosphorus in the water column (median = 0.04 µM; Boyer et al. 1997), relative to the sediment (median = 0.34 µM; Fourqurean et al. 1992*b*), and first order nutrient uptake kinetics in these low nutrient systems (Gras et al. 2003; Nielsen et al. 2006). Recent chamber studies show inorganic P in the water column of Florida Bay

to be rapidly sequestered by the water column, rather than the benthos, particularly during phytoplankton blooms (Nielsen et al. in press). Thus, as seagrasses take up the majority of nutrients from the porewater and translocate them to the leaves, where nutrients are concentrated, the loss to the water column as leaves rapidly senesce on the short shoots, as was found in this study, could stimulate autotrophic and/or heterotrophic production in the water column through a “nutrient pump”. Rapid water column nutrient uptake (Nielsen et al. in press) may mask benthic fluxes of nutrients to the water column inorganic pool, which remains low in the bay (Boyer et al. 1997), even across a sediment nutrient gradient (Fourqurean et al. 1992*b*; Zhang et al. 2004; Nielsen et al. 2006).

The magnitude of leaf nutrient release into the water column of the bay, assuming a bay-wide seagrass biomass of 46 g dwt m^{-2} (Hall et al. 1999), indicates the significance of seagrass N and P recycling in Florida Bay. Approximately 11 µmol P m^{-2} d^{-1} and 210 µmol N m^{-2} d^{-1} were estimated to be released by senescing leaves still attached to the short shoots, which on a yearly basis for the entire bay (2,220 km^2 area; Rudnick et al. 1999) would be 266 metric tons of P and 2,383 metric tons of N yr^{-1}, using a conservatively high rate of resorption, 31% P and 23% N (Stapel and Hemminga 1997). If no resorption is assumed, these rates increase to 506 metric tons of P and 6,513 metric tons of N yr^{-1}. Considering the rough estimated inputs of 580 metric tons of TP and 14,000 metric tons of TN entering Florida Bay each year, primarily (~90% for P and N) via advection from the Gulf of Mexico (Rudnick et al. 1999), the estimated recycling via seagrass leaves of the total estimated external P and N loads is substantial both with, 46% of the P and 17%, and without, 87% of the P and 47%, accounting for resorption.

Based on results from this study, the contribution to this recycling is region specific across the bay resulting from differences in both biomass allocation and senescing leaf nutrient retention. Nutrient recycling via the seagrass pool is depicted as a conceptual model identifying the contribution of different seagrass components to nutrient fluxes in western, central and eastern Florida Bay (Fig. 3.11). Standing leaf biomass increases significantly from east to west across the trophic gradient in the bay, as previously documented in the literature (Zieman et al. 1989; Hall et al. 1999); however, the lowest above to below-ground biomass ratio occurs in the eastern bay. The greater allocation to below-ground tissue in the P depleted eastern bay may be a response to P limitation, but lower above-ground productivity and nutrient sequestration as a whole was found to be significantly lower in the eastern bay. Despite the differences in biomass allocation across sites in the bay, the most significant nutrient flux was always from attached seagrass leaves to the water column as they senesced on the short shoot. These rates of nutrient release from attached leaves were related to nutrient availability, with the western and northcentral sites having ~5-fold greater flux rates than the eastern nutrient-poor site. These patterns of seagrass nutrient recycling may sustain east-west trophic gradients in the bay and potentially influence the initiation of recurrent phytoplankton blooms in the western and central regions of the bay (Phlips and Badylak 1996; Phlips et al. 1999). Therefore, while the porewater nutrient pool is the primary source for inorganic nutrients for seagrass in the bay, based on first order uptake kinetics, the water column receives the highest efflux from seagrasses as they decompose, which is enhanced by increased trophic state.

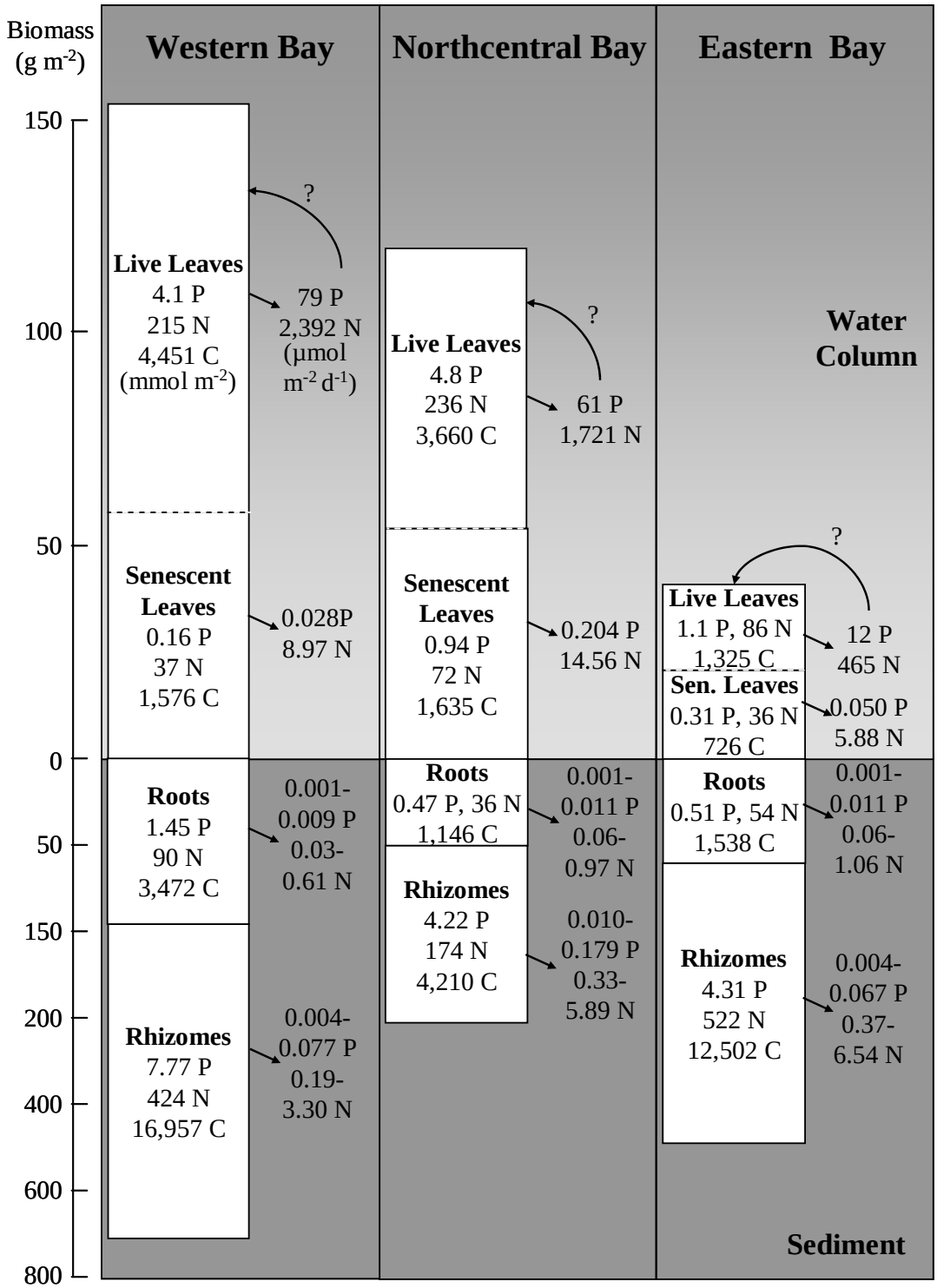

Figure 3.11. Nutrient standing stocks (mmol m^{-2}) and fluxes (µmol m^{-2} d^{-1}) into the water column and sediment from *Thalassia testudinum* above- and below-ground tissue in western, northcentral, and eastern Florida Bay. Below-ground biomass densities are based on ~30 cm depth cores. See methods for a detailed description of nutrient flux calculations and assumptions. The amount of N and P resorbed by leaves is still in question.

Senescent leaves also contributed to nutrient flux to the water column, but at the sediment-water interface as detritus, and significantly less than live leaves (Fig. 3.11). This flux was dominated by the central bay, accounted for by the higher initial leaf nutrient content at this site and high senescent leaf decay rates ($k = 0.008\text{-}0.013\ d^{-1}$), resulting in >4-fold higher P and ~2-fold higher N flux than eastern and western bay sites, respectively (Fig. 3.11). Interestingly, the eastern and western bay sites, the two end members of the sediment P gradient (Zhang et al. 2001) had relatively similar fluxes of P from senescent leaves, explained by the high live leaf nutrient turnover in the west and low nutrient sequestration in the east. These results indicate that the deposition of nutrients to sediments in the western and central basins of the bay, with a clearly high sediment P content, is most likely cycled via sedimentation of phytoplankton in the water column, not via seagrass leaf detritus, which is low in nutrients. Consistent with this idea, senescent leaf decay constants in this study ($k = 0.003\text{-}0.013\ d^{-1}$) are relatively low, and within the range reported for decaying seagrass leaves ($k = 0.001\text{-}0.017\ d^{-1}$) from both tropical and temperate species (Harrison 1989), indicating that for seagrasses in general, slow rates of leaf decay may be related to the high efflux of live leaf nutrients. Greater rates of decay were found for detached live leaves of *T. testudinum* allowed to decompose in the water column ($k = 0.015\text{-}0.045\ d^{-1}$; Harrison 1989; Fourqurean and Schrlau 2003). These data are consistent with the more rapid loss of nutrients found in this study for live leaves still attached to the short shoots, compared to senescing leaves in the detrital pool.

Although seagrass biomass belowground can surpass that of above ground, particularly in late successional species such as *T. testudinum*, the nutrient content and

flux of nutrients are lower than those estimated for live leaves based on our data from Florida Bay (Fig. 3.11). Belowground decomposition of root and rhizome tissues is, however, still an important direct nutrient source to sediments and pore water. Even though literature values for belowground productivity ranges an order of magnitude, giving a wide range of flux estimates, rhizome nutrient fluxes were in general 10 times higher than those from roots (Fig. 3.11). While the decay rates for these belowground tissues were similar, the loss rates of nutrient mass and productivity rates for rhizomes was higher than roots, explaining their higher nutrient flux rates. If data were available on the mass specific productivity for belowground tissues of *T. testudinum*, these differences between roots and rhizomes may even be greater, and show more significant differences across sites. These boundary setting calculations, presented as a conceptual model (Fig. 3.11), illustrate the relative importance of seagrass nutrients being recycled primarily through live leaf senescence in the water column, rather than the detrital pool.

Because of the extremely high rates of nutrient loss in the water column of live leaves, it is quite unlikely that these nutrients are being resorbed. Also, in seagrasses the meristematic new leaf growth is in the central interior portion of the short shoot, while in this study we found the major change in nutrients are between the brown and yellowing portion of the senescing leaves at the apex, suggesting that nutrients are being leached via decomposition on the leaf tips, rather than being resorbed. Also, because BLBK had the lowest senescent leaf nutrient decline in relation to percent decomposing tissue, resorption appeared to be lowest at this eastern P-limited site. Although these findings contradict many terrestrial and aquatic plant studies which show active plant resorption with nutrient limitation (Shaver and Melillo 1984; Pugnaire and Chapin 1993; Van

Heerwaarden et al. 2003; Rejmankova 2005), our results compare well to studies on the Indonesian seagrasses *T. hemprichii* and *Enhalus acoroides*, which had lower resorption efficiencies at nutrient-limited sites (Stapel and Hemminga 1997). If the high rates of leaching observed in this study, probably not accounted for by true resorption, occur in seagrasses from other regions, previous estimates of nutrient resorption in seagrasses, based on nutrient declines in senescent leaves, may have been overestimated. Previous resorption studies consider nutrient leaching to be insignificant based on ^{15}N tracer work in the temperate seagrass *Zostera marina*, which showed that <10% of ^{15}N was lost to the external medium following a one-week incubation under N-rich conditions (Borum et al. 1989). However, it is well documented that nutrient leaching occurs rapidly during the initial stages of seagrass decay (Rublee and Roman 1982; Kenworthy and Thayer 1984; Blum and Mills 1991; this study). Rapid leaf decay and subsequent leaching may be more prevalent in tropical seagrasses, particularly since the nutrient declines in this study (29-95% P and 45-86% N) are greater than resorption efficiencies calculated from previous studies (up to 51% P and 68% N; Borum et al. 1989; Pedersen and Borum 1993; Stapel and Hemminga 1997; Hemminga et al. 1999; Stapel et al. 2001; Lepoint et al. 2002).

In conclusion, in shallow tropical/subtropical estuaries dominated by the seagrass *T. testudinum*, a considerable amount of nutrients can be released into the water column from attached seagrass leaves. Thus, seagrasses may serve as nutrient pumps, transferring N and P from the porewater back to the overlying water column. This nutrient release increases with site trophic state potentially influencing eutrophication processes in nutrient limited seagrass-dominated estuarine systems, such as Florida Bay. Thus, there are linkages between site trophic state and seagrass nutrient recycling; but rather than an

effect on plant nutrient resorption, enhanced seagrass leaf decomposition increases nutrient fluxes to the water column, probably influencing the initiation of recurrent phytoplankton blooms in Florida Bay.

3.5. LITERATURE CITED

Aerts, R. 1996. Nutrient resorption from senescing leaves of perennials: are there general patterns? J. Ecol. 84(4): 597-608.

Blum, L. K. and A. L. Mills. 1991. Microbial growth and activity during the initial stages of seagrass decomposition. Mar. Ecol. Prog. Ser. 70: 73-82.

Borum, J., L. Murray, and W. M. Kemp. 1989. Aspects of nitrogen acquisition and conservation in eelgrass plants. Aquat. Bot. 35: 289-300.

Boyer, J. N., J. W. Fourqurean, and R. D. Jones. 1997. Spatial characterization of water quality in Florida Bay and Whitewater Bay by multivariate analyses: zones of similar influence. Estuaries 20(4): 743-758.

Chapin, F. S., III. 1980. The mineral nutrition of wild plants. Annu. Rev. Ecol. Syst. 11:233-260.

Chapin, F. S., R. A. Kedrowski. 1983. Seasonal changes in nitrogen and phosphorus fractions and autumn retranslocation in evergreen and deciduous taiga trees. Ecology 64(2): 376-391.

Debusk, W. F. and K. M. Reddy. 2005. Litter decomposition and nutrient dynamics in a phosphorus enriched everglades marsh. Biogeochemistry 75: 217-240.

Erftemeijer, P. L. A. and J. J. Middelburg. 1995. Mass balance constraints on nutrient cycling in tropical seagrass beds. Aquat. Bot. 50: 21-36.

Fourqurean, J. W. and J. C. Zieman. 1991. Photosynthesis, respiration and whole plant carbon budget of the seagrass *Thalassia testudinum*. Mar. Ecol. Prog. Ser. 69: 161-170.

Fourqurean, J. W., J. E. Schrlau. 2003. Changes in nutrient content and stable isotope ratios of C and N during decomposition of seagrasses and mangrove leaves along a nutrient availability gradient in Florida Bay, USA. Chem. Ecol. 19(5): 373-390.

Fourqurean, J. W., J. C. Zieman, and G. V. N. Powell. 1992*a*. Phosphorus limitation of primary production in Florida Bay: evidence for C:N:P ratios of the dominant seagrass *Thalassia testudinum*. Limnol. Oceanogr. 37: 162-171.

Fourqurean, J. W., J. C. Zieman, and G. V. N. Powell, 1992*b*. Relationships between porewater nutrients and seagrasses in a subtropical carbonate environment. Mar. Biol. 114: 57-65.

Fourqurean, J. W., R. D. Jones, and J. C. Zieman. 1993. Processes influencing water column limitation of phytoplankton biomass in Florida Bay, FL, USA: inferences from spatial distributions. Estuar. Coast. Shelf Sci. 36: 295-314.

Gras, A. F., M. S. Koch, and C. J. Madden. 2003. Phosphorus uptake kinetics of a dominant tropical seagrass *Thalassia testudinum*. Aquat. Bot. 76: 299-315.

Hall, M. O., M. J. Durako, J. W. Fourqurean, and J. C. Zieman. 1999. Decadal changes in seagrass distribution and abundance in Florida Bay. Estuaries 22 (2): 445-459.

Harrison, P. G. 1989. Detrital processing in seagrass systems: a review of factors affecting decay rates, remineralization, and detritivory. Aquat. Bot. 23: 263-288.

Hemminga, M. A. 1998. The root/rhizome system of seagrasses: an asset and a burden. J. Sea Res. 39: 183-196.

Hemminga, M. A., C. M. Duarte. 2000. Seagrass Ecology. Cambridge University Press, Cambridge, United Kingdom. 298 p.

Hemminga, M. A., N. Marba, and J. Stapel. 1999. Leaf nutrient resorption, leaf lifespan and the retention of nutrients in seagrass systems. Aquat. Bot. 65: 141-158.

Hemminga, M. A., P. G. Harrison, and F. van Lent. 1991. The balance of nutrient losses and gains in seagrass meadows. Mar. Ecol. Prog. Ser. 71: 85-96.

Kenworthy, W. J. and G. W. Thayer. 1984. Production and decomposition of the roots and rhizomes of seagrasses, *Zostera marina* and *Thalassia testudinum*, in temperate and subtropical marine ecosystems. Bull. Mar. Sci. 35(3): 364-379.

Larkum, A. W. D., A. J. McComb, and S. A. Shepherd. 1989. Biology of Seagrasses. Elsevier Science Publishers, Amsterdam. 842 p.

Lepoint, G, O. Defawe, S. Gobert, P. Dauby, and J.-M. Bouquegneau. 2002. Experimental evidence for N recycling in the leaves of the seagrass *Posidonia oceanica*. J. Sea Res. 48: 173-179.

Lopez, N. I., C. M. Duarte, F. Vallespinos, J. Romero, and T. Alcoverra. 1998. The effect of nutrient additions of bacterial activity in seagrass (*Posidonia oceanica*) sediments. J. Exp. Mar. Biol. Ecol. 224: 155-166.

Menendez, M., D. Carlucci, M. Pinna, F. A. Comin, and A. Basset. 2003. Effect of nutrients on decomposition of *Ruppia cirrhosa* in a shallow coastal lagoon. Hydrobiologia 506-509: 729-735.

Nielsen, O. I., M. S. Koch, and C. J. Madden. in press. Inorganic phosphorus uptake in a carbonate-dominated seagrass ecosystem. Estuaries.

Nielsen, O. I., M. S. Koch, H. S. Jensen, and C. J. Madden. 2006. *Thalassia testudinum* phosphate uptake kinetics at low in situ concentrations using a ^{33}P radioisotope technique. Limnol. Oceanogr. 51(1): 208-217.

Patriquin, D. 1973. Estimation of growth rate, production and age of the marine angiosperm *Thalassia testudinum*. Carib. J. Sc. 13: 111-124.

Pedersen, M. F. and J. Borum. 1993. An annual nitrogen budget for a seagrass *Zostera marina* population. Mar. Ecol. Prog. Ser. 101: 169-177.

Phlips, E. J. and S. Badylak. 1996. Spatial variablility in phytoplankton standing crop and composition in a shallow inner-shelf lagoon, Florida Bay, Florida. Bull. Mar. Sci. 58: 203-216.

Phlips, E. J., S. Badylak, and T. C. Lynch. 1999. Blooms of the picoplanktonic cyanobacterium *Synechococcus* in Florida Bay, a subtropical inner-shelf lagoon. Limnol. Oceanogr. 44(4): 1166-1175.

Pugnaire, F. I. and F. S. Chapin, III. 1993. Controls over nutrient resorption from leavesof evergreen Mediterranean species. Ecology 74(1): 124-129.

Rejmankonva, E. 2005. Nutrient resorption in wetland macrophytes: comparison across several regions of different nutrient status. New Phytol. 167: 471-482.

Rublee, P. A. and M. R. Roman. 1982. Decomposition of turtlegrass (*Thalassia testudinum*) in flowing sea-water tanks and litterbags: compositional changes and comparison with natural particulate matter. J. Exp. Mar. Biol. Ecol. 58: 47-58.

Rudnick, D. T., Z. Chen, D. L. Childers, J. N. Boyer, and T. D. Fontaine, III. 1999. Phosphorus and nitrogen inputs to Florida Bay: the importance of the Everglades watershed. Estuaries 22(2): 398-416.

Shaver, G. R. and J. M. Melillo. 1984. Nutrient budgets of marsh plants: efficiency concepts and relation to availability. Ecology 65(5): 1491-1510.

Stapel, J. and M. A. Hemminga. 1997. Nutrient resorption from seagrass leaves. Mar. Biol. 128: 197-206.

Stapel, J., M. A. Hemminga, C. G. Bogert, and Y. E. M. Maas. 2001. Nitrogen (^{15}N) retention in small *Thalassia hemprichii* seagrass plots in an offshore meadow in South Sulawesi, Indonesia. Limnol. Oceanogr. 46: 24-37.

Valiela, I., J. M. Teal, S. D. Allen, R. V. Etten, D. Goehringer, and S. Volkmann. 1985. Decomposition in salt marsh ecosystems: the phases and major factors affecting disappearance of above-ground organic matter. J. Exp. Mar. Biol. Ecol. 89: 29-54.

Van Heerwaarden, L. M., S. Toet, and R. Aerts. 2003. Nitrogen and phosphorus resorption efficiency and proficiency in six sub-arctic bog species after 4 years of nitrogen fertilization. J. Ecol. 91: 1060-1070.

Van Tussenbroek, B. I. 1998. Above- and below-ground biomass and production by *Thalassia testudinum* in a tropical reef lagoon. Aquat. Bot. 61: 69-82.

Xie, Y., D. Yu, and B. Ren. 2004. Effects of nitrogen and phosphorus availability on the decomposition of aquatic plants. Aquat. Bot. 80: 29-37.

Zhang, J.-Z., C. J. Fischer, and P. B. Ortner. 2004. Potential availability of sedimentary phosphorus to sediment resuspension in Florida Bay. Global Biochem. Cycles 18: GB4008, doi: 10.1029/2004GB002255.

Zieman, J. C. 1974. Methods for the study of the growth and production of turtle grass, *Thalassia testudinum.* Aquaculture 4: 139-143.

Zieman, J. C., J. W. Fourqurean, and R. L. Iverson. 1989. Distribution, abundance, and productivity of seagrasses and macroalgae in Florida Bay. Bull. Mar. Sci. 44: 292- 311.

CHAPTER 4

THE POTENTIAL ROLE OF SULFIDE OXIDATION AND SEDIMENT DISSOLUTION IN RELEASING PHOSPHORUS FROM CARBONATE SEAGRASS SEDIMENTS IN FLORIDA BAY

4.0. Introduction

Seagrass primary production in carbonate environments is frequently limited by inorganic phosphorus (P*i*) availability (e.g. Short et al. 1990, Fourqurean et al. 1992) resulting from low external terrestrial P loads and high sediment affinity for P*i* in these systems. Phosphorus in carbonate sediments is strongly bound to the solid phase carbonate matrix, e.g. as calcium-fluoro-apatite (CFA; Kitano et al., 1978; de Kanel and Morse, 1978; Ruttenberg and Berner, 1993; Jensen et al., 1998; Millero et al., 2001; Koch et al., 2001; Zhang et al., 2004), but also other P and F bearing carbonate phases occur (e.g. Rude and Aller, 1991). Jensen et al. (1998) showed that inorganic P (P*i*) can be mobilized from solid phase carbonate pools in shallow seagrass sediments of Bermuda, but no experiments have been conducted specifically linking carbonate dissolution and subsequent P availability for seagrass sequestration. In Bermuda sediments, the maximum concentration of P*i* and fluoride (F^-), indicators of CFA dissolution, was found at the greatest rooting depth of the dominant tropical seagrass in the Atlantic-Caribbean region, *Thalassia testudinum*. Ku et al. (1999) and Burdige et al. (2002) suggest that oxygen released from *T. testudinum* roots enhance sulfide oxidation, as well as aerobic mineralization of organic matter in the sediment. As both of these metabolic oxidation processes generate acidity in the form of sulfuric and carbonic acids, they have the potential to cause dissolution of carbonate sediments and a concomitant release of sediment-bound P and F. A low pH in seagrass carbonate sediments with high (mM) porewater sulfide levels was observed by Morse et al., (1987), Ku et al., (1999) and Koch et al., (2007) in Florida Bay. Burdige et al. (2002) also found evidence for enhanced carbonate dissolution shown by increased Ca^{2+} and ΣCO_2 in porewater of dense seagrass beds of the Bahamas. Similarly, Yates and Halley (2006) calculated that carbonate sediment dissolution rates were highest in seagrass sites at night in Florida Bay, resulting from high respiration rates.

Based on a relatively simple stoichiometry of 2:1 or 1:1 between carbonate dissolution and sulfate reduction rates (SRR), depending on the pore water pH and dominant speciation of H_2S (Hu and Birdige, 2007), all sulfide produced in iron-poor carbonate sediments could be reoxidized within the sediment if sufficient oxygen is supplied (Ku et al., 1999). Using a stoichiometry of 2:1, Burdige et al. (2002) calculated that published rates of carbonate dissolution of 4-11 mmol m^{-2} d^{-1} in non-vegetated sediments from Florida Bay (Rude and Aller, 1991) could be accounted for by sulfide oxidation consuming ~15% of the daily net production of oxygen produced by *T. testudinum* via sulfate reduction-oxidation coupling. Lee and Dunton (2000) also showed that diurnal porewater sulfide varied in sediment vegetated with *T. testudinum*, indicating that sufficient oxygen can be provided during the day to re-oxidize most of the sulfide generated at night via SR. Thus, there is indirect evidence that SRR in seagrass beds and subsequent sulfide oxidation may promote carbonate dissolution in depositional environments where carbonates are dominated by aragonite and high-Mg calcite (Walters et al. in press); although Hu and Burdige (2007) suggest organic mater oxidation and CO_2 production may also be important for generating the metabolic acidity that drives carbonate dissolution in more oligotrophic systems. Regardless of the dominant metabolic pathway driving dissolution, the relationship between carbonate dissolution to P*i* availability in pore waters of carbonate-dominated seagrass systems remains elusive.

In the present study, we experimentally examined carbonate sediment dissolution in a subtropical seagrass-dominated ecosystem, Florida Bay, with a focus on understanding the relationship between pH, carbonate dissolution, and desorbtion of P*i*, and the potential influence of site-specific SR rates. We also examined the potential for P*i* that was released from dissolution to be resorbed onto carbonates across a nutrient gradient in the bay. In some of our earlier work (Jensen et al., 1998), it was shown that nearly all sediment Ca and F could be mobilized at pH 4.0 using an acetic acid buffer (or in

0.5 M HCl) applying a sequential extraction scheme. Along with the dissolution of this carbonate matrix, the majority of sediment inorganic and organic P was released. We also observed that P*i* could be extracted in preceding extraction steps with $MgCl_2$ or BD reagent at neutral pH, likely representing a surface bound P*i* fraction, assumed to be in dynamic equilibrium with porewater P*i*. To follow up on these initial experiments in Bermuda and to better understand P-cycling in carbonate-seagrass environments in Florida Bay, we traced P*i* in sediment dissolution experiments using sediment from four different locations in Florida Bay, representing the end members of a well established sediment P gradient (Zhang et all, 2004; Nielsen et al., 2006). We also measured SRR at these sites to estimate potential sulfide oxidation rates and P-mobilization through carbonate dissolution. Further, patterns of P*i* adsorption onto and incorporation into carbonate sediments in the eastern (P-limited) and western (P-enriched) bay sites were examined by adding $^{33}PO_4^{3-}$ to sediment slurries and following the rates at which they became homogeneously labeled by the exchangeable and matrix-bound P pools.

4.1. Methods

4.1.1. Sampling Sites

Florida Bay is a shallow (< 2m) semi-enclosed estuarine lagoon at the southern tip of the Florida peninsula (Fig. 4.1). The sediment is predominantly aragonite (50-60%) and high-Mg calcite (30-40%) generated internally by primarily calcareous algae and in situ precipitation, and composed of a very low silicate fraction (Walter and Burton, 1990; Rude and Aller, 1991; Walters et al., in press; Lyon et al., 2004) and low Fe (Chambers et al., 2001; Zhang et al., 2004). Extensive seagrass meadows of the tropical seagrass *T. testudinum* dominate primary production in the bay decreasing in biomass from west to northeast as a consequence of P availability (Fourqurean and Zieman, 2002). This trophic gradient is well established by sediment P concentrations (Zhang et al., 2004), sediment P adsorption

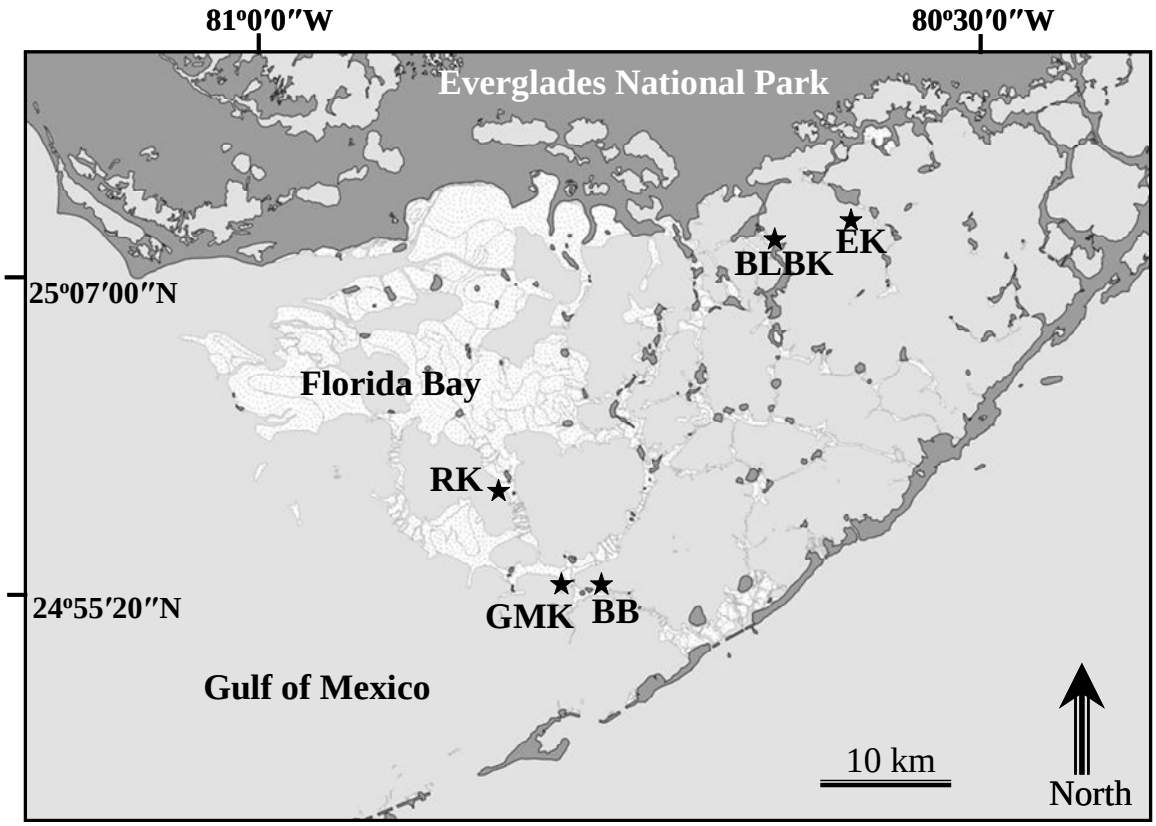

Figure 4.1. Study sites in Florida Bay, a semi-enclosed lagoonal estuary, at the southern terminus of the Florida Peninsula, bounded to the north by the Everglades, to the south by the Florida Keys and Gulf of Mexico to the west. Sediment for SRR and dissolution experiments were collected from eastern bay sites: Eagle Key (EK) and Black Betsy Key (BLBK) and western bay sites: Rabbit Key (RK) and Buchanan Bank (BB). Radiotracer experiment with 33P was conducted with sediment from EK and Green Mangrove Key (GMK). Numerous mangrove islands (dark grey) and mudbanks (light grey) are noted.

isotherms (Nielsen et al., 2006) and leaf C:P ratios (Fourqurean et al., 1992). Sites chosen for this study (Fig. 4.1) include three sites in the western bay, Buchanan Bank (BB; 24°54’55.9” N; 80°45’24.2” W), Green Mangrove Key (GMK; 24°54’55.9” N/80°45’24.2” W) and Rabbit Key (RK; 24°58’50”N/80°50’11”W), high sediment P sites, and two sites in the northeastern bay, Eagle Key (EK;

25°09’32.4” N/80°34’58.6” W) and Black Betsy Key (BLBK; 25°08’23”N/ 80°38’51”W), low sediment P sites, all dominated by *T. testudinum*. The more enriched western sites are also characterized as having relatively higher porewater sulfide concentrations (4-6 mmol L^{-1}) relative to eastern sites (≤ 2 mmol L^{-1}) (Barber and Carlson, 1993; Carlson et al., 1994; Koch et al., 2007).

4.1.2. P mobilization experiment

Seagrass sediment (2-10 cm) from BB, RK, BLBK and EK was collected via coring (March 2005; 20 cm diameter cores) and subsequently sieved (2 mm) to remove large rhizomes and roots. The wet sediment (20 g) was added to ambient seawater (80 mL) from the sites. The resulting sediment slurries were placed on a shaker table and pre-incubated for 12 h prior to the start of the experiment. To examine sediment carbonate dissolution and subsequent release of P as pH was lowered through acidification, four different concentrations of sulfuric acid: 0, 150, 400 and 800 µmol H_2SO_4 (~10-50 µmoles cm^{-3} sediment; n=3) were added to sediment from each site. While the sediment treatments were similar on a sediment volume basis, differences in the bulk densities across sites resulted in variable amounts of acid amendments per g dry wt sediment; therefore, results are normalized to moles of H_2SO_4 per g dry weight where appropriate. Release of P*i*, F^- and Ca^{2+}, as well as pH changes in the slurries, were monitored throughout the experiment at time 0, 2, and 6 h. The pH of the slurry was measured directly, while P*i*, F^- and Ca^{2+} were measured after filtering (GF/F) a subsample (15 mL) of the sediment-water slurry. Inorganic soluble reactive P*i* was determined using standard colorimetric methods (Koroleff, 1983) with a detection limit of 20 nmol L^{-1}. Inorganic fluoride was determined using a combined F^- electrode (Orion 96-09) with 1:1 addition of low-level TISAB. The resolution at

ambient seawater F^- concentration was ±1.8 μmol L^{-1}. Dissolved Ca^{2+} was determined by AAS (Perkin Elmer) also using standard methods.

After acid treatments, wet sediment in the seawater slurry underwent several sequential extractions to quantify P and F pool adsorbed to carbonates. The extraction procedure followed a modified two-step extraction scheme developed for carbonate sediment by Jensen et al. (1998). In the first step, the sediment was transferred to 60 mL centrifuge tubes to which 30 mL of 1 mol L^{-1} $MgCl_2$ was added and put on a shaker table for 1 h. After centrifugation and decanting, the sediment was washed in 30 mL of 0.5 mol L^{-1} NaCl. The wash supernatant was added to the $MgCl_2$ and brought up to volume with H_2O (100 ml). The second step was a 1 h extraction with a BD-reagent (0.11 M Na-dithionite and 0.11 M $NaHCO_3$) followed by two BD washes and one NaCl wash, and brought to volume with H_2O (200 mL). The first extraction step extracts loosely adsorbed P while the second step extracts both Fe-bound P and P loosely-bound to the surface of carbonates (Jensen et al. 1998). In siliclastic temperate sediments $MgCl_2$ extracts loosely adsorbed surface bound P*i* with BD extraction considered highly specific for Fe-bound P (Jensen and Thamdrup 1993). However, Jensen et al. (1998) have shown that in carbonate sediment BD extracts both Fe and surface-bound *i*P without concurrent release of Ca^{2+}, which is also supported by a lack of correlation between reactive Fe oxides and BD-extractable P in the bay by Zhang et al. (2004). Subsequently, P*i* and F^- concentration in the extracts was measured as stated above. Standard curves were prepared in the specific matrix extract solutions. Control extractions were also run without acid dissolution as a control.

4.1.3. Sediment Characteristics

Porosity, dry:wet wt ratios and grain size (<63 µm reported in %) were determined on sediment from all sites. Total Ca, F and P concentrations were quantified by combusting the dried sediment (550°C, 3 h) and subsequently dissolving the pellet in 1 mol L^{-1} HCl (120°C, 1 hour) and analyzed as above; with the exception of extracts requiring neutralization (NaOH) for F^- measurements. Solid fraction inorganic P (TP*i*) was determined by dissolving the sediment in cold 0.5 M HCl and analyzing the extract for soluble reactive P*i*.

4.1.4. Sediment P-pool labeling experiment

We used a unique radiotracer technique to examine sediment P exchange in eastern fine-grained P-poor sediment from EK (83% <63 µm) and coarser P-rich sediment from GMK (34% <63 µm). This technique is based on the principle that $^{33}PO_4^{3-}$, when added to sediment slurries in trace amounts, will undergo isotopic exchange with any surface-bound or solid fraction $^{31}PO_4^{3-}$ reservoir at different exchange rates depending on the exchangeability potential of the sediment particles. Wet sediment (20 g) was kept in suspension in P-free artificial seawater (100 mL) on a shaker table and carrier-free $^{33}PO_4^{3-}$ (1 µCi) added to the slurry. The activity of $^{33}PO_4^{3-}$ in the slurry water was followed for 4 h, after which the distribution of the tracer in the exchangeable and matrix bound fractions ($MgCl_2$-extractable, BD-extractable, and HCl-extractable P*i*, respectively, see above) was determined by sequential extraction at time 4.66, 7.66, 33, and 55 h. $^{33}PO_4^{3-}$ in solution was measured on a GF/F filtrate while solid pool tracer distribution was measured on the particles retained on the filter. Radioactivity was measured on a scintillation counter (Beckman LS 6500 Liquid Scintillation Counter) using standard techniques and correcting for background, decay, and quenching with known activity.

4.1.5. Sulfate reduction rates (SRR)

SRR were determined on sediment cores (diameter 3.5 cm; n=4) from EK, BLBK, BB, and RK in October 2005 and July 2006 to relate dissolution of carbonates to potential sulfide oxidation. Intact cores from each site were injected with $^{35}SO_4^{2-}$ (2 μl of 1 μCi) through silicon stopper holes on two sides at 2 cm intervals down to 14-18 cm depth (after Jørgensen, 1978). Cores were selected within seagrass beds between short shoots to minimize seagrass tissue in the cores. Cores were incubated for 2 h at in situ temperature (26 ^{o}C October and 31 ^{o}C July). Post-incubations, cores were carefully sliced into 2 cm intervals and immediately transferred into zinc acetate (10 mL of 1 mol L^{-1}) for sulfide fixation. Subsequently, the sediment was washed with 10 mL of 1 mol L^{-1} zinc acetate to remove excess $^{35}SO_4^{2-}$. Reduced ^{35}S-pools were retrieved using a two-step distillation method described by Fossing and Jørgensen (1989) and radioactivity was immediately counted on a scintillation counter. SRR were calculated as the percent recovery of radiolabelled sulfur in the acid volatile sulfide (AVS) and chromium reducible sulfide (CRS) pools. Porewater sulfate was measured using a separate non-radioactive core at 2 cm intervals. Sediment was transferred into centrifuge tubes and centrifuged to extract porewater that was stored frozen until analysis of sulfate using ion-chromatography.

4.2. Results

4.2.1. General Sediment Characteristics - Solid Phase

General sediment characteristics showed relatively similar levels of F across sites, while Ca and P levels showed more distinct differences in eastern versus western bay sites (Table 4.1). Western bay sites were generally lower in total Ca than eastern bay sites, although Ca levels were high at all sites. Total sediment phosphorous (TP) and inorganic solid phase phosphorus (TP*i*) closely followed the

established trophic gradient for the bay with more P enrichment in the western bay sites. The importance of the inorganic solid phase P pool is shown by this fraction representing approximately 50±2% of the TP pool at all four sites (46-53%). Sediment F levels were similar across sites, but tended to be lower in the eastern bay. The molar ratios of fluoride to calcium are indicative of sediment dominated by easily dissolvable aragonite and high-Mg calcite in support of the supposition that dissolution could be an important mechanism in recycling P in bay sediments. Further, inorganic solid phase pools indicate a greater potential release of solid phase inorganic P (TP*i*) in the western bay sediment with a 2-5-fold higher TP*i*:Ca ratio than eastern bay sediments.

4.2.2. Sulfuric acid addition experiment

Sulfuric acid addition to the carbonate sediment in slurries resulted in a lower pH at the first time measurement (1 h) at all sites except BLBK, with decreasing pH a function of increasing acid treatment level (Fig. 4.2). All sites had similar pH levels in response to acid treatments by 6 h. Concomitant with the decline in pH from sediment acidification, Ca^{2+}, F^{-} and P*i* was dissolved and recovered in the seawater slurry water or from the exchangeable pool depending on site (Fig. 4.2, Table 4.2). Despite Ca^{2+} mobilization at all sites, P*i* measured in the slurry water was only significantly different from controls at Rabbit Key (Table 4.2), the site with the highest sediment TP and TP*i* (Table 4.1). Sequential extraction of the surface bound P pools at the end of the experiment showed that a portion of the mobilized P*i* was surface bound, either in the loosely adsorbed $MgCl_2$ fraction or in the more strongly adsorbed BD fraction (Table 4.2). The Fe content, and especially oxidized Fe, in Florida Bay is extremely low, thus the fraction captured in the BD extracts was probably still surface-bound, even though it was not recovered in the $MgCl_2$ exchangeable fraction. Significant extractable P*i* in one or both of the surface bound pools was found at RK, BB and BLBK (Table 4.2). Only at EK were the

Table 4.1. Sediment total inorganic Ca, F and TP*i*, and total P (TP), molar ratios of fluoride to calcium and inorganic P to calcium and fluoride, and bulk density (bd, wet wt), porosity, and % sediment < 60 µm at Eagle Key (EK), Black Betsy Key (BLBK), Buchannan Bank (BB) and Rabbit Key (RK) in Florida Bay. Elemental and ratio values represent means ± SD (n=3). Sediment bd and porosity are depth averages (0-14 cm).

	(mmol gdw^{-1})	(µmol gdw^{-1})			Molar Ratios ($x10^{-3}$)			gdwt cm^{-3}		%
Site	Ca	F	TP*i*	TP	F:Ca	TP*i*:Ca	TP*i*:F	bd	Porosity	<63µm
EK	9.23	28.78 ± 1.30	0.81 ± 0.02	1.77 ± 0.06	3.11	0.09	28	0.70	0.66	83
BLBK	9.29	31.51 ± 3.14	1.12 ± 0.02	2.22 ± 0.05	3.39	0.12	36	0.91	0.73	69
BB	8.90	58.43 ± 6.29	2.35 ± 0.03	4.40 ± 0.03	6.57	0.26	40	0.34	0.84	63
RK	7.80	35.56 ± 3.92	4.66 ± 0.16	9.48 ± 0.25	4.56	0.60	131	0.25	0.89	59

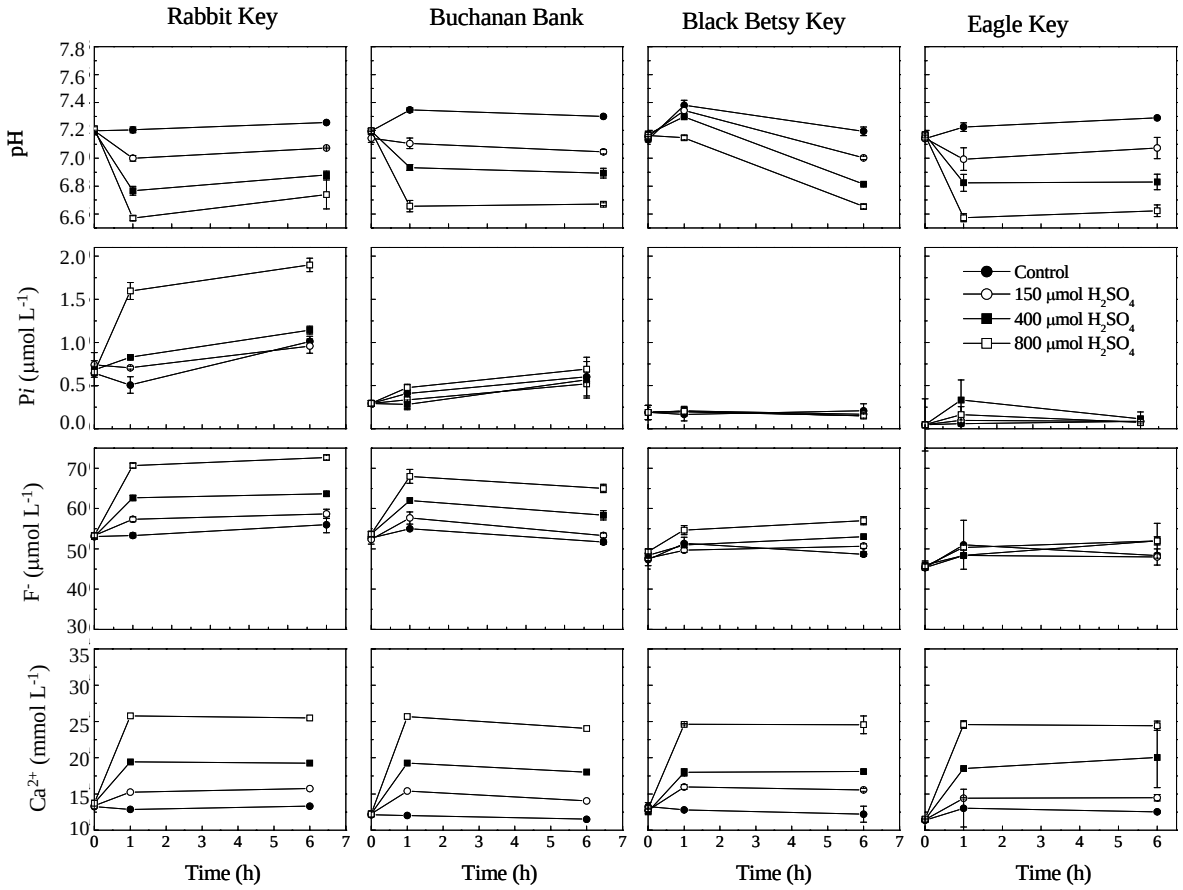

Figure 4.2. Efflux of inorganic P (P*i*), fluoride (F^-) and Ca^{2+} into the seawater sediment slurry (soluble phase) as a function of decreasing pH exposed to 3 different acidification treatments (see legend) and control over time in the 6 h incubation (n=3).

Table 4.2. Soluble reactive phosphorus (ΔP_i), fluoride (ΔF^-), and calcium (ΔCa^{2+}) mobilized in seawater (SW) after acidification treatments (150, 400, and 800 µmol H_2SO_4) and ΔSRP and ΔF^- re-adsorbed but recovered in specific sequential extracts with $MgCl_2$ (loosely adsorbed) and BD (strongly adsorbed). Values are represented as changes in concentration compared to control treatments with no acid dissolution; (*) represent significant changes. Σ represents the sum of SRP or F^- in the three sequential fractions (SW, $MgCl_2$, and BD).

	150 µmol H_2SO_4				400 µmol H_2SO_4				800 µmol H_2SO_4			
Site	SW	MgCl	BD	**Σ**	SW	MgCl	BD	**Σ**	SW	MgCl	BD	**Σ**
						ΔSRP (nmol g dw^{-1})						
EK	0.04	0.08	10.47	**10.60**	0.43	0.07	-16.50	**-16.00**	0.08	0.09	-9.96	**-9.79**
BLBK	-0.08	-0.60	1.66*	**0.98***	-0.16	-0.07	2.26	**2.03**	-0.16	-0.01	4.46*	**4.29***
BB	-0.62	0.28	3.43	**3.10**	-0.43	1.33*	8.78	**9.67**	0.65	2.59*	8.78	**12.13**
RK	0.07	1.94	34.66*	**36.66***	2.29*	5.26	48.62*	**56.17***	12.10*	22.11	48.67*	**82.87***
						ΔF^- (nmol g dw^{-1})						
EK	-0.07	7.48	12.72*	**20.13**	10.84	6.54	28.23	**45.61***	13.66	9.06	58.52*	**81.23***
BLBK	2.91	2.63	-17.01	**-11.47**	9.16	7.95	4.33	**21.44**	21.81*	12.26*	19.26	**53.34**
BB	17.15	0.64	18.31	**36.10**	43.86*	2.93	39.54	**86.33***	93.83*	8.16*	63.40*	**165.39**
RK	34.19	0.32	-22.52	**11.98**	104.28*	16.61*	-38.19	**82.69***	213.63*	27.17*	-72.89	**167.91**
						ΔCa^{2+} (µmol g dw^{-1})						
EK	7.6*				31.0*				50.6*			
BLBK	16.9*				28.9*				54.9*			
BB	19.4				48.6				94.1			
RK	29.6				70.9				152.8			

changes in surface bound P insignificant across all acidification treatments and were not recovered in sequential extractions (Table 4.2). If we examine the total amount of P*i* extracted as dissolved and surface resorbed, relative to controls without acid treatment, there was an increasing amount of P recovered with a clear east-west distinction (Fig. 4.3) along the sediment TP and TP*i* gradient (Table 4.1).

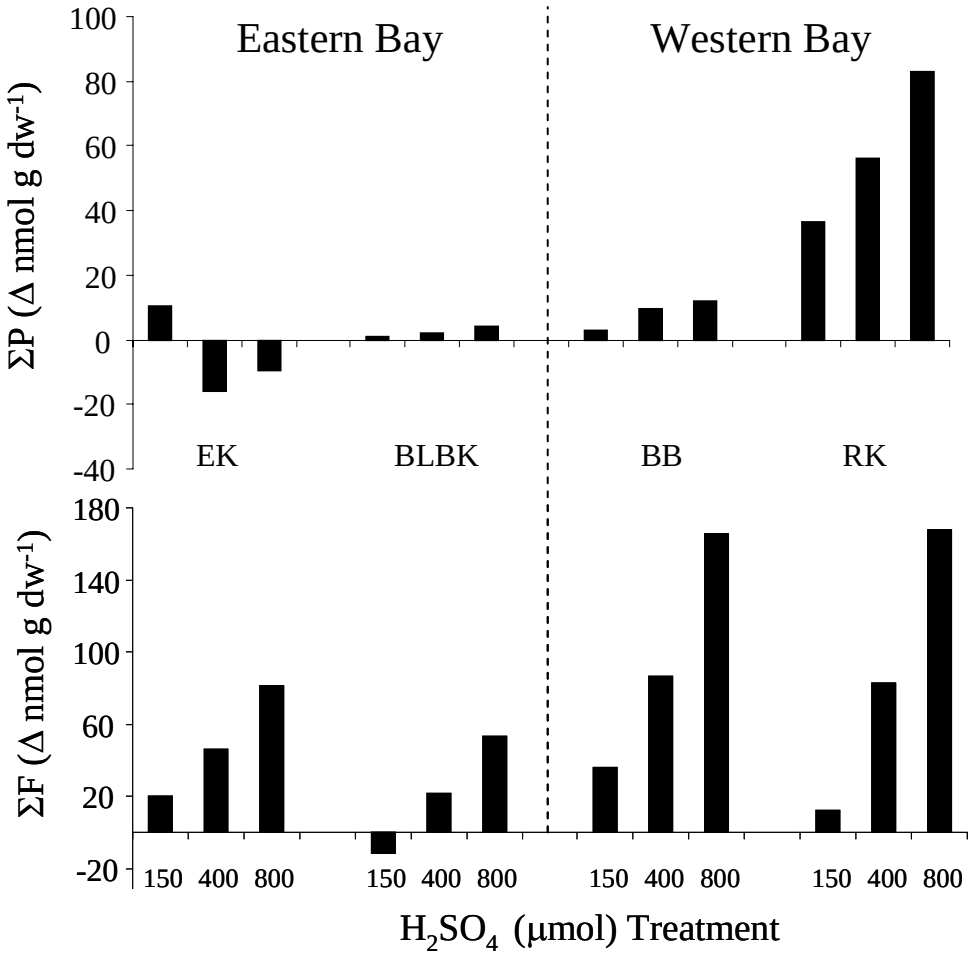

Figure 4.3. Total P and F recovered from the soluble (seawater) and exchangeable (HCl and BD extractable) pools after dissolution with sulfuric acid comparing eastern (Eagle Key [EK]and Black Betsy Key[BLBK]) and western (Rabbit [RK] Key and Buchanan Bank [BB]) bay sites.

Fluoride mobilization to the water phase of the sediment slurry with acidification followed the same trend as observed for P*i* with the greatest F^- release at the western sites, RK and BB, with significant increases also at BLBK (Fig. 4.2). Consistent with P*i* results, F^- was also mobilized to both the slurry water and recaptured as a surface-bound pool on the carbonate sediments in the slurry. While no significant release of F^- to the slurry water was found at EK, all four stations had significant F^- recovery in the adsorbed solid phase pools (Table 4.2). The pattern of recovery for the adsorbed pool, however, did not follow total F or P content in the sediment (Table 4.1), rather tended to be higher in the western than eastern bay sites, particularly under the highest sulfuric acid treatments (Fig. 4.3).

The relationship between the amounts of P dissolved and the sulfuric acid concentrations added, normalized to per gram dry weight sediment, followed a general pattern of increasing flux with higher acid additions, with the exception of EK (Fig. 4.4). At RK, this correlation was linear ($R^2 = 0.74$; Fig. 4.4). For Ca^{2+}, slopes ranged between 0.78 and 0.97, with no significant differences between sites. The near 1:1 relationship indicates an approximate equimolar reaction between sulfuric acid and carbonate sediment mineralization. This was further supported by the observation of gas formation (CO_2) immediately after acid was added to the carbonate sediment slurries. This ratio may be unique for the experimental study while in nature the sediment will receive a much slower exposure to sulfuric acid, probably resulting in a ratio closer to 1:2. Similar to results for Ca^{2+}, F^- was mobilized equally across sites independent of location and with no significant difference in slope. The molar ratio of F^- and Ca^{2+} that effluxed upon acidification ranged from 1.29×10^{-3} to 1.78×10^{-3} (Table 4.3), a significantly lower F:Ca ratio than determined for the bulk sediment (Table 4.1), indicating preferential dissolution of a F^- poor carbonate fraction.

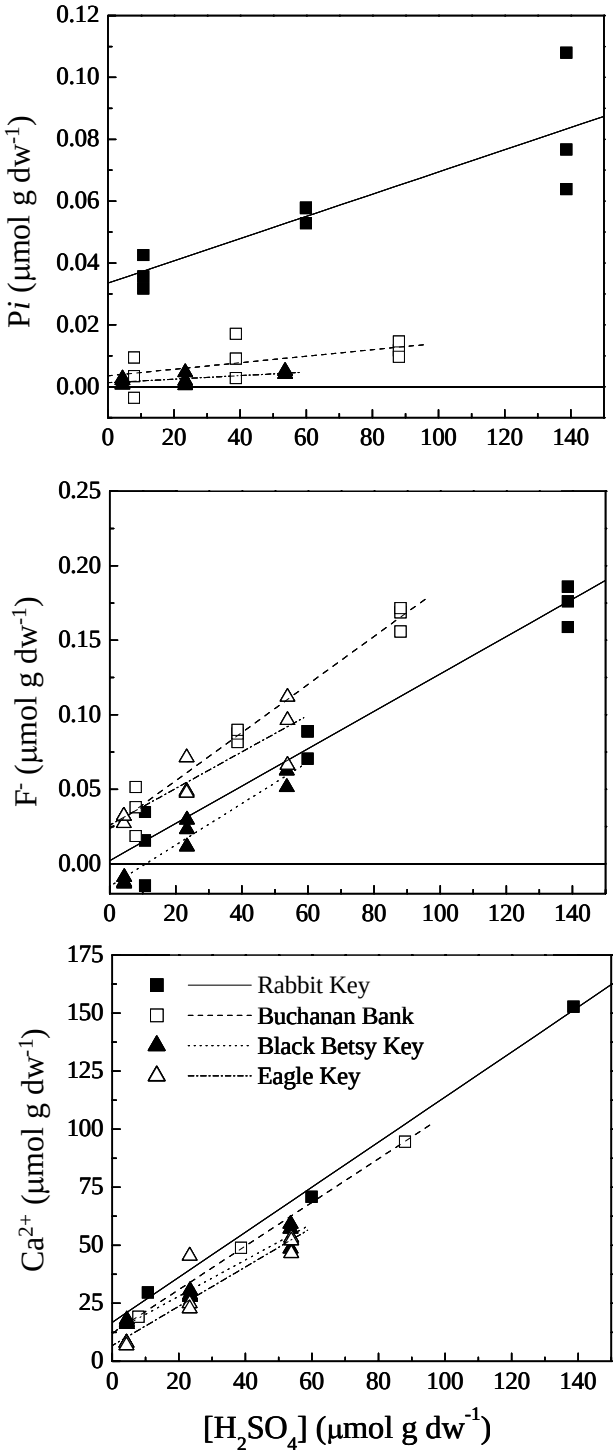

Figure 4.4. Relationship between sulfuric acid additions and release of inorganic P (P*i*), fluoride (F^-) and Ca^{2+} into the seawater sediment slurry (soluble phase) normalized to per g dw^{-1} for eastern (Eagle Key and Black Betsy Key) and western (Rabbit Key and Buchanan Bank) bay sites.

Table 4.3. Ratios between P*i*, F^-, and Ca^{2+} mobilized after sulfuric acid additions. The ratios are calculated from the slopes generated from Figure 3. No significant (ns) P*i* mobilization was found at Eagle Key.

	Atomic Ratios (x 10^{-3})		
	F:Ca	P:Ca	P:F
EK	1.45	ns	ns
BLBK	1.78	0.07	41
BB	1.71	0.11	66
RK	1.29	0.37	282

As shown previously, P*i* mobilization was only significant at RK, BB and BLBK, thus, P*i* efflux in response to sulfuric acid additions, per gram sediment dry weight, can only be calculated for three sites. The highest slopes were found at RK and lowest at BLBK (Fig. 4.4), but less P*i* was mobilized and subsequently recovered (Table 4.2) than predicted from the bulk TP*i* sediment distribution among sites across the sediment trophic gradient in the bay (Table 4.1). This either indicates dissolution of a relatively P-poor carbonate fraction, or more likely, a large re-adsorption and subsequent incorporation into solid phase P pools not recovered by the sequential extraction scheme applied. Re-adsorption was less pronounced for F^- than for P*i* and Ca^{2+} re-crystallization, if occurring, was only a small fraction of the $CaCO_3$ that was dissolved (Table 4.2). Thus Ca^{2+} and to some extent also F^- may be considered indicators of P*i* release from the carbonate matrix when observed in elevated concentrations (e.g. Jensen et al., 1998), even if elevated concentrations of P*i* are not observed in the pore water.

4.2.3. Tracer experiment

$^{33}PO_4^{3-}$ amended to sediment slurries rapidly adsorbed to the carbonate particles with 0.35% and 1.1% left in the water after 60 min at EK and GMK, respectively (Fig. 4.5). At the eastern bay site (EK), $^{33}PO_4^{3-}$ was distributed in proportion with the cold phosphate after 4 h with 25% found in the surface adsorbed P-pools, 2.6% in the $MgCl_2$ and 22.4 % in the BD extractions and 75% within the carbonate matrix (Table 4.4). However, in the western bay at GMK, $^{33}PO_4^{3-}$ was primarily found in the surface bound pools from where it only slowly redistributed into the HCl-extractable carbonate matrix pool. Even after 55 h, only 54% of the $^{33}PO_4^{3-}$ was recovered in the surface adsorbed pools.

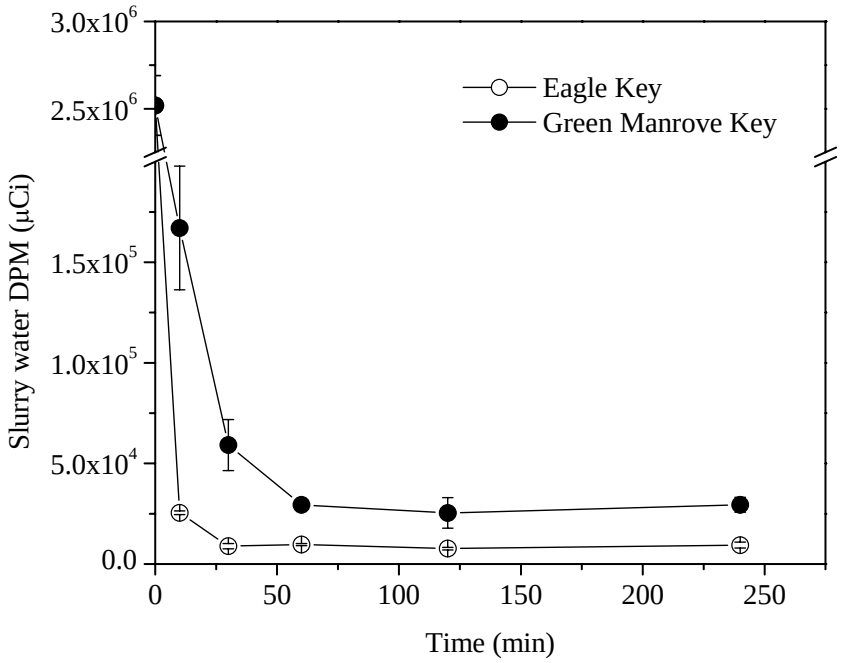

Figure 4.5. Changes in the ^{33}P radioactivity over time in the aqueous phase of the sediment slurry over time, using sediment from Eagle Key and Green Mangrove Key, eastern and western bay sediments, respectively.

Table 4.4. Distribution of ^{33}P (%) in various P-pools as a function of time following addition of trace amounts of $^{33}PO_4^{3-}$ to sediment slurries from the western Florida Bay (Green Mangrove) and the northeastern Florida Bay (Eagle Key) sites. The percentage distribution of $^{31}PO_4^{3-}$ in the sediments is also shown. Values represent mean ± SD (n=3).

		Relative ^{33}P distribution (%)				^{31}P dist (%)
		4.66 h	7.66 h	33 h	55 h	
GM	$MgCl_2$	26.8 ± 2.9	22.8 ± 3.7	16.1 ± 1.7	16.1 ± 0.4	5.4 ± 1.2
	BD	42.7 ± 1.3	44.4 ± 2.2	39.5 ± 0.9	36.9 ± 0.2	20.1 ± 0.9
	HCl	30.5 ± 1.6	32.8 ± 1.5	44.4 ± 2.6	47.0 ± 0.2	74.5 ± 2.0
EK	$MgCl_2$	3.8 ± 0.0	3.5 ± 0.1	2.3 ± 0.1	2.6 ± 0.2	5.7 ± 0.4
	BD	22.8 ± 0.3	24.2 ± 0.2	20.6 ± 1.3	22.9 ± 1.9	17.1 ± 1.8
	HCl	73.5 ± 0.3	72.1 ± 0.3	77.1 ± 1.2	74.5 ± 1.8	77.2 ± 1.7

4.2.4. Sulfate reduction rates

The highest SRR were measured in the more enriched western bay sediments, with respect to P availability, and in the upper 0-2 cm of sediment (Fig. 4.6). Depth integrated rates in the top 14 cm were 2-fold higher at RK and BB (43-85 mmol m^{-2} d^{-1}) compared to BLBK and EK (27-32 mmol m^{-2} d^{-1}; Table 4.5). Seasonality was only observed at Rabbit Key where rates in the fall were almost twice the rates in June, although high variance was also observed (Fig. 4.6).

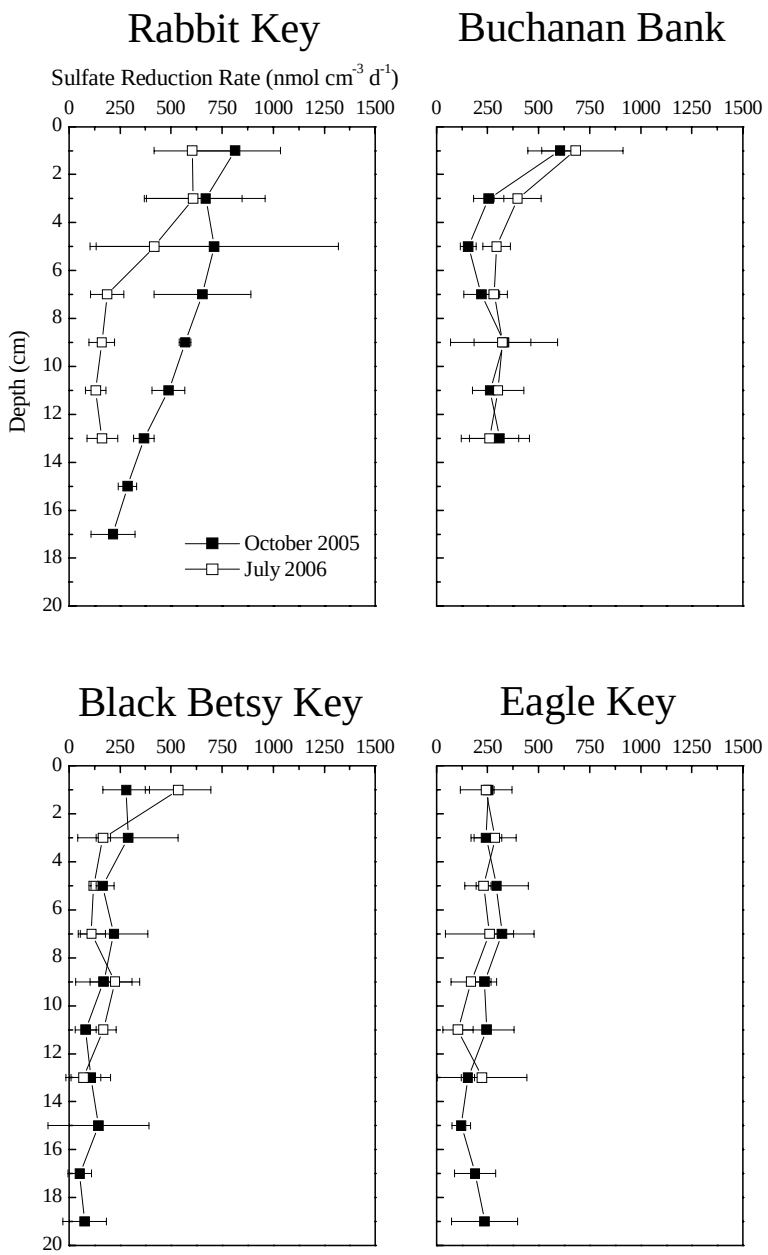

Figure 4.6. Depth profiles of microbial sulfate reduction rates incubated at in situ temperatures in intact sediment cores October 2005 (27°C) and July 2006 (31°C) from western (Rabbit Key and Buchanan Bank) and eastern (Black Betsy Key and Eagle Key) Florida Bay.

Table 4.5. Seasonal variations in sulfate reduction rates (SRR) integrated to14 cm depth and mean SRR normalized to sediment volume in seagrass sediments from Eagle Key (EK), Black Betsy Key (BLBK), Buchanan Bank (BB) and Rabbit Key (RK) in Florida Bay. Values are mean ± SD (n=3 cores).

Site	Date	$\Sigma SRR_{0\text{-}14\ cm}$ (mmol m^{-2} d^{-1})	SRR (nmol cm^{-3} d^{-1})
EK	Oct 2005	34.9 ± 3.1	249.3 ± 21.9
	July 2006	30.3 ± 4.3	216.1 ± 23.2
BLBK	Oct 2005	26.2 ± 4.6	187.3 ± 33.1
	July 2006	28.0 ± 5.5	199.6 ± 26.4
BB	Oct 2005	42.7 ± 3.6	304.8 ± 95.2
	July 2006	50.7 ± 14.6	362.5 ± 104.5
RK	Oct 2005	85.4 ± 19.4	610.3 ± 138.8
	July 2006	45.4 ± 18.1	324.2 ± 129.2

4.3. Discussion

Rates of microbial sulfate reduction and release of P*i* from acidification of carbonate sediment was greatest in the western region of Florida Bay where high sediment nutrient loads (Zhang et al., 2004; Nielsen et al., 2006), primarily from Gulf of Mexico sources (Rudnick et al., 1999), result in extremely dense seagrass meadows (Fourqurean et al. 1992), following the general trend of higher SRR with increasing organic matter in seagrass sediments (Holmer et al., 2006). SRR were approximately 2-fold higher on average at the western (305-610 nmol cm^{-3} d^{-1}) than eastern (187-249 nmol cm^{-3} d^{-1}) bay sites with a depth integrated (14 cm) areal rate of 43-85 and 26-36 mmol m^{-2} d^{-1}, respectively. Using closed chamber SO_4^{2-} incubation experiments, we have calculated similar rates of SR at western (BB, 372 nmol cm^{-3} d^{-1}) and eastern (EK, 123

nmol cm^{-3} d^{-1}) bay sites (Koch et al., in press). Our estimates are comparable to those determined by Walter et al. (in press) for sediments of mudbank and island fringe sites in the central bay (70-579 nmol cm^{-3} d^{-1}) also using the $^{35}SO_4^{2-}$ radiolabelling technique, albeit at slightly higher temperatures (32°C). However, they calculate a 2-fold higher depth (18-22 cm) integrated area SRR (82-274 mmol m^{-2} d^{-1}) which are greater than maximum estimates reported by Holmer et al. (2006) for tropical seagrass sediments in east Asia (<138 mmol m^{-2} d^{-1}) using a depth profile of 0-10 cm. Some of these discrepancies in areal SR estimates are probably explained by the depth of integration, which were down to 14 cm in the current study, 10 cm by Holmer and colleagues, and 18-22 cm by Walter et al. Although there are some variances in area estimates due to depth integration, there is general agreement on the rates of SR from Florida Bay on a sediment volume basis, and these rates conform to those found in other warm tropical climes (reviewed by Holmer et al., 2006). Thus, as a first approximation our SRR data can be used to estimate sulfide generation potential sulfide reoxidation rates assuming unity between these redox couples.

In contrast to Fe-rich siliciclastic coastal sediments, where reduced sulfide is readily incorporated into solid phase FeS pools, such as pyrite (e.g. Berner, 1984), sulfides accumulate in the porewaters in organic rich low-Fe carbonate sediments, such as Florida Bay. Several authors (Barber and Carlson, 1993; Carlson et al., 1994; Lyons et al., 2004; Walter et al., in press) have shown sulfide levels in the bay to be in the millimolar range (2-7 mM), with higher concentrations in western bay sediments, corresponding to higher SRR (Koch et al., in press, this study) and organic matter loading from dense seagrass meadows and higher algal productivity (Zieman et al., 1998; Phlips et al., 1999). Although sulfide concentrations are high in porewaters of the bay, there is mounting evidence, based on $^{18}O_{SO4}$ signatures and the lack of sulfate depletion in porewater profiles, that rapid recycling occurs between redox states of S (Walter and

Burton, 1990; Ku et al., 1999; Moreira et al., 2004). Exceptions have been found though on some highly organic mudbank sites without seagrass which act as a “closed system” and reoxidation of S^{2-} is limited (Lyons et al., 2004). However, sites in the bay with appreciable seagrass meadows indicate a high capacity to efficiently oxidize sulfides (Ku et al., 1999; Koch et al., 2007; Walter et al., in press), similar to other carbonate systems (Burdige and Zimmerman, 2002). A complete recycling of sulfide within the sediment means that there is no net-formation of sulfuric acid but as SR is occurring in a large depth profile sulfide oxidation will be restricted to the much narrower root zone or sites of bioturbation. If we assume that sulfide oxidation is in unity with reduction, the acid generated by sulfide oxidation can be approximated by SRR applying a 1:1 stoichiometry, although this conversion does not consider loss of H_2S through plants or other bioturbation processes. As a first approximation, if we consider all sulfides generated from SR were reoxidized, sulfide oxidation would contribute the equivalent of 1.4±0.66 and 0.27±0.09 µmol H_2SO_4 gdwt^{-1} d^{-1} at western and eastern bay sites, respectively. At that rate it would take 80±11 and 205±63 days to generate the H_2SO_4 amendments of our highest acid additions, 112±36 and 53±0.2 µmol H_2SO_4 gdwt. Under these H_2SO_4 treatments, pH values dropped in the sediment slurry to 6.6-6.8, on par with those found in porewaters of Florida Bay (6.6-6.7 and 6.8-6.9 in western and eastern sites, respectively, Koch et al., in press; Walter and Burton, 1990). These results indicate that the acidification levels generated in this study by H_2SO_4 represent those that can occur over time in the bay with relatively high SRR and rapid reoxidation of sulfides, the volumetrically dominant acid-generating reaction driving dissolution in bay sediments (Ku et al., 1999; Walter et al., in review). In Florida Bay sediment pH is reportedly low, consistent with the fact that in low Fe systems, sulfide accumulation buffers pH between 6.6 and 6.9 (Walter and Burton, 1990). Higher porewater pH (7.25-8.25) has been reported in high

density seagrass meadows in the Bahamas (Burdige and Zimmerman, 2002) and dissolution in these systems is thought to primarily be driven by organic matter mineralization and CO_2-generated acidity (Hu and Burdige, 2007), although sulfide oxidation may also play an important role.

Regardless of the metabolic processes driving dissolution, it is generally agreed that there is significant dissolution of carbonate sediments occurring in both Florida Bay and the Bahamas through metabolic oxidation. This acid-driven dissolution could liberate P*i* from the large TP*i* pool in these systems. In our experiments, although the acid treatment varied among sites on a sediment dry wt basis as a results of differences in the bulk density, acid treatments within the same range (10-53 µmol H_2SO_4 gdw^{-1}) across treatments released P*i* preferentially from western bay sites, and particularly at RK. Phosphorus flux normalized to acid per g dry wt of sediment were 0.60, 0.14, and 0.08 nmol P*i* released per µmol H_2SO_4 amended at RK, BB and BLBK, respectively, with no detectable release of P from EK. The P*i* release rates between western and eastern bay sites span 1-2 orders of magnitude, while differences in the TP*i* concentrations of the sediment are only 2-4 fold higher in western than eastern bay sites. These data suggest that the linkage between P*i* release and acidification may be confounded by the mechanism by which P*i* is incorporated by carbonate sediments; either adsorbed onto carbonates and/or incorporated into the carbonate matrix, as well as the chemical make up of the source sediment. These geochemical processes will subsequently control the susceptibility of the carbonate matrix associated with TP*i* to release P in response to acidification either by sulfide oxidation and/or metabolic acid accumulation.

Although sediments across Florida Bay are dominated by $CaCO_3$ (81-94%, Zhang et al., 2004) source carbonates at our western bay sites had molar ratios indicative of sediment

dominated by easily dissolvable aragonite and high-Mg calcite with approximately 2-fold higher F:Ca ratios compared to eastern bay sites. While acid readily dissolved carbonate sediments in both eastern and western bay sites, the percentage of the total sedimentary Ca dissolved per g dry weight sediment, for example at our highest acid treatment, per µmol of acid added was 1.03, 1.12, 1.23 and 1.43 at EK, BLBK, BB and RK, identifying western bay carbonates as more susceptible to dissolution. This fact, and the high TP*i* pool in the western bay, probably explains the larger release of P*i*, the majority which was recovered in the surface bound pool from RK and BB in this study. While RK and BB released the greatest amounts of P*i* in this study, the molar fraction of F:Ca in our acid dissolved pool from all sites was similar among eastern and western bay sites (1.29-1.78 x 10^{-3}), indicating that the carbonate matrix that did dissolve was chemically similar. The implication here is that regardless of the variance in organic matter decomposition (SRR and carbonic acid production) across sites and potential acid generation from these processes, there would not be a concomitant P*i* release to the porewaters or easily exchangeable pool from carbonate dissolution across the bay. Based on this study, F:Ca ratios and acidification at levels generated by SR may be better indicators of TP*i* availability under high rates of SR and subsequent oxidation in seagrass-dominated bay sediments, compared to extremely low pH (< 4) extracts that dissolve the entire $CaCO_3$ pool (Koch et al., 2001; Zhang et al., 2004). We also conclude from this that F^- and Ca^{2+} increases in pore-water may be a valid indicator of P*i* mobilization from the carbonate matrix, as suggested by Jensen et al. (1998).

In strong contrast to western bay sites, EK sediments in the northeastern bay strongly bounded P*i* to the point where no P recovery was made from the dissolved or adsorbed P pools after treatment with 53 µmol H_2SO_4 $gdwt^{-1}$. This result can be explained in two ways, P was not released with acid dissolution, which appears very unlikely based on the $CaCO_3$ that was

dissolved, or P was rapidly (< 1h) adsorbed and incorporated into a non-exchangeable P pool. In a previous experiment by the authors on P*i* adsorption-de-sorption equilibrium (Nielsen et al., 2006), the crossover concentration (Ce0) where P*i* is no longer adsorbed, was extremely low (0.017 µmol L^{-1}) at EK, 10-times lower than a western bay site (GM), indicating the high capacity for eastern bay sediments to adsorb P*i*. Small carbonate grain sizes <10 µm have been shown to be important in P adsorption; and more specifically, Florida Bay sediments have been defined as having high surface energies resulting from small particle size (Walter et al., in press). Comparing among sites in this study, EK had the smallest carbonate particles, where 83% of the sediment was less than 63 µm, and most of this residual pool was probably even smaller. Sediment sequential extraction data from EK sediment, following acid dissolution, suggest that, if the dissolved P pool was resorbed, it was not incorporated into a readily exchangeable pool, but rather tightly adsorbed or incorporated into the carbonate matrix.

The second important mechanism that may have influenced P*i* recovery in this study post dissolution is the potential for re-crystallization and/or reincorporation of P*i* into a matrix with fine carbonate particles at eastern bay sites. Although our Ca^{2+} flux data do not support the idea that appreciable amounts of re-crystallization of carbonates occurred, which may have influenced re-sequestering of P*i*, re-crystallization of biogenic aragonites and high-Mg calcites have been found in Florida Bay and Bahamian porewaters with sediments of high specific surface areas (Hu and Burdige, 2007; Walter et al., in press). Specific surface areas of 2 m g^{-1} have been estimated for the bay by Walter and Morse (1985) giving a critical volume to area (V:A) value of 0.7 x 10^{-3} cm, below a critical value of 1 x 10^{-3} cm, shown to promote fine crystallite formation (Walter et al., in press). Walter et al (in press) calculated that 3.3 times more carbonate is dissolved by SR than released by net dissolution, with the remainder being re-crystallized. Because our P*i*:Ca

concentrations are so low, both in the solid (0.09×10^{-3}) and dissolved phase ($<0.07 \times 10^{-3}$), we cannot rule out the potential for the incorporation of P*i* released at EK back into a carbonate matrix via a small amount of $CaCO_3$ re-crystallization, which was within the variance of our Ca^{2+} measurement, and thus, not recovered in the exchangeable pool.

The potential for tight resorption of P*i* released from EK is also supported by the rapid rate of isotope exchange of ^{33}P*i* into the HCl-extractable TP*i* pool at this site. We examined the rate of ^{33}P isotope exchange into surface adsorbed and matrix incorporated P pools for carbonate sediments collected from eastern and western sites in the bay. After only 5 h, 73% of the radioactivity was detected in HCl-extractable $CaCO_3$-bound pools in eastern bay sediments, while only 31% of radioactivity was found during this same time in western bay sediments. Even after 55 h, the majority of radioactivity was still found in the surface-bound exchangeable pool at the western bay site. Thus, while the apportionment of TP*i* in the various pools in the bay are similar based on ^{31}P (this study, Zhang et al., 2004), the rates of incorporation, and perhaps binding efficiency (Nielsen et al., 2006), may explain low P*i* in porewaters in the eastern versus western regions of the bay (Fourqurean et al., 1992), and the inability to recover P*i* post acidification from EK sediments in this study.

Although several studies of shallow carbonate platforms of south Florida dominated by seagrass indicate the high potential for SR and subsequent reoxidation of sulfides that can generate enough acidity, along with organic matter decomposition, to dissolve an appreciable amount of carbonates, the complexities and spatial variance in these processes has been appreciated (Ku et al., 1999; Lyons et al., 2004; Hu and Burdige, 2007; Walter et al., in press). Overlying these complexities, as indicated by the present study, is the clear non-linearity between calcium carbonate dissolved and P*i* released from Florida Bay carbonates, based on the

limited sites examined. The present study indicates a high efflux of P*i* at western bay sites with dissolution exemplified by RK sediments. At RK, SRR (1.9 µmol SO_4^{2-} gdwt^{-1} d^{-1}) could dissolve ~2.8 µmol Ca gdwt^{-1} d^{-1}, applying a 2:1 ratio of Ca dissolved to SR (Walter and Burton, 1990; Ku et al., 1999), generating 1.5 nmol P*i* gdwt^{-1} sediment d^{-1} from the TP*i* pool based on P*i* release calculated as a function of $CaCO_3$ dissolution in this study. On an area basis, using an integration of 14 cm depth, this P*i* supply equates to 53 µmol m^{-2} d^{-1} from bacterial SR and dissolution of $CaCO_3$, which is ~50% (53 µmol P m^{-2} d^{-1} to 14 cm) of the daily P requirement for *T. testudinum* (~100 µmol P m^{-2} d^{-1}), and together with P regenerated from mineralization of organic material (66 µmol P m^{-2} d^{-1}; with a C:P 2,000 and 2 mol C per mol SO_4^{2-} reduced), would provide a surplus of P*i*, probably contributing to the lack of seagrass P limitation in the western bay. It is not as clear for eastern bay sites whether seagrass productivity could be supported by nutrients generated by carbonate dissolution, even if SRR or carbonic acid production would produce enough acid to drive the pH to 6.5. More work is needed on the mechanisms of incorporation of P into the solid phase $CaCO_3$ pool across the bay which significantly influences the retention of TP*i*, even when subjected to acidification.

In addition, the temporal dynamics of the seagrass meadows need to be considered and how these biological shifts in community control net precipitation or net dissolution reactions. When seagrass meadows are active, they could be important sites of net $CaCO_3$ dissolution, but when die-offs occur, as they frequently do in western Florida Bay (Hall et al., 1999; Borum et al., 2005; Koch et al., in press), they may become supersaturated with respect to overlying water aragonite because of high SRR and increasing alkalinity promoting $CaCO_3$ precipitation (Lyons et. al., 2004), and limits on aerobic respiration, which may lead to the co-precipitation of P*i*. Clearly more work is required in understanding these processes and how changes in temperature

with climate change, and seagrass production through eutrophication, may affect these biogeochemical interactions and influence nutrient cycling in shallow carbonate seagrass ecosystems, such as Florida Bay.

4.4. References

Barber, T.R., Carlson, P.R., 1993. Effects of seagrass die-off on benthic fluxes and porewater concentrations of ΣCO_2, ΣH_2S, and CH_4 in Florida Bay Sediments. In: Oremland, R.S. (Ed.), Biogeochemistry of Global Change: Radiatively Active Trace Gases. Chapman and Hall, New York, pp. 530-550.

Berner, R.A., 1984. Sedimentary pyrite formation: an update. Geochim. Cosmochim. Acta. 48, 605-615.

Borum, J., Pedersen, O., Greve, T.M., Frankovich, T.A., Zieman, J.C., Fourqurean, J.W., Madden, C.J., 2005. The potential role of plant oxygen and sulphide dynamics in die-off events of the tropical seagrass, Thalassia testudinum. J. Ecol. 93, 148-158.

Burdige, D.J., Zimmerman, R. C., 2002. Impact of seagrass density on carbonate dissolution in Bahamian sediments. Limnology and Oceanography 47, 1751-1763.

Carlson, P.R., Yarbro, L.A., Barber, T.R., 1994. Relationship of sediment sulfide to mortality of Thalassia testudinum in Florida Bay. Bull. Mar. Sci. 54, 733-746.

Chambers, R.M., Fourqurean, J.W., Macko, S.A., Hoppenot, R., 2001. Biogeochemical effects of iron availability on primary producers in a shallow marine carbonate environment. Limnol. Oceanogr. 46, 1278-1286.

Cline, J.D., 1969. Spectrophotometric determination of hydrogen sulfide in natural waters. Limnol. Oceanogr. 14 (3), 454-458.

De Kanel, J. & Morse, J.W. 1978 The chemistry of orthophosphate uptake from seawater on to calcite and aragonite. Geochimica et Cosmochimica Acta 42, 1335-1340.

Fossing, H., Jørgensen, B.B. 1989. Measurement of bacterial sulfate reduction in sediments: Evaluation of a single-step chromium reduction method. Biogeochemistry 8:205-222.

Fourqurean, J.W., Zieman, J.C., Powell, G.V.N., 1992a. Phosphorus limitation of primary production in Florida Bay: Evidence from C:N:P ratios of the dominant seagrass *Thalassia testudinum*. Limnol. Oceanogr. 37, 162-171.

Fourqurean, J. W., and J. Zieman. 2002. Nutrient content of the seagrass *Thalassia testudinum* reveals regional patterns of availability of nitrogen and phosphorus in the Florida Keys USA. Biogeochemistry **61**: 229-245.

Hall, M.O., Durako, M.J., Fourqurean, J.W., Zieman, J.C., 1999. Decadal changes in seagrass distribution and abundance in Florida Bay. Estuaries, 22 (28), 445-459.

Holmer, M., Pedersen, O., Ikejima, K., 2006. Sulfur cycling and sulfide intrusion in mixed southeast Asian tropical seagrass meadows. Bot. Mar. 49 (2), 91-102.

Hu, X., Burdige, D.J. 2007. Enriched stable carbon isotopes in the pore waters in carbonate sediments dominated by seagrasses: Evidence for coupled carbonate dissolution and reprecipitation. Geochimica et Cosmochimica Acta 71:129-144.

Jensen, H.S., McGlathery, K.J., Marino, R. & Howarth, R.W. 1998 Forms and availability of sediment phosphorus in carbonate sand of Bermuda seagrass beds. *Limnology and Oceanography* 43, 799-810.

Jørgensen, B.B. 1978. A comparison of methods for the quantification of bacterial sulfate reduction in coastal marine sediments. Geomicrobiology Journal 1, 11-27.

Kitano, Y., Okumura, M. & Idogaki, M. 1978 Uptake of phosphate ions by calcium carbonate. *Geochemical Journal* 12, 29-37.

Koch, M. S., R. E Benz, and D. T. Rudnick. 2001. Solid-phase phosphorus pools in highly organic carbonate sediments of northeastern Florida Bay. Estuar. Coast. Shelf Sci. **52**: 279-291.

Koch, M.S., Schopmeyer, S.A., Holmer, M., Madden, C.J., Kyhn-Hansen, C. 2007. *Thalassia testudinum* response to the interactive stressors hypersalinity, sulfide and hypoxia. Aquat. Bot. 87: 104-110.

Koch, M.S., Schopmeyer, S.A., Nielsen, O.I., Kyhn-Hansen, C., Madden, C.J. in press. Conceptual model of seagrass die-off in Florida Bay: Links to biogeochemical processes. Journal Experimental Marine Biology and Ecology.

Koroleff, F. 1983. Determination of phosphorus, p 125-139. *In*: Grasshoff, K., M. Ehrhardt, and K. Kremling (eds.). Methods of seawater analysis. Verlag Chemie, Weinheim.

Ku, T.C.W., Walter, L.M., Coleman, M.L., Blake, R.E., Martini, A.M., 1999. Coupling between sulfur recycling and syndepostitonal carbonate dissolution: Evidence from oxygen and sulfur isotope composition of pore water sulfate, South Florida Platform, U.S.A. Geochim. Cosmochim. Ac. 63 (17), 2529-2546.

Lyons, T.W., Walter, L.M., Gellaty, A.M., Martini, A.M., Blake, R.E. 2004. Sites of anomalous organic remineralization in the carbonate sediments of South Florida, USA: The sulfur cycle and carbonate-associated sulfate. In: Amend, J.P., Edwards, K.J., Lyons, T.W. (Eds.), Sulfur Biogeochemistry- Past and Present. Geological Society of America Special Paper 379, pp. 161-176.

Millero, F., F. Huang, X. R. Zhu, X. W. Liu, and J. Z. Zhang. 2001. Adsorption and desorption of phosphate on calcite and aragonite in seawater. Aquat. Geochem. **7**: 33-56.

Moreira, N., Walter, L.M., McKenzie, J., Vasconcelos, C., McCall, P. 2004. Role of sulfide oxidation in dolomitization: sediment pore water geochemistry of a modern hypersaline lagoon system. Geology 32: 701-704.

Morse, J. W., Zullig, J.J., Iverson, R.L., Choppin, G. R., Mucci, A., Millero, F.J., 1987. The influence of seagrass beds on carbonate sediments in the Bahamas. Marine Chemistry 22 (1), 71-83.

Nielsen, O.I., Koch, M.S., Jensen, H.S., Madden, C.J., 2006. Thalassia testudinum phosphate uptake kinetics at low in situ concentrations using a ^{33}P radioisotope technique. Limnol. Oceanogr. 50 (1), 208-217.

Phlips, E.J., Badylak, S., Lynch, T.C., 1999. Blooms of the picoplanktonic cyanobacterium Synechococcus in Florida Bay, a subtropical inner-shelf lagoon. Limnology and Oceanography 44, 1166-1175.

Rosch, K., Koch, M.S. in review. Seagrass (*Thalassia testudinum*) nutrient recycling in Florida Bay, a subtropical carbonate-dominated estuary.

Rude, P.D., Aller, R. C., 1991. Fluorine mobility during early diagenesis of carbonate sediment: An indicator of mineral transformations. Geochimica Acta 55, 2491-2509.

Rudnick, D. T., Z. Chen, D. L. Childers, J. N. Boyer, and T. D. Fontaine III. 1999. Phosphorus and nitrogen inputs to Florida Bay: the importance of the Everglades watershed. Estuaries 22:398-416.

Ruttenberg, K.C. & Berner, R.A. 1993 Authigenic apatite formation and burial in sediments from non-upwelling, continental margin environments. Geochimica et Cosmochimica Acta 57, 991-1007.

Short, F.T., Davis, M.W., Gibson, R.A., Zimmerman, C.F., 1985. Evidence for phosphorus limitation in carbonate sediments of the seagrass *Syringodium filiforme*. Estuar. Coast. Shelf. Sci. 20, 419-430.

Walter, L.M., Burton, E.A. 1990. Dissolution of recent platform carbonate sediments in marine pore fluids. American Journal of Science 290: 601-643.

Walter, L.M., Ku, T.C.W., Muehlenbachs, K., Patterson, W.P., Bonnell, L. in press. Controls on the $\delta^{13}C$ of dissolved inorganic carbon in marine pore waters: An instructive example from biogenic carbonate sediments (south Florida Platform). Deep Sea Research.

Yates, K.K., Halley, R. B. 2006. Diurnal variation in rates of calcification and carbonate sediment dissolution in Florida Bay. Estuaries and Coasts. 29(1):24-39.

Zhang, J.Z., Fisher, C.J., Ortner, P.B., 2004. Potential availability of sedimentary phosphorus to sediment resuspension in Florida Bay. Global Biogeochem. Cy. 18, GB4008. . doi:10.1029/2004GB002255.

Zieman, J.C., Fourqurean, J.W., Iverson, R.L., 1989. Distribution, abundance, and production of seagrasses and macroalgae in Florida Bay. Bull. Mar. Sci. 44, 292-311.